Science Sub-Component
Climate Change Action Fund, Environment Canada

Downscaling of Global Climate Model Outputs for Flood Frequency Analysis in the Saguenay River System

Project no. S02-15-01

Paulin Coulibaly and Yonas B. Dibike

Department of Civil Engineering / School of Geography and Geology
McMaster University
Hamilton, ON
L8S 4L7

Collaborators: François Anctil and Bruno Larouche

Hamilton, ON
June 2004

Downscaling Global Climate Model Outputs for Flood Frequency Analysis in the Saguenay River System

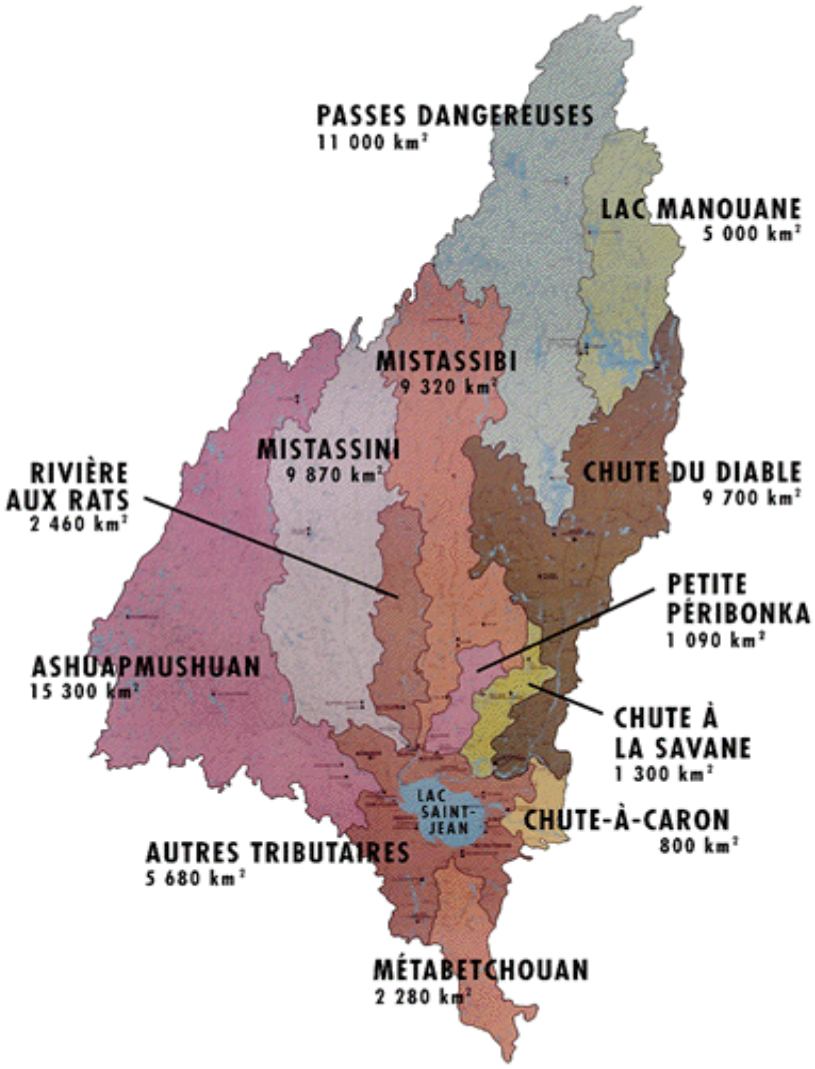

Final Report

by

Paulin Coulibaly and Yonas B. Dibike

Financial Support:
The Government of Canada Climate Change Action Fund

June, 2004

Project participants:

Mr. Jean Paquin, Hydrologist, ALCAN Company, Jonquiere, Quebec

Mr. Sajjad M. Khan, PhD candidate, Department of Civil Engineering, McMaster University

Mr. Xiaogong Shi, M.A.Sc. candidate, Department of Civil Engineering, McMaster University

Starting date: November 1, 2002

Ending date: June 30, 2004

Project summary:

The Global Climate Models (GCMs) used to simulate the present climate and project future climate are generally not designed for local or regional climate change impact studies. While GCMs demonstrated significant skill at the continental and hemispherical scales, they are inherently unable to represent local or subgrid-scale features and dynamics such as local topographical features and convective cloud processes. However, most hydrological models used in climate change impact studies need to simulate sub-grid scale phenomenon and therefore require input data (such as precipitation and temperature) at similar sub-grid scale (i.e. high resolution). Therefore, there is a need to convert (or 'downscale') the GCM outputs into high resolution daily precipitation and temperature series appropriate for local or regional scale hydrological impact studies.

The issues of 'downscaling' the outputs of GCM to a scale appropriate to hydrological impact studies are investigated. Canadian GCM data as well as data from eleven meteorological and nine hydrometric stations in the Saguenay watershed in Quebec were used in the study. Three types of dynamic artificial neural networks namely time lagged feedforward neural network (TLFN), Elman and Jordan recurrent neural networks, with different inherent representations of temporal information, are investigated for downscaling daily precipitation and temperature data. The performance of the optimal DANN model is compared to benchmarks from a statistical downscaling model (SDSM) and a stochastic weather generator (LARS-WG). Overall, the downscaling results for the current period (1961-2000) suggest that the TLFN is the most efficient of the DANN models tested for downscaling both daily precipitation and temperature series. Furthermore, the test results indicate that the optimal DANN model mostly outperforms the statistical and stochastic models for the downscaling of precipitation at most of the meteorological stations. With respect to the future 'business as usual' climate scenario, both the DANN and the SDSM models have predicted increasing trends in average annual precipitation between 15% and 40% in the study area while no significant trend was predicted with LARS-WG. Downscaled temperature data corresponding to all the three models show a comparable and consistently increasing trend in the mean annual temperature ranging between 3 to 5 ^{o}C for the next 100 years.

Moreover, simulations of river flows and reservoir inflows in the region were performed with lumped conceptual as well as physically based and distributed hydrological models. All simulations under climate change scenario showed that precipitation and temperature data downscaled with DANN and SDSM resulted in an increase in river flows and reservoir inflows as well as earlier spring-peaks, except for the summer months where reduction of flow is observed. While the data downscaled with DANN and SDSM resulted in an increase in mean annual flow of about 15% and 40% in the coming 100 years, the one downscaled with LARS-WG resulted in a decrease in mean annual flow of up to 10%. This is a clear indication of how the outcome of a hydrologic impact study (or any other impact study based on downscaled data) can be affected by the choice of any one particular downscaling technique over the other. In most cases, the DANN model appears to provide trade-off results between the SDSM and the LARS-WG model.

The flood frequency analysis completed on the simulated peak flows indicated an overall increasing trend in the frequencies of flood events in most of the major rivers in the Saguenay watershed. The study also indicated that, on average, the GCM output downscaled with DANN gave relatively larger increases in the magnitude of less frequent events (events with high return periods) than those downscaled with SDSM and LARS. SDSM seems to result in a relatively smaller increase in the frequency of flood events for the next 100 years than the other two. Overall, the results of the frequency analysis of peak flows simulated with all the three hydrological models are found to be relatively consistent. However, simulations made with HBV-96 seem to give the highest increase in the frequency of peak flow followed by WATFLOOD and CEQUEAU.

Table of Contents

1. Introduction

Human activities, primarily the burning of fossil fuels and changes in land cover and use, are nowadays believed to be increasing the atmospheric concentrations of greenhouse gases. This alters energy balances and tends to warm the atmosphere which will result in climate change. Some reports indicate that mean annual global surface temperature has increased by about 0.3 - 0.6^{o}C since the late 19th century and it is anticipated to further increase by 1–3.5°C over the next 100 years (IPCC, 1995). These changes in global climate appear to most severely affect the mid and high latitudes of the Northern Hemisphere, where temperatures have been noticeably getting warmer since 1970s (IPCC, 2001). Such changes in climate will have significant impact on local and regional hydrological regimes, which will in turn affect ecological, social and economical systems. Therefore, the study of the various impacts of climate change on hydrological regimes over the coming century has become a priority, both for process research and for water and watershed management and development strategies. Nevertheless, most of the studies in Canada have mainly focused on assessing the potential implication of climate change on water resources at regional or local level. These studies showed the vulnerability of the water resources such as lowering of water levels in the Great Lakes and reduced flows in St. Lawrence River, earlier spring peak flows, drought conditions in the Prairies, etc (Mehdi et al., 2002). Despite the undeniable importance of those studies for long-term planning, they give very little information on the changes in flow regimes in rivers, particularly the extreme flood or drought conditions.

Climate-change impact studies on flood regimes in Canada have been relatively rare until recently, basically because Global Circulation Models (GCMs), which are widely used to simulate future climate scenarios, do not provide hourly or daily rainfall reliable enough for flood regime modeling. To correctly model the flood regime of a catchment, continuous rainfall-runoff simulation at hourly or at least at daily time steps is necessary. In practice, daily rainfall series at a catchment corresponding to future climate scenarios can be derived from GCM outputs using the so called ‘downscaling techniques’. Even if GCMs are run at higher resolution, appropriate downscaling technique will still be necessary for impact studies (Wilby et al., 2002). Though these conversion methods do not correct the GCM model inaccuracies, they can provide future daily rainfall scenarios relevant to impact studies on flood regime. There are various downscaling techniques available, but it is not clear which one provides the most reliable estimates of daily rainfall corresponding to different scenarios. Therefore, to allow a proper evaluation of climate-change impact on flood regime at regional or local scale throughout Canada, it appears important to first evaluate thoroughly existing downscaling methods, and then to try to propose a better solution. This study aims to investigate and evaluate the more promising downscaling techniques, and provide a thorough inter-comparison study using the Saguenay – Lac-Saint-Jean (SLSJ) watershed in northern Québec as an experimental site. The Saguenay basin is a well known flood prone area as many Canadians still remember the year-1996 flood in this region. Therefore, this study will also address some important questions regarding the Saguenay River such as “Is this historical and damaging flood event part of the current climate

change? What would be the probable frequency and magnitude of such event in this region under the changing climate conditions?" In this way this study fills an important gap in our understanding of climate change impact on flood regime in this region. Furthermore, with more than three hundred reservoirs and dams in the Saguenay watershed, the study will have a significant implication by providing scientific basic and recommendations for future water resources systems management and planning in the region.

The general objective of this study is, therefore, to carry out an inter-comparison study of the most popular downscaling methods available for daily rainfall and temperature scenarios construction with that of the dynamic neural network downscaling technique. In other words, in addition to assessing the impact of global warming on flood trends and magnitude in the Saguenay region, the study will also provide a general framework for selecting appropriate precipitation and temperature downscaling model for future flood regime analysis anywhere in Canada. Therefore, the specific objectives of the study can be described as to:

- Evaluate stochastic and statistical downscaling methods for flood regime assessment in the Saguenay watershed;
- Develop dynamic neural network downscaling methods to improve daily rainfall and temperature scenarios generation;
- Assess the uncertainty associated with the downscaling techniques;
- Investigate the possible hydrological impact of climate change in Saguenay region based on the downscaled precipitation and temperature scenario data

Before going to the main tasks accomplished in the study, a brief preview of climate change and related impacts on water resources is provided in the next sections.

1.1. Climate change

Climate refers to the average, or typical, weather conditions observed over a long period of time for a given area; while weather is the condition of the atmosphere at any given place and time involving factors such as temperature, precipitation, direction and speed of wind, and the amount of water vapor in the air. The overall state of the global climate is determined by the balance of solar and terrestrial radiation budgets. How this energy balance is regulated depends upon the fluxes of energy, moisture, mass and momentum within the global climate system.

The climate system is made up of five components, the atmosphere, the oceans, the cryosphere, the biosphere and the geosphere. Arguably there is a sixth component, an anthropogenic system, man-kind. In the last 200 years, through increased utilization of the world's resources, humans have begun to influence the global climate system, primarily by increasing the Earth's natural greenhouse effect which is widely believed to cause climate change. Climate change, as defined in IPCC, refers to statistically significant variations that persist for an extended period, typically decades or longer. It includes shifts in the frequency and magnitude of sporadic weather events as well as the slow continuous rise in global mean surface temperature (IPCC 3rd report, 2001). The natural greenhouse

effect, in which certain gases in the atmosphere prevent some of the energy that otherwise goes from earth to space, has for millennia warmed the earth's surface (Bruce, et al, 2000). However, the earth's climate system has demonstrated unprecedented changes both in global and regional scales since the pre-industrial era, with some of these changes attributed to human activities. Emission of greenhouse gases and aerosols and their increasing concentration in the atmosphere continue to alter the atmosphere in ways that are expected to affect the climate. In terms of radiative forcing by greenhouse gases emitted through human activity, carbon dioxide (CO_2) and methane (CH_4) are the first and second most important, respectively. The increase in atmospheric CO_2 is nowadays widely believed to be caused mainly by fossil-fuel burning and land use change including deforestation. The increase in CH_4 can be identifies with emissions from energy use, livestock, rice agriculture, and landfill. Increase in concentration of other greenhouse gases such as tropospheric ozone (O_3) are also attributed to fossil-fuel combustion as well as other industrial and agricultural emissions.

An increasing number of observations gives a collective picture of a warming Earth and other changes in the climate system. The mean annual global surface temperature has increased by about 0.3 - 0.6^{o}C since the late 19th century and it is anticipated to further increase by 1–3.5°C over the next 100 years (IPCC, 1995). At the same time, changes in sea level, snow cover, ice extent, and precipitation are consistent with a warming climate near the Earth's surface. However, substantial differences are projected in regional changes in climate compared to the global mean change. All these changes are expected to continue under all IPCC emissions scenarios during the 21st century. As the climate system shifts to a new equilibrium, each of its components and sub-components will respond to the complex interaction of feedback loops. Climate impacts can therefore be expected to occur throughout the system. Some of the major impact areas identified (IPCC, 1990b) include agriculture, forestry, natural ecosystems, hydrology and water resources, human settlements and health, and oceans and coastal zones. Global-mean surface temperature increase, regional temperature increases, precipitation increases and decreases, soil moisture availability, climatic variability and the occurrence of extreme events such as hurricanes are all likely to influence the nature of these impacts.

1.2. Climate models

The Earth's climate results from interactions between many processes in the atmosphere, ocean, land surface and cryosphere. The interactions are complex and extensive (as shown in Figure 1), so that quantitative predictions of the impact on the climate of greenhouse gas increases cannot be made just through simple intuitive reasoning. For this reason, computer models have been developed which try to mathematically simulate the climate system, including the interactions between the system components. The models, however, must simplify what is a very complex climate system. This is in part due to the limited understanding of the climate system, and partly the result of computational restraints.

The basic laws and other relationships necessary to model the climate system are expressed as a series of equations. Simplification may be achieved in terms of spatial dimensionality, space and time resolution, or through parameterization of the processes that are simulated. The simplest models are

zero order in spatial dimension where the state of the climate system is defined by a single global average. Other models include an ever increasing dimensional complexity, from 1-D, 2-D and finally to 3-D models. Whatever the spatial dimension of a model, further simplification takes place in terms of spatial resolution. The time resolution of climate models varies substantially, from minutes to years depending on the nature of the models and the problem under investigation. Parameterisation involves the inclusion of a process as a simplified (sometimes semi-empirical) function rather than an explicit calculation from first principles. Sub-grid scale phenomena have to be parameterized as it is not possible to deal with these explicitly while other processes may be parameterized to reduce the amount of computation required. Once all the above specifications are set, solving the final equations is usually achieved with numerical techniques such as finite difference or finite element methods. Such models can be used to simulate climate on a variety of spatial and temporal scales. It is therefore important to consider the model resolution, in both time and space i.e. the time step of the model as well as the horizontal and vertical scales.

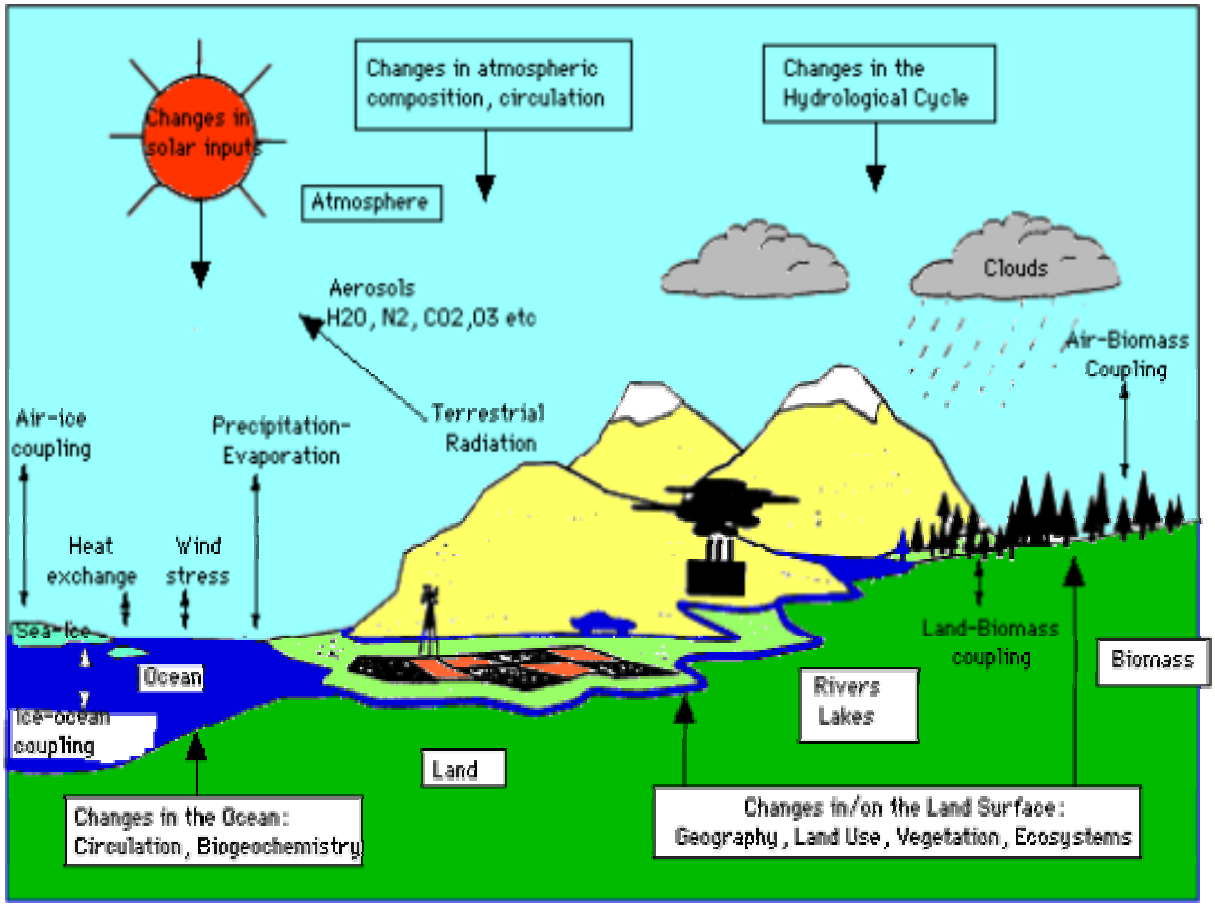

Figure 1: Schematic view of the processes and interactions in the global climate system (based on Fig 1.1 of the 1995 IPCC Science Assessment).

The ultimate purpose of a model is to identify the likely response of the climate system to a change in any of the parameters and processes which control the state of the system. The climate response occurs in order to restore equilibrium within the climate system. For example, the climate

system may be perturbed by the radiative forcing associated with an increase in carbon dioxide (a greenhouse gas) in the atmosphere. The aim of the model is then to assess how the climate system will respond to this perturbation, in an attempt to restore equilibrium.

The mathematical models generally used to simulate the present climate and project future climate with forcing by greenhouse gases and aerosols are generally referred to as GCMs (General Circulation Models or Global Climate Models). GCMs represent the most sophisticated attempt to simulate the climate system. The 3-D model formulation is based on the fundamental laws of physics consisting of: a) conservation of energy; b) conservation of momentum; c) conservation of mass; and d) the "Ideal Gas Law". These models typically divide the atmosphere and ocean into a horizontal grid with a horizontal resolution of 2° to 4° latitude and longitude, with 10 to 20 layers in the vertical. Such computer models numerically solve the fundamental equations for each atmospheric grid box, while taking into account the transfer of those quantities between grid boxes. They also consider, often in parameterized form, the physical processes within the boxes, including sources and sinks of these quantities. Since the models contain thousands of grid points, GCMs are computationally expensive. However, being 3-D, they can provide a reasonably accurate representation of the average planetary climate, and unlike simpler models, can simulate global and continental scale processes in detail (see Figure 2).

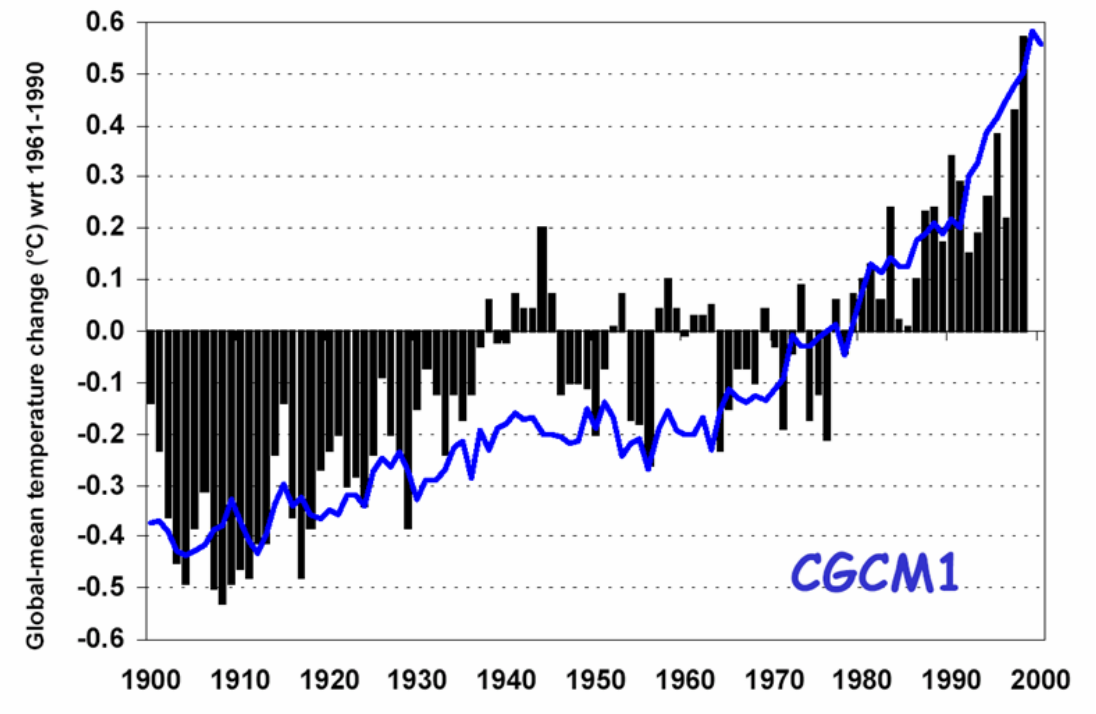

Figure 2: The global mean temperature change since 1900 as simulated by the Canadian climate model (CGCM1) forced with changes in natural and human-made factors (solid line), and compared with observations (bar chart).

Nevertheless, most GCMs are not able to simulate synoptic (regional) meteorological phenomena such as tropical storms, which play an important part in the latitudinal transfer of energy

and momentum. The spatial resolution of GCMs is also limited in the vertical dimension. Consequently, many boundary layer processes must be parameterized. Moreover, since the oceans have such a large heat capacity, and can transfer heat around the globe, it is vital to couple atmosphere and ocean models in order to simulate climate variability and changes. This has led to the development of coupled atmosphere ocean models. Over the past decade, the sophistication of such models has increased and their ability to simulate present and past climates has substantially improved. In general, GCMs can be considered to simulate reasonably accurately the global and continental-scale climate, but confidence is still lacking in its ability to simulate correctly the regional detail.

1.3. Hydrological impacts of climate change

Changes in global climate will have significant impacts on local hydrological regimes, which will consequently have ramification on ecological as well as social and economic systems. Some of these effects include changes in stream flows which support aquatic ecosystems, navigation, hydropower, irrigation systems, etc. There may also be a significant change in the frequency and severity of floods and droughts.

The projected global climate change in the coming century may have both beneficial and adverse environmental impact, but the larger the changes and the rate of change in climate, the more adverse effect predominate (IPCC, 2001). Moreover, relatively small climatic variations can create large changes in water resources, especially in arid and semi-arid regions. Consequently, watersheds where water resources are already stresses under current conditions are most likely to be highly vulnerable to these possible changes in mean climatic conditions and extreme events. In general, climate change is projected to reduce stream flow and groundwater recharge in many part of the world but to increase it in some other areas. The amount of change varies depending on the projected rainfall (especially rainfall intensity) and projected evaporation. However, the climatic impacts on hydrology at the regional scale are uncertain, and will be influenced by a complex mix of temperature, precipitation, evaporation, soil moisture availability and runoff changes. The effects of climate changes on water scarcity, water quality, and the frequency and intensity of floods and droughts is expected to increase the challenges for water and flood management in the 21st century. Therefore, the potential impacts of such variations in the future climate need to be taken into consideration by policy and decision makers when managing water resources and making plans for the future (Mehdi et al., 2002).

Among the most important projected impacts of the climate change scenarios on Canadian water resources are: declines in low seasonal river flows and lake levels and higher water temperature in most of southern Canada, decline in groundwater levels and quality in populated southern regions, greater frequency of high intensity rainfalls that would increase soil erosion, flash floods and storm sewer overflow (Bruce et al., 2000). Besides, annual flood peaks are expected to be lower in most regions but occasional very large floods are likely to occur in vulnerable river systems such as Fraser, Red, and tributaries of St. Lawrence (e.g. Saguenay). However, one of the challenges in hydrologic impact studies is the difficulty to draw a line between the one caused solely by climate change and the rest caused by any other activities different from climate change.

1.4. Downscaling Global Circulation Models outputs

The mathematical models used to simulate the present climate and project future climate with forcing by greenhouse gases and aerosols are generally referred to as General Circulation Models or Global Climate Models (GCMs). These global models are generally not designed for local climate change impact studies and do not permit a good estimation of hydrological responses to climate change at local or regional scale. While they demonstrated significant skill at the continental and hemispherical scales and incorporate a large proportion of the complexity of the global system, they are inherently unable to present local subgrid-scale features and dynamics (Wigley et al., 1990; Carter et al., 1994). Therefore, there is a need to couple GCM with hydrological model which will provide a framework in which to conceptualize and investigate the relationship between climate and water resources. In climate change impact studies, such hydrological model is usually required to simulate sub-grid scale phenomenon and therefore require input data (such as precipitation and temperature) at similar sub-grid scale. However, the spatial resolution of GCMs remains quite coarse, in the order of 300 x 300 km, and at that scale, the regional and local details of the climate which are influenced by spatial heterogeneities in the regional physiography are lost. GCMs are therefore inherently unable to represent local subgrid-scale features and dynamics, such as local topographical features and convective cloud processes. Therefore, there is the need to convert the GCM outputs into at least a reliable daily rainfall and temperature time series at the scale of the watershed to which the hydrological impact is going to be investigated. The methods used to convert GCM outputs into local meteorological variables required for reliable hydrological modeling are usually referred to as 'downscaling' techniques.

There are various downscaling techniques available to convert GCM outputs in to daily meteorological variables appropriate for hydrologic impact studies. However, it is not yet clear which method provides the most reliable estimates of daily rainfall and temperature for the future horizon. The most widely used statistical downscaling methods are the multiple linear regression and stochastic weather generation. However, the interest in nonlinear regression methods, namely, artificial neural networks (ANN), is nowadays increasing because of their high potential for complex, nonlinear and time-varying input-output mapping. Although the weights of an ANN are similar to nonlinear regression coefficients, the unique structure of the network and the non-linear transfer function associated with each hidden and output nodes allows ANNs to approximate highly nonlinear relationships. Moreover, while other regression techniques assume a functional form, ANNs allow the data to define the functional form. The simplest form of ANN (i.e. multilayer perceptron) is reported to give similar results compared to multiple regression downscaling methods (Schoof and Pryor, 2001). Furthermore, ANN model was found to account for some heavy rainfall events, while they were not identified by the linear regression downscaling technique (Weichert and Burger, 1998). More recently, Cannon and Whitfield (2002) found that an ensemble ANN downscaling model was capable of predicting changes in stream flows using only large-scale atmospheric conditions as model input. Nevertheless, some studies have also shown that standard ANN method commonly used for hydrologic variables modeling, is not well suited to temporal sequences processing, and often yields

sub-optimal solutions (Coulibaly et al. 2001a). There are, however, other categories of neural networks that have feedback connections and are thus inherently dynamic in nature. Dynamic neural networks (DANNs) are topologies designed to include time relationships explicitly in the input-output mappings and the application of feedback enables the networks to acquire *state* representations, which make them more suitable for complex nonlinear system modelling (Gautam and Holz, 2000).

This report attempts to highlight the applicability of dynamic artificial neural networks as downscaling methods for improving daily rainfall and temperature estimates. The study specifically focuses on DANNs such as time lagged feed-forward neural networks (TLFN) and different types of recurrent neural networks (RNN). In addition, emphasis is given to evaluating and comparing the optimal DANN method with the most commonly used stochastic and multiple regression-based downscaling methods. The best downscaling results are then used to evaluate the hydrologic impact of climate change on river flows in the Saguenay watershed in Northern Quebec, Canada. To simplify the presentation of investigated methods and their results, the remainder of the report is organized as follows. Section 2 provides an overview of the downscaling methods. In section 3, the topologies and learning algorithms of the DANN methods are introduced. Section 4 provides a brief description of the study area and the experiment data. In section 5, results from the downscaling experiment are reported and discussed. Section 6 presents the results of hydrological impact analysis. Section 7 summarizes the findings and provides some conclusions.

2. Downscaling Methods: An Overview

Spatial 'downscaling' is the means of relating the large scale atmospheric predictor variables to local or station-scale meteorological records. Such downscaled data could then be used as input to hydrological models to evaluate possible impacts of different climate change scenarios. There is a variety of downscaling techniques in the literature, but in practice two major approaches can be identified at the moment, namely, *dynamic downscaling* and *empirical (statistical) downscaling*.

2.1. Dynamic downscaling

Dynamic downscaling approach is a method of extracting local-scale information by developing and using limited-area models (LAMs) or regional climate models (RCMs) with the coarse GCM data used as boundary conditions. The basic steps are then to use the GCMs to simulate the response of the global circulation to large-scale forcing and the nested RCM to account for sub-GCM grid scale forcing such as complex topographical features and land cover heterogeneity in a physically-based way; and thus enhance the simulation of atmospheric circulations and climate variables at fine spatial scales. RCMs have recently been developed that can attain horizontal resolution in the order of tens of kilometers or less over selected areas of interest. Compared with GCMs, the resolution of these RCMs is much closer to that of distributed-parameter hydrological models and that even makes coupling of such models possible.

However, while RCMs are the most informative downscaling approach, they also have several limitations. RCMs still require considerable computational resources and they are as expensive to run as GCMs (Xu, 1999). Even though RCMs operate on some high-resolution grid point scales, the results will still be in the form of spatial averages. These models may not meet the needs of spatially explicit models of hydrological systems, and there may remain the need to downscale the results from such models to individual sites or localities for impact studies**.** Such site specific downscaling is usually done with relatively simpler empirical techniques as explained in the following section.

2.2. Empirical (statistical) downscaling

Empirical downscaling starts with the premise that the regional climate is the result of interplay of the overall atmospheric, or oceanic, circulation as well as of regional topography, land-sea distribution and land use. As such, empirical/ statistical downscaling seeks to derive the local scale information from the larger scale through inference from the cross-scale relationship using some random or deterministic functions. In most cases, the regional climate is seen as a random process conditioned upon a driving large-scale climate regime. Therefore, the confidence that may be placed in downscaled climate change information is foremost dependent on the validity of the large-scale fields from GCM. For instance, derived variables (not fundamental to the GCM physics, but derived from the physics) such as precipitation are usually not as robust information at the regional and local scale (Trigo and Palutikof, 1999). Conversely, tropospheric quantities like temperature or geopotential height are intrinsic parameters of the GCM physics and are more skilfully represented by GCMs.

Formally, the concept of regional climate being conditioned by the large-scale state may be written as:

$$R = F(L) \quad (1)$$

where R represents the predictand (a regional or local climate variable), L is the predictor (a set of large-scale climate variables), and F a deterministic/stochastic function conditioned by L and has to be found empirically from observation or modeled data sets.

When using downscaling for assessing regional climate change, three implicit assumptions are made (von Storch et al, 2000): (1) the predictors are variables of relevance and are realistically modeled by the GCM; (2) the predictors employed fully represent the climate change signal; and (3) the relationship is valid also under altered climate condition (which may not be provable). A diverse range of empirical/ statistical downscaling techniques have been developed over the past few years and each method generally lies in one of the three major categories, namely, regression (transfer function) methods, stochastic weather generators and weather typing schemes.

Regression downscaling techniques

Regression-based downscaling methods rely on direct quantitative relationship between the local scale climate variable (predictand) and the variables containing the larger scale climate information (predictors) through some form of regression. Individual downscaling schemes differ according to the choice of mathematical transfer function, predictor variables or statistical fitting procedure. To date, linear and non-linear regression, artificial neural networks, canonical correlation and principal component analysis have all been used to derive predictor-predictand relationships (Conway et al., 1996; Schubert and Henderson, 1997).

One of the well recognized statistical downscaling tools that implements a regression based method is the *Statistical Down-Scaling Model* (SDSM) (Wilby, et al., 2002). SDSM reduces the task of statistically downscaling daily weather series into a number of discrete processes such as (1) screening of potential downscaling predictor variables to identifies those large-scale predictor variables which are significantly correlated with observed station (predictand) data; (2) calibration of the model to determine model parameters which results in the best relationship between observed climate variables representing the current condition and the corresponding local metrological data; (3) validation of the models through synthesis of daily weather data using an independent data set of observed predictors as input; (4) generation of ensembles of future weather data using the validated model and GCM-derived predictor variables corresponding to future climate scenario; and (5) diagnostic testing/analysis of data by calculating the statistical characteristics of both the observed and synthetic data for further comparison. In this study, the SDSM is used as a benchmark model as it appears one the most widely used for precipitation and temperature downscaling.

In general, the main appeal of regression-based downscaling is the relative ease of their application. However, these models often explain only a fraction of the observed climate variability (especially when the predictand is precipitation). Downscaling future extreme events using

regression-based models may also be problematic since these phenomena usually tend to lie at the margins or beyond the range of the calibration data set (Wilby, et al, 2002).

Stochastic weather generators

Weather generators are statistical models of observed sequences of weather variables. They can also be regarded as complex random number generators, the output of which resembles daily weather data at a particular location. There are two fundamental types of daily weather generators, based on the approach to modeling daily precipitation occurrence: the Markov chain approach (Hughes et al., 1999) and the spell-length approach (Wilks, 1999). In the Markov chain approach, a random process is constructed which determines a day at a station as rainy or dry, conditional upon the state of the previous day, following given probabilities. If a day is determined as rainy, then the amount is drawn from yet another probability distribution. In case of spell-length approach, instead of simulating rainfall occurrences day by day, spell-length models operate by fitting probability distribution to observed relative frequencies of wet and dry spell lengths. In either case, the statistical parameters extracted from observed data are used along with some random components to generate a similar time series of any length. In stochastic downscaling, the parameters of the weather generator are conditioned upon a large-scale state, or the relationships between daily weather generator parameters and climatic averages can be used to characterize the nature of future daily statistics on the basis of more readily available time-averaged climate-change information (Wilks and Wilby, 1999). The resulting weather generator models are then used to simulate daily series of indefinite lengths representative of the altered climate.

One well known stochastic downscaling tools is the stochastic weather generator called *Long Ashton Research Station Weather Generator* (LARS-WG) (Semenov and Barrow, 1997, 2002). LARS-WG can be used for the simulation of weather data at a single site under both current and future climate conditions. This weather generator consists of three main steps. The first step in the weather generation process is the *analysis* of the observed station data in order to calculate the weather generator parameters, i.e., the statistical characteristics of the data. The analysis process uses semi-empirical distributions, i.e., frequency distributions calculated from the observed data, for wet and dry series duration, precipitation amount etc. The resulting parameter file is then used in the generation process. Then, LARS-WG *generates* synthetic weather data by combining a scenario file, containing information about changes in precipitation amount, wet and dry series duration, mean temperature and temperature variability, with the parameter files generated in the first step. If LARS-WG is being used to generate synthetic data in order to determine how well the model is simulating observed conditions, then the scenario file contains no changes. However, if LARS-WG is being used to generate daily data for a particular scenario of climate change, then the scenario file will contain the appropriate monthly changes in the different statistical parameters such as mean value and variability of the time series to be estimated. The scenario files are prepared based on the relative changes in statistical parameters calculated from the GCM outputs representing the different scenarios corresponding to future time periods. Finally, LARS-WG simplifies the procedure for

determining how well it is simulating observed conditions by providing the *Qtest* option. In this step, the statistical characteristics of the observed data are compared with those of synthetic data generated using the parameters derived from the observed station data. The LARS-WG is used herein as the second benchmark downscaling model.

Weather typing schemes

Weather typing approaches involve grouping local, meteorological variables in relation to different classes of atmospheric circulation. Future regional climate scenarios are constructed, either by resampling from the observed variable distribution (conditional on the circulation patterns produced by a GCM), or by first generating synthetic sequences of weather pattern using Monte Carlo techniques and resampling from the generated data. The mean, or frequency, distribution of the local climate is then derived by weighting the local climate states with the relative frequencies of the weather classes. Climate change is then estimated by determining the change of the frequency of weather classes. However weather typing are inadequate basis for simulating rare or extreme events, and entirely dependent on stationary circulation-to-surface climate relationships. Potentially the most serious limitation is that precipitation changes produced by changes in the frequency of weather patterns are seldom consistent with the changes produced by the host GCM unless additional predictors such as atmospheric humidity are employed (Wilby et al., 2002).

A more detailed review of exciting downscaling methods a preliminary investigation of their relative performance can be found on the first progress report (Dibike & Coulibaly, 2003).

3. Dynamic Artificial Neural Network (DANN) Downscaling Method

A neural network can, in general, be characterized by its architecture, which is represented by the pattern of connections between the nodes, its method of determining the connection weights, and the activation or transfer functions that it employs. As a result, ANNs constitute a diverse family of networks whereby the functionality of each type of network is determined by the network topology, the individual neural network characteristics, and the learning or training strategy employed. Within the last decade, the study of artificial neural networks has experienced a huge resurgence due to the development of more sophisticated algorithms and the emergence of powerful computational tools (ASCE, 2000a). Multilayer perceptrons (MLPs), which constitute probably the most widely used network architecture, are composed of a hierarchy of processing units organized in a series of two or more mutually exclusive sets of neurons or layers. The information flow in the network is restricted to a flow, layer by layer, from the input to the output, hence also called feedforward network. While feedforward neural networks are popular in many application areas, they lack the temporal delays and/or the feedback connections necessary to provide a dynamic model. There are, however, more recent explorations of neural networks that have either time delays or feedback connections and are thus inherently dynamic in nature.

In temporal problems, the measurements from a given system are no longer a set of independent elements, but functions of time. A single sensor produces a sequence of measurements that are linked by an order relation, defining the signal time structure. If one changes the order of the samples, one may be distorting the time signal, and changing its frequency content, so sample order should be preserved in temporal processing (Principe et al., 2000). To exploit the signal time structure, the neural network must have access to the time dimension. Since natural systems are mostly causal, the search is restricted to the past of the signal. Physical structures that store the past of a signal are called *short-term memories*, or simply *memory structures* and it is now possible to incorporate memory structures into a neural network.

There are different ways of introducing ‘memory’ in a neural network in order to develop a dynamic neural network. *Time lagged feedforward networks* (TLFN) and *Recurrent networks* (RNN) are the two major groups of candidate dynamic neural networks mostly used in time series analysis (Dibike et al. 1999; Coulibaly et al. 2001a,b).

3.1. Time-Lagged Feedforward Networks (TLFN)

A dynamic neural network can be formulated by replacing the neurons of a multilayer perceptron (MLP) with a memory structure, which is sometimes called a *tap delay line*. If the memory structure is incorporated only with the input neurons, then it is called focused time lagged feedforward neural network (TLFN). The size of the memory layer (the tap delay) depends on the number of past samples that are needed to describe the input characteristics in time and it has to be determined on a case-by-case basis. TLFN uses *delay-line* processing elements (PE) which implements memory by delay, that is, by simply holding past samples of the input signal as shown in Figure 3.

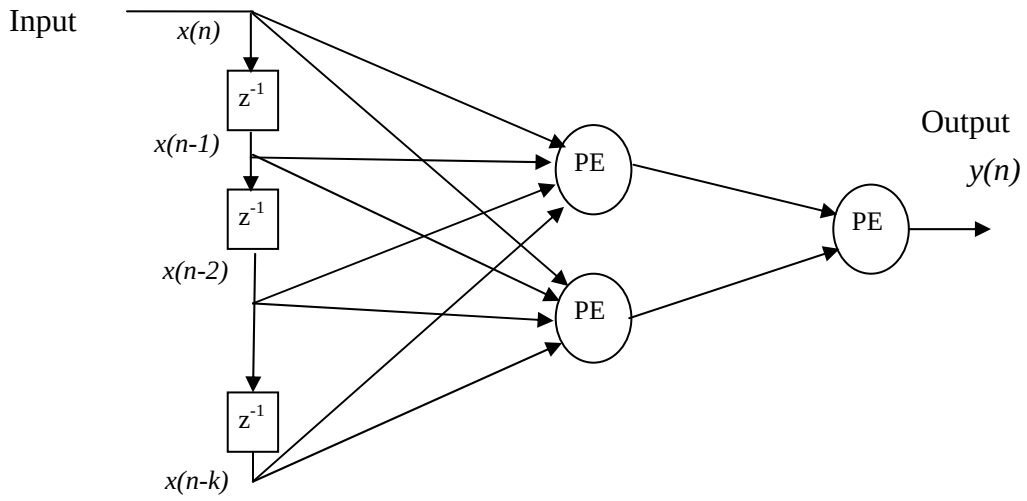

Figure 3. A focused TLFN with one input variable, one hidden layer and a tap delay line with $k + 1$ taps

The output of TLFN network with one hidden layer is given by:

$$y(n) = \varphi_1\left(\sum_{j=1}^{m} w_j y_j(n) + b_0\right) = \varphi_1\left(\sum_{j=1}^{m} w_j \varphi_2\left(\sum_{l=0}^{k} w_j(l)x(n-l) + b_j\right) + b_0\right) \quad (2)$$

where m is the size of the hidden layer, w_j are the weights in the network and φ_1 and φ_2 are transfer functions at the output and hidden layers respectively. For the case of multiple inputs (of size p), the delay-line with a memory depth k can be represented by:

$$\begin{aligned} (n) &= \left[x(n), x(n-1), ..., x(n-k+1)\right] \\ x(n) &= \sum_{j=1}^{p} x_j(n) \end{aligned} \quad (3)$$

where $x(n)$ represents the input pattern at time step n, $x_j(n)$ is an individual input at the n^{th} time step and $\boldsymbol{x}(n)$ is the combined input to the processing elements at time step n. Such delay-line only "remembers" k samples in the past.

An interesting feature of the TLFN is that the tap delay line at the input does not have any free parameters; therefore the network can still be trained with the classical backpropagation algorithm. The TLFN topology has been successfully used in nonlinear system identification, time series prediction (Coulibaly et al. 2001b), and temporal pattern recognition (Principe et al., 2000). However, a more flexible memory depth can be achieved by implementing *memory by feedback* where $x(n)$ in Equation 3 is represented as

$$x(n) = (1-\mu)x(n-1) + \mu\left(\sum_{j=1}^{p} x_j(n)\right) + b \qquad (4)$$

where (1-μ) is the feedback parameter. The memory depth of the PE can be controlled by changing the parameter μ instead of the whole network topology. Such types of networks are referred to as Gamma memory neural networks (GMN) and when μ = 1, the GMN becomes TLFN.

3.2. Recurrent Neural Networks (RNN)

Recurrent neural networks are composed of networks with feedback connections among some or all neurons which form closed loops in the network topology. The architectural layout of a recurrent network takes many different forms. However, the popular way to recognize (and ultimately to reproduce) sequences has been to use partially recurrent networks. In this case, the network connections are mainly feedforward, but include a carefully chosen set of feedback connections. The introduction of recurrence allows the network to remember relevant temporal patterns from the recent past, while at the same time not significantly complicating the network training. Simple recurrent networks like Jordan networks (Jordan, 1986) and Elman networks (Elman, 1990), are primarily feedforward structures with additional feedback loops for implementing the dynamics. The specific group of units which receive feedback signals from the values already obtained at the previous time steps are known as *context units* and they form a *context layer*. Elman's context layer receives input from the hidden layer, while Jordan's context layer receives input from the output layer. Both Jordan and Elman networks (see Figure 4) have fixed feedback parameters and there is no recurrency in the input-output path; therefore, they can be approximately trained with a backpropagation algorithm.

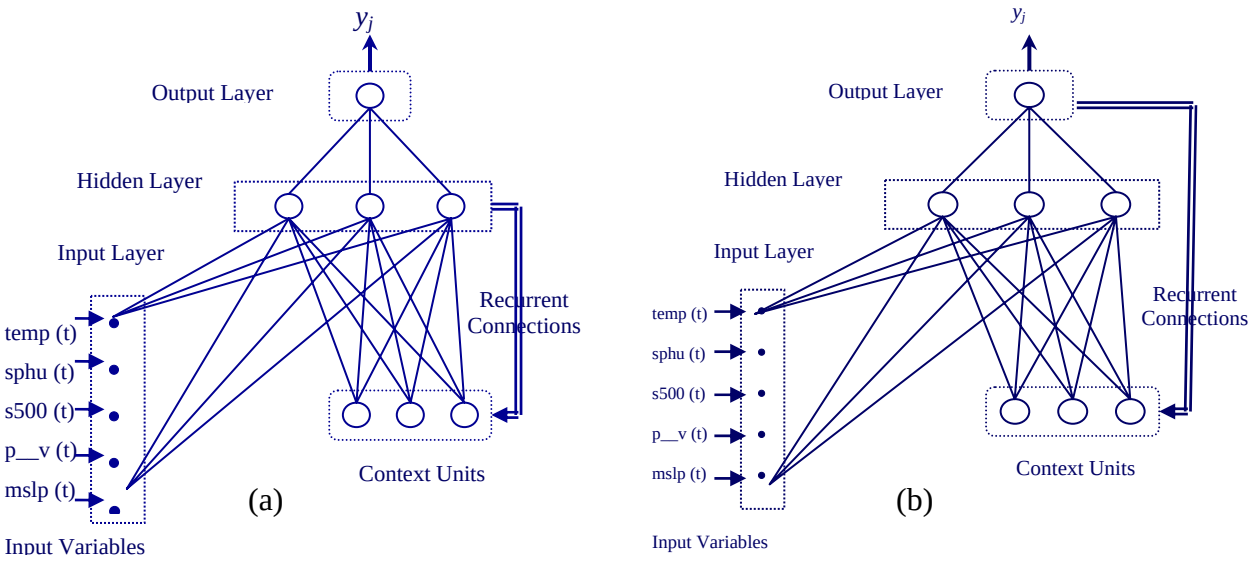

Figure 4. (a) Elman (a) and (b) Jordan Recurrent Neural Networks with their feedback connections.

In general, if the present value of the model input is denoted by *x(n)*, and the corresponding value of the model output by *y(n+1)*, then the dynamic behaviour of a generic recurrent network is described by

$$y(n+1) = F(y(n), y(n-1),..., y(n-k+1), x(n), x(n-1),..., x(n-k+1)) \quad (5)$$

where *F* represent the functional form of the recurrent network. Such recurrent networks are sometimes referred to as a *nonlinear autoregressive with exogenous inputs (NARX) models* (Haykin, 1999).

The other type of recurrent network that is identified by a hidden layer that feeds back upon itself using adaptable weights is referred to as *fully recurrent network*. On the other hand, *partially recurrent networks* (PRN) start with a fully recurrent net and add a feed-forward connection that bypasses the recurrency, effectively treating the recurrent part as a state memory. These types of recurrent networks can have an infinite memory depth and thus find relationships through time as well as through the instantaneous input space.

The fundamental difference between the adaptation of the weights in static and recurrent networks is that only in the latter the local gradients depend on the time index. Therefore, recurrent networks may also employ different types of learning methods, such as backpropagation through time (BPTT) (Williams and Zipser, 1995). In BPTT, the goal is to compute the gradient over the training set trajectory. Since the gradient decomposes over time, this can be achieved by computing the instantaneous gradients and summing the effect over time. During BPTT the activation is sent through the network and each processing element stores its activation locally for the entire length of the trajectory. At each time step the network output is also computed and stored. At the end of the trajectory, the errors are generated at the output and a vector of errors is used to update the network weights.

4. Study Area and Data

The study area selected in this research project for the application of downscaling methods and evaluation of hydrologic impact of climate change is the Saguenay–Lac-Saint-Jean (SLSJ) hydrologic system in northern Quebec (see Figure 5). The total area of the river system is about 73,800 square kilometres and it extends between 70.5^o to 74.3^o West and between 47.3^o to 52.2^o North. Saguenay is a well known flood prone area as many Canadians still remember the year-1996 flood of this river. During the period of July 19-21, 1996, a rapidly developing low pressure system with a sea level pressure drop of 20 mb in 24 hours produced heavy rainfall over the Saguenay basin in Quebec. The average precipitation over this period was about 200 mm over an area of 5000 square kilometers. This resulted in the collapse of the dikes at lakes Kénogami and Ha!Ha!. The ensuing floods caused severe damage to eight communities downstream of these lakes, leading to seven deaths and property damage (Yu et al, 1997).

Observed daily data of large-scale predictor variables representing the current climate condition is derived from the national centre for environmental prediction (NCEP) reanalysis data set (Kistler, et al, 2001). The GCM output used for this study is the result of the IPCC "IS92a" forcing scenario in which the change in greenhouse gases (GHG) forcing corresponds to that observed from 1900 to 1990 and increases at a rate 1% per year thereafter until year 2100. The direct effect of sulphate aerosols (A) is also included. This climate change condition corresponds to the so called 'business as usual' scenario and the corresponding data for the study area is extracted from the Canadian Global Climate Model (CGCM1) outputs at the grid point 50^oN, 71^oW. This is the closest grid point to the study area where CGCM1 output is available. The CGCM1 data set consist of large-scale predictor variables listed in Table 1. All predictors in this data set, with the exception of wind direction, have been normalized with respect to the 1961-1990 mean and standard deviation and were made available by the Canadian Climate Impacts Scenarios (CCIS) project. The data is divided into four distinct periods, namely, the current (covering the forty years period between 1961 and 2000), the 2020s (2010-2039), the 2050s (2040-2069) and the 2080s (2070-2099) to facilitate trend analysis.

Moreover, observed (historical) precipitation and temperature data at thirteen metrological stations and stream flow data from eleven hydrometric stations distributed over the watershed (see Table 2 and 3) are used in this research. The observed and downscaled precipitation and temperature data at these stations are used in the modelling and analysis of hydrologic impact of the anticipated climate change in the watershed. However, the downscaling exercise at one of the stations located near Chute-du-Diable (station ID 7061560 located at 48.75^o N and 71.7^o W) is considered for a more in-depth analysis of the downscaling model performances and reporting. The station has forty years of daily precipitation and temperature records representing the current climate (1961 till 2000).

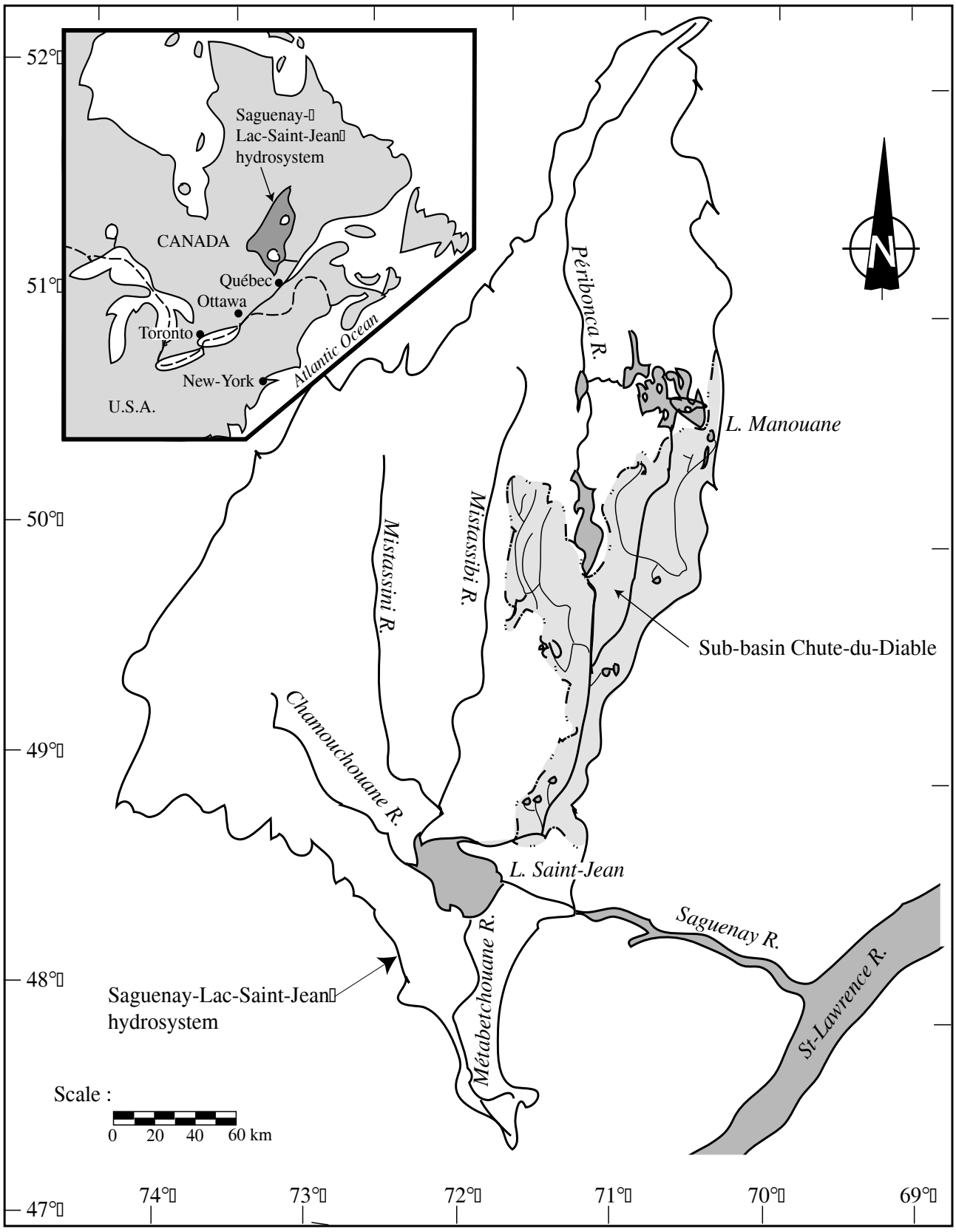

Figure 5: Location map of the Saguenay–Lac-Saint-Jean watershed and the sub-basin Chute-du-Diable

Table 1. Large-scale predictor variables obtained from CGCM1 outputs

Daily variable	Description
temp	Mean temperature
mslp	Mean sea level pressure
p500	500 hPa geopotential height
p850	850 hPa geopotential height
rhum	Near surface relative humidity
shum	Near surface specific humidity
s500	Specific humidity at 500 hPa height
s850	Specific humidity at 850 hPa height
**_f	Geostrophic airflow velocity
**_z	Vorticity
**_u	Zonal velocity component
**_v	Meridional velocity component
**th	Wind direction
**zh	Divergence

** indicates p_, p5 or p8 which represent the variable values near surface, at 500 hPa height or 850 hPa height, respectively. All predictors, with the exception of wind direction, have been normalized with respect to the 1961-1990 mean and standard deviation.

Table 2. Metrological stations where observed precipitation and temperature data are used for the downscaling and hydrological modeling exercise

Meteorological Station Name	Station Location (in degrees)		
	Latitude	Longitude	Altitude (m)
Bagot	48.3	71.0	159
Benoit	51.53	71.1	549
Bonard	50.7	71.0	506
Chute-Du-Diable	48.75	71.7	174
Chute-Des-Passes	49.9	71.25	399
Chiba	49.8	74.5	387
Cygnes	49.9	72.9	405
Long	50.5	72.95	468
Machisque	50.9	71.8	543
Metabetchouan	48.4	71.96	220
Mistassibi 2	49.4	71.9	183
Normandin	48.83	72.55	137
Roberval	48.5	72.27	179

Table 3. Hydrometric stations where observed river flow data are used for the hydrological modeling and impact analysis

Hydrometric Station	**Station Location (in degrees)**		
Name	Latitude	Longitude	Altitude (m)
Metabetchouan	48.38	71.99	220
Ashuapmushuan aval	48.69	72.49	111
Ashuapmushuan amont	49.28	73.36	305
Mistassini	48.89	72.26	117
Mistassibi	48.90	72.21	116
Petite Péribonca	48.81	72.05	104
Serpent	49.69	71.37	305
Manouane	49.88	70.93	241
Blanches_2	51.01	70.70	498
Mistassini_2	49.95	72.72	265
Mistassibi_3	49.85	72.08	-

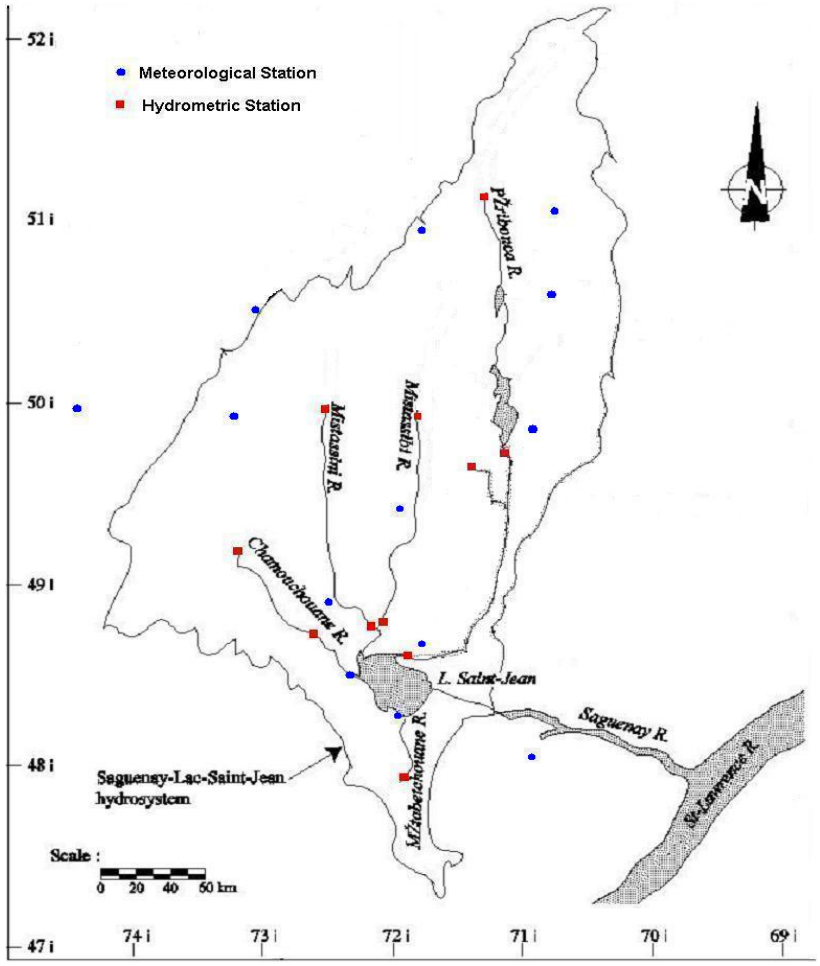

Figure 5b: Location map of the metrological and hydrometric stations in the Saguenay–Lac-Saint-Jean watershed

5. Downscaling Daily Precipitation and Temperature

Daily total precipitation (solid and liquid) as well as daily maximum and minimum temperature data were the predictand variables considered for the downscaling experiments. From the forty years of observed data representing the *current* climate, the first 30 years (1961-1990) are considered for calibrating the downscaling models while the remaining ten years of data (1991-2000) are used to validate those models. The different parameters of each model are adjusted during calibration to get the best statistical agreement between observed and simulated meteorological variables. During the calibration of precipitation downscaling models, in addition to the mean daily precipitation and daily precipitation variability for each month, monthly average dry and wet-spell lengths constituted the performance criteria. For the cases of Tmax and Tmin, mean and standard deviation of these variables corresponding to each month were considered as performance criteria.

The downscaling experiment was conducted with the two statistical (SDSM and LARS-WG) and the three types of dynamic neural network methods (TLFN, Elman, Jordan) presented in sections 2 and 3. For SDSM and all DANNs, selecting the most relevant predictor variables is the first and important task in the downscaling process. This step is not required for LARS-WG since stochastic downscaling depends only on the precipitation and temperature values simulated by the GCM. In the case of SDSM, the task of screening the most relevant predictor variables is achieved with linear correlation analysis and scatter plots (between the *predictors* and the *predictand* variables). Observed daily data of large-scale *predictor* variables representing the current climate condition (derived from the NCEP reanalysis data set) is used to investigate the percentage of variance explained by each *predictand-predictor* pairs. In general, the correlation between the predictor variables and each predictand is very low in case of precipitation compared to that of maximum and minimum temperature. Moreover, the strength of individual *predictors* varies on a month by month basis; therefore, the most appropriate combination of *predictors* has to be chosen by looking at the analysis output of all the twelve months. However, the final choice is made by considering whether the identified variables and relationships are physically sensible for the particular experiment and study site. A step by step procedure for screening predictor valuables with SDSM can be found in the first progress report (Dibike & Coulibaly, 2003).

A slightly different approach is used for the case of DANN. First the networks are trained with all (the twenty two) predictor variables as input to the networks. Then a sensitivity analysis is done to determine the most relevant predictors which need to be selected for further retraining. Sensitivity analysis provides a measure of the relative importance among the predictors (inputs of the neural network) by calculating how the model output varies in response to variation of an input. The network learning is disabled during this operation such that the network weights are not affected. The basic idea of sensitivity analysis is that the inputs to the neural network are shifted slightly and the corresponding change in the output is reported. Each input is varied between its mean +/- standard deviation while all other inputs are fixed at their respective means. The network output is then computed for a specified number of above and below the mean. This process is repeated for each

input. The sensitivity is calculated by dividing the standard deviation of the output by the standard deviation of the input which was varied to create the output. The results of such analysis in downscaling precipitation with TLFN are plotted in Figures 6 for the Chute-du-Diable stations. Eight of the most relevant predictor variables are selected for each neural network by identifying those to which the network is found to be more *sensitive*. The neural network is then retrained with the few selected predictor variables till acceptable validation performance is achieved. The predictor variables identified for simulating daily precipitation as well as daily maximum and minimum temperature at Chute-du-Diable stations with the different downscaling techniques are summarized in Table 4a,b&c. Similar procedures were followed to identify the predictor variables for downscaling precipitation and temperature data at the remaining twelve meteorological stations. The results show that, even though the set of variables selected as most relevant to each of the downscaling methods is not identical, some large scale predictor variables such as *s500* (specific humidity at 500 hPa height) or *s850* (specific humidity at 850 hPa height), *p_v* (meridional wind velocity component at different levels), *p850* (850 hPa geopotential height), temp (mean surface temperature) and *shum* (near surface specific humidity) are found to be most relevant predictors in most of the cases. Each set of selected predictor variables are then used to calibrate and validate the corresponding dynamic neural network downscaling method.

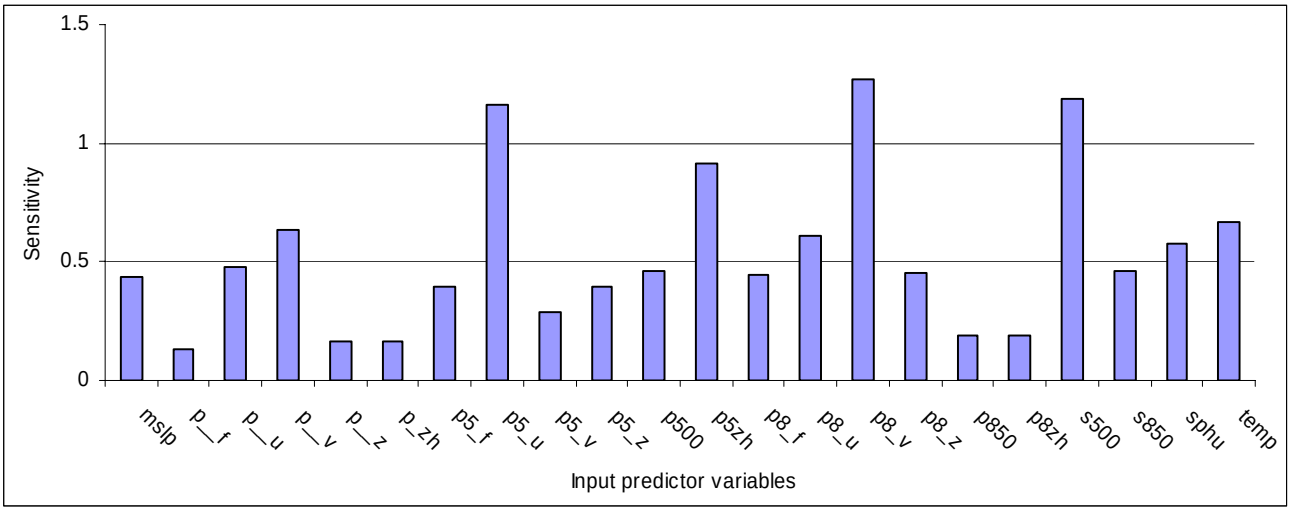

Figure 6. Sensitivity of a TLFN (in downscaling precipitation at Chute-du-Diable) to each of the predictor variables used as input to the network.

Table 4a. Large scale predictor variables selected for predicting daily precipitation at Chute-du-Diable with different downscaling methods.

CD_Prec	temp	mslp	p500	p850	sphu	s500	p__u	p5_u	p8_u	p__v	p8_v	p_zh	p5zh	p8zh
SDSM	x					x				x	x			x
TDN	x				x	x		x	x	x	x		x	
Elman	x	x		x	x	x	x	x			x			
Jordan	x	x	x	x	x			x		x	x			

Table 4b. Large scale predictor variables selected for predicting daily maximum temperature at Chute-du-Diable with different downscaling methods.

Cd_Tmax	temp	mslp	p500	p850	sphu	s500	s850	p__z	p8_u	p__u	p__v
SDSM	x		x		x	x	x				x
TDN	x	x		x	x		x	x		x	x
Elman	x		x		x	x	x	x	x	x	
Jordan	x	x		x	x		x		x	x	x

Table 4c. Large scale predictor variables selected for predicting daily minimum temperature at Chute-du-Diable with different downscaling methods.

Cd_Tmin	temp	mslp	p500	p850	sphu	s850	p__z	p__v	p_zh	p8zh
SDSM	x		x		x	x	x	x		
TDN	x	x		x		x	x	x	x	x
Elman	x	x	x	x	x	x		x	x	
Jordan	x	x	x	x	x		x		x	x

5.1. Downscaling models validation results

As explained earlier, from the forty years of data representing the *current* climate, the first 30 years (1961-1990) are considered for calibrating the downscaling models while the remaining ten years of data (1991-2000) are used to validate those models. In downscaling daily maximum and minimum temperature values, all the downscaling methods showed acceptable performance on the validation data sets. However, the validation result in downscaling precipitation data is that, while all of the downscaling models estimate the mean monthly precipitation quite well, only the two statistical methods (SDSM and LARS) and one of the DANN method (TLFN) resulted in a satisfactory performance in terms of good agreements in the other monthly precipitation statistics (such as standard deviations and average wet and dry-spell lengths) between the observed and simulated values. The performances of the other DANN methods, namely the Elman and Jordan networks were not satisfactory. For the sake of visual comparison, the validation performance of SDSM, TLFN and Elman network in downscaling the precipitation and temperature data at the Chute-du-Diable station is presented in Figure 7 and 8 respectively. The bar charts in these figures clearly show the difference in performance between these methods in terms of average monthly statistics of the observed and downscaled precipitation and temperature data. Similar results corresponding to the other downscaling methods are presented in Annex A. Therefore, the TLFN will be the only DANN model considered for further analysis herein. Thus, further discussion in this report will mainly be based on the results of the three successful downscaling models, namely SDSM, LARS and TLFN (referred to as the optimal DANN model at this stage).

The differences (or residuals) between the observed and simulated values corresponding to downscaling of daily precipitation as well as daily maximum and minimum temperatures are provided in Table 5. Specifically, the residuals shown in Table 5 are differences between mean daily values corresponding to each month for the validation period (1991-2000). Amongst the three downscaling methods, LARS-WG reproduces the wet and dry-spell lengths of precipitation better

than that of SDSM and DANN. While SDSM has under-estimated the wet-spell length through out the year, DANN has most of the time overestimated these values. In downscaling maximum and minimum temperature, the performance of all the three methods is very good. However, LARS-WG slightly overestimates the daily minimum temperatures for some months while it underestimates the same for the remaining months of the year. Seasonal analysis of the validation results (presented in Table 6) also shows that, the DANN has consistently resulted in lower root mean square error (RMSE) in simulating precipitation for each of the four seasons. While all the three methods demonstrated good performance in downscaling temperature values, SDSM and DANN resulted in lower RMSE than LARS-WG. However, the higher RMSE statistics for LARS-WG does not necessarily imply very poor performance because of the inherent stochasticity introduced in this method.

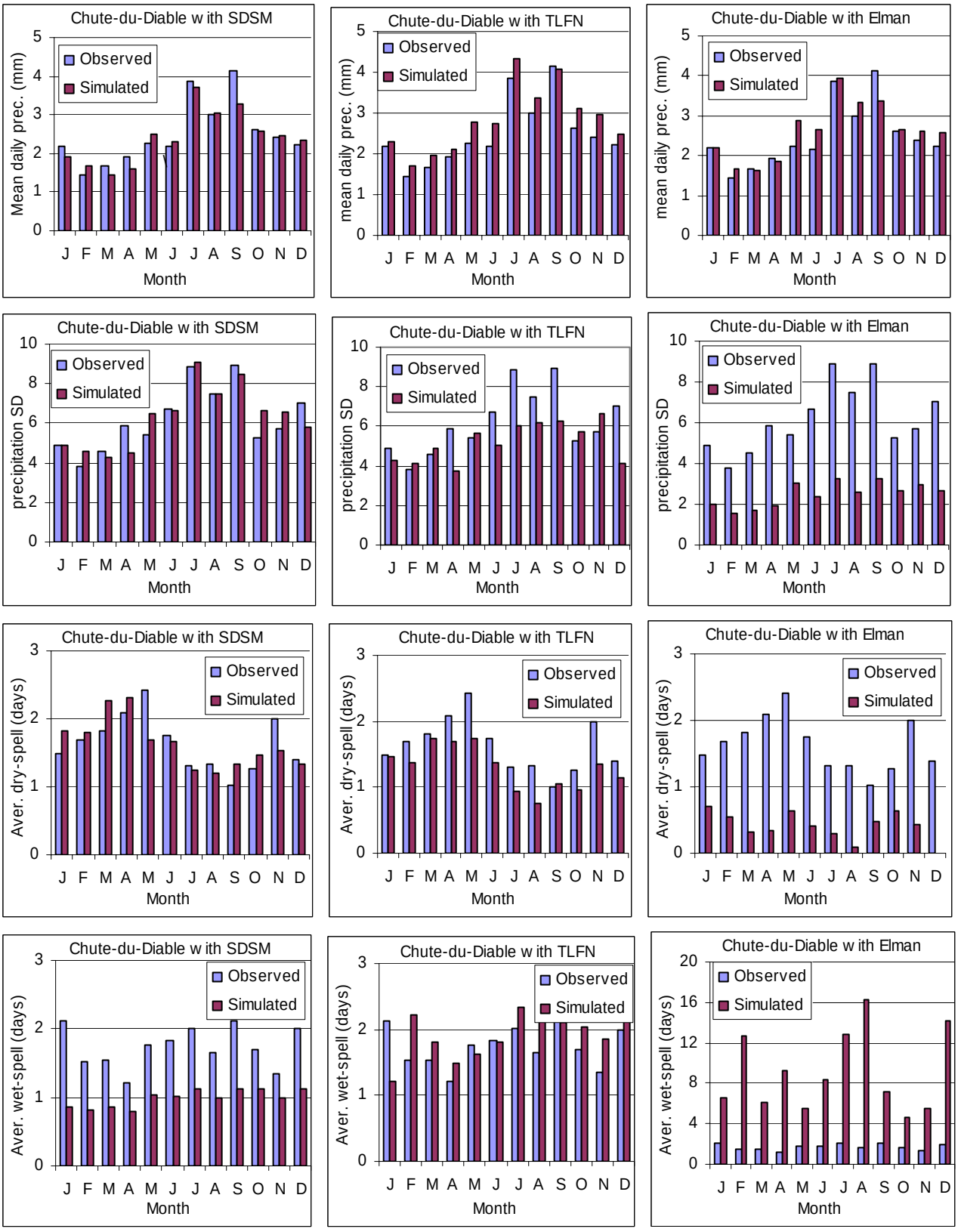

Figure 7. Validation performances of the three downscaling methods (SDSM, TLFN & Elman) in downscaling daily precipitation data at Chute-du-Diable

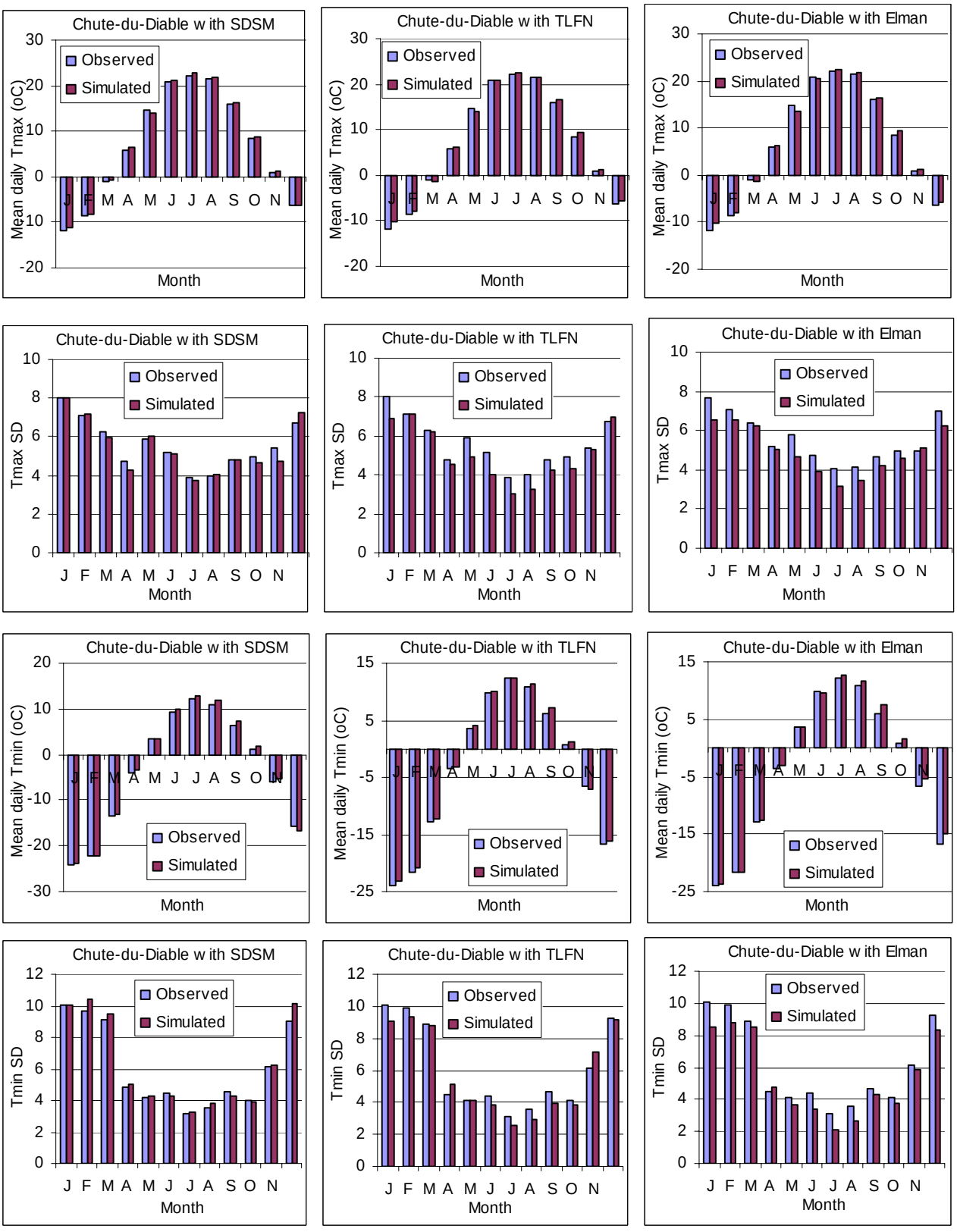

Figure 8. Validation performances of the three downscaling methods (SDSM, TLFN & Elman) in downscaling daily maximum and minimum temperature data at the Chute-du-Diable

Diable for the validation period (1991-2000)

	Mean daily precipitation (mm)			Mean Wet-Spell length (days)			Mean Dry-spell length (days)			Mean daily Tmax (°C)		
	SDSM	LARS	DANN	SDSM	LARS	DANN	SDSM	LARS	DANN	SDSM	LARS	DANN
January	-0.29	-0.14	-0.58	-1.26	0.02	-0.97	0.33	-0.03	0	0.8	0.5	0.88
February	0.24	-0.07	0.45	-0.70	-0.02	0.23	0.12	-0.12	-0.56	0.2	-0.1	0.82
March	-0.23	-0.05	0.32	-0.69	0.00	0.75	0.45	-0.05	-0.58	0.4	-0.3	-0.22
April	-0.33	-0.10	-0.42	-0.42	0.07	-0.04	0.22	-0.05	-0.79	0.6	0.1	0.21
May	0.26	-0.14	0.62	-0.72	0.02	-0.34	-0.74	-0.01	-0.85	-0.6	-0.4	-0.74
June	0.15	0.10	0.04	-0.82	0.06	0.23	-0.09	-0.01	-0.97	0.4	-0.3	-0.01
July	-0.16	0.09	0.93	-0.90	0.11	1.38	-0.07	-0.03	-0.38	0.6	0.1	0.22
August	0.03	0.01	0.64	-0.66	0.05	1.46	-0.12	0.02	-0.8	0.4	-0.6	-0.03
September	-0.86	-0.07	-0.36	-1.00	-0.01	0.4	0.32	-0.04	-0.08	0.2	-0.1	0.48
October	-0.05	-0.15	0.85	-0.57	0.04	0.25	0.20	0.03	-0.48	0.4	0.2	0.93
November	0.06	-0.10	0.96	-0.35	-0.05	0.01	-0.47	-0.06	-0.66	0.4	-0.3	0.36
December	0.14	-0.14	0.59	-0.87	-0.11	1.24	-0.05	-0.09	-0.66	0.0	0.6	0.9

Table 6. Downscaling model validation *RMSE* seasonal statistics of meteorological data at Chute-du-Diable

		Seasons			
Predictands	**Models**	Winter	Spring	Summer	Autumn
P (mm)	SDSM	38.96	67.68	74.57	68.85
	LARS	45.01	47.67	70.71	63.19
	DANN	55.62	33.47	42.71	81.94
Tmax (°C)	SDSM	0.93	1.34	0.83	0.87
	LARS	2.26	1.58	1.59	1.85
	DANN	1.08	1.36	0.67	0.94
Tmin (°C)	SDSM	1.52	1.02	0.90	0.98
	LARS	2.69	1.00	1.09	1.36
	DANN	1.42	0.96	0.42	0.30

5.2. Downscaling GCM outputs corresponding to a climate change scenario

Once the downscaling models have been calibrated and validated, the next step is to use these models to downscale the future climate change scenario simulated by the GCM. In this case, this means, the selected large-scale predictor variables to be used as input to each of the downscaling models are taken from CGCM1 simulation output. This data covers the four distinct periods (Current, 2020s, 2050s and 2080s) corresponding to the 'business as usual' scenario explained is section 4. The monthly statistics of the DANN downscaling results for daily precipitation as well as daily maximum and minimum temperature data corresponding to the two meteorological stations are summarized and plotted in Figures 9. Similar plots corresponding to the SDSM and LARS-WG downscaling techniques can be found in Annex B. Table 7 summarizes the comparative downscaling results of the three methods by presenting the average changes (increase or decrease) between the current condition and each simulation periods.

The DANN downscaling results in Figures 9 indicate an increasing trend both in the mean daily precipitation and precipitation variability at each station. However, the plots show no significant trend for the average wet and dry-spell length. The figures also show consistent increasing trend both in the Tmax and Tmin values for all months of the year. Once again, no significant trend is observed when it comes to the variability of monthly Tmax and Tmin values. Similar results are observed with the precipitation and temperature data downscaled with SDSM. However, the increase in precipitation corresponding to SDSM is much higher than that of DANN (see Table 7). Downscaling with LARS-WG, on the other hand, resulted in no significant increasing trend in the future precipitation while the increases in temperature are similar to those predicted with the other two methods.

Table 7. Changes in annual average values at Chute-du-Diable from the current condition as predicted by the different downscaling models

	Average Increase / Decrease								
	Precipitation (%)			Tmax (^{o}C)			Tmin (^{o}C)		
	SDSM	LARS	DANN	SDSM	LARS	DANN	SDSM	LARS	DANN
2020s	10.8	0.56	4.45	1.3	1.23	1.09	1.3	1.23	1.47
2050s	16.7	1.01	1.84	2.5	2.40	2.27	2.5	2.40	2.82
2080s	31.7	0.40	16.02	4.5	4.22	4.51	4.4	4.22	5.20

Similarly, Tables 8 summarize the simulated increase or decrease in seasonal values of the meteorological variables between the current (1961-2000) and the 2080s (2070-2100) time periods for each of the downscaling methods. The results show that both SDSM and DANN predicted a significant increase in precipitation. However, the over all increase simulated by SDSM is higher that that of DANN. Moreover, while SDSM simulation gave the highest increase in precipitation at Chute-du-Diable in winter and at Chute-des-passes in Spring, DANN simulation gave the highest increase at both stations to be in Winter. LARS-WG, on the other hand predicted a very marginal precipitation increase in winter, spring, and autumn, with a small decrease (-6.82%) in summer. In

the case of temperature downscaling, all the three methods gave comparable results with the highest simulated increase in both Tmax and Tmin being in winter while the lowest increase being in autumn.

In general, while SDSM downscaling results predicted an average increase in annual precipitation between the current and the 2080s climate of about 32% at Chute-du-Diable while the DANN model has predicted for the same period an increase in average annual precipitation about 16%. However, LARS-WG downscaling results at both stations have not shown any significant change in precipitation for the same time period. At the same time, downscaling result for daily Tmax and Tmin values corresponding to all the three models show a comparable and consistently increasing trend. For both the Tmax and Tmin, the highest increase is predicted for the winter season, while the lowest increase is predicted for the autumn season. Moreover, downscaling with DANN resulted in a slightly higher increase in temperature than the other two downscaling methods. Finally, the results suggest an average increase in the mean annual temperature values in the study area of about 4 to 5 ^{o}C for the next 100 years. Similar downscaling results of a few other metrological stations is presented in Table 9. More precipitation and temperature downscaling results corresponding to the other meteorological stations can be found in Appendix A.

Table 8. Average increase / decrease in seasonal values at Chute-du-Diable between the current (1961-2000) and the 2080s (2070-2100) simulation periods

		Seasons			
		Winter	Spring	Summer	Autumn
Predictands	Models	Average Increase / Decrease			
P (%)	SDSM	49.05	29.17	21.54	28.82
	LARS	6.52	-3.68	-3.91	13.06
	DANN	26.60	5.11	17.39	17.82
Tmax (^{o}C)	SDSM	5.10	4.48	4.78	3.66
	LARS	5.12	4.40	3.97	3.38
	DANN	6.29	4.89	3.82	3.04
Tmin (^{o}C)	SDSM	6.66	4.28	4.02	2.67
	LARS	5.12	4.40	3.97	3.38
	DANN	7.51	5.50	3.71	3.07

Table 9. Average increase / decrease in annual values between the current (1961-2000) and the 2080s (2070-2100) simulation periods at some of the stations in the watershed

	Average Increase / Decrease								
	Precipitation (%)			Tmax (^{o}C)			Tmin (^{o}C)		
	SDSM	LARS	DANN	SDSM	LARS	DANN	SDSM	LARS	DANN
Benoit	22.3	5.0	25.5	4.3	4.4	5.3	3.7	4.3	4.7
Chute_des_Passes	44.0	0.1	27.6	4.7	4.2	4.76	4.02	4.2	5.08
Chute-du-diable	31.7	0.4	16.0	4.5	4.2	4.51	4.4	4.4	5.20
Cygnes	23.8	4.4	19.7	3.8	4.1	4.3	3.9	4.2	5.5
Misbi2	29.6	2.2	25.1	3.9	4.3	4.8	3.9	4.4	4.8

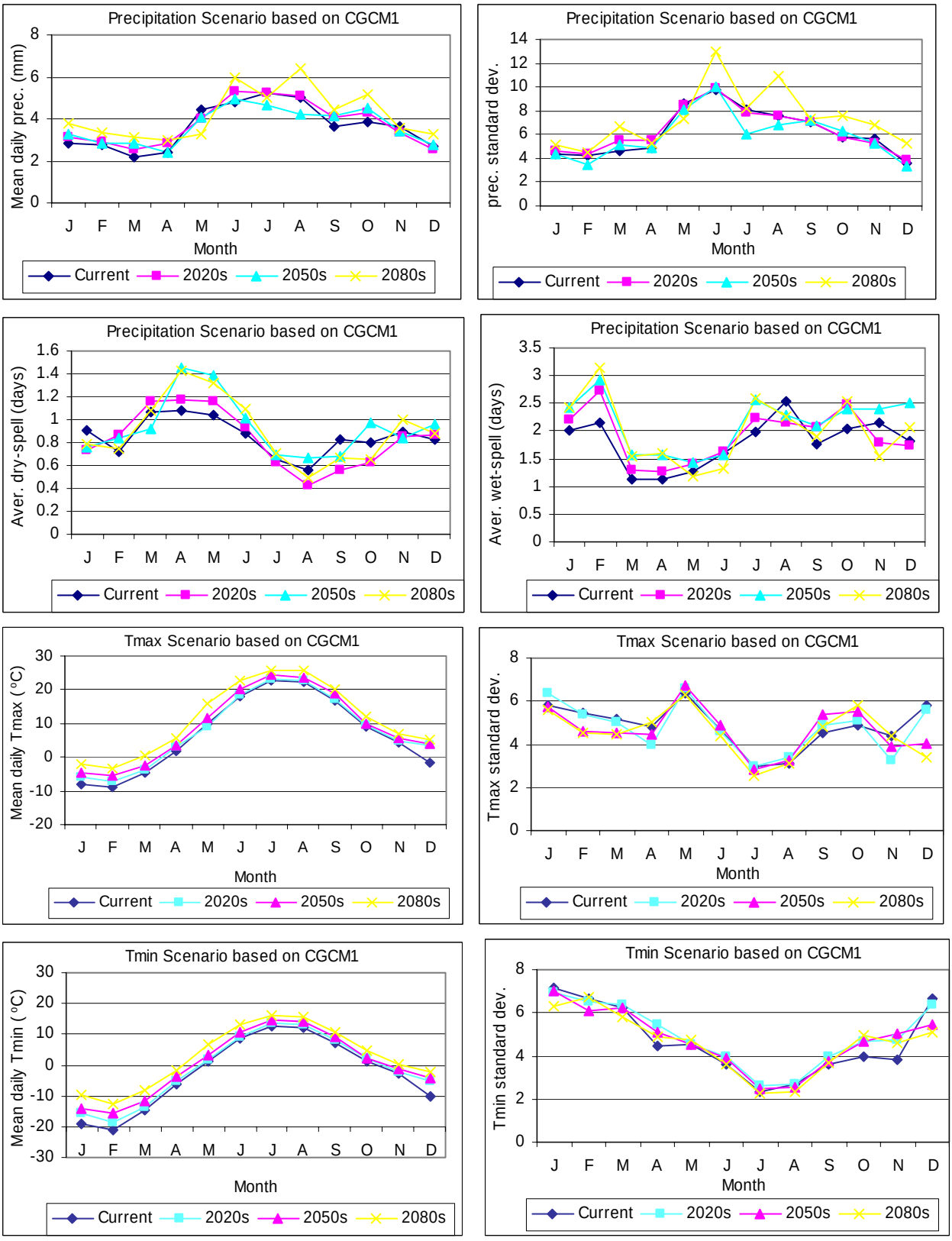

Figure 9. General trend in precipitation and temperature at Chute-du-Diable corresponding to a climate change scenario downscaled with DANN

6. Uncertainty Analysis

Questions of reliability of downscaling results may arise because of the presence of model errors and uncertainties in the estimates of means and variances of downscaled data. Those errors and uncertainties result from the concept (assumptions) on which the downscaling models are based and from the data used. Assessing model errors and quantification of uncertainty in downscaled meteorological variables is particularly useful in identifying the most accurate and most reliable downscaling model that can be used in hydrologic modelling of climate change impact studies. This section describes the various steps in exploratory data analysis, model errors evaluation and uncertainty estimation. Exploratory data analysis is a graphical approach of data analysis to investigate normality, outliers and serial correlations in a data set. This guides one to choose either parametric or nonparametric approach to be used in assessing model errors and uncertainties. Model errors evaluation deals with the deviations in the estimates of means and variances between observed and simulated data at a certain statistical significance level while uncertainty estimation helps to identify uncertainties in the estimates of means and variances in terms of their 95% confidence intervals. A number of literatures describe various types of uncertainty quantification techniques. Ang and Tang (1984) quantified uncertainties in terms of coefficient of variations (can be defined as standard deviation/mean), which describe uncertainties associated with inherent randomness in the system. Kaleris et al. (2001) characterized uncertainty in the downscaling model by the deviation between the measured and simulated cumulative probability distributions of the historic temperature and precipitation data.

The uncertainty analysis here includes daily precipitation as well as daily maximum and minimum temperature at the Chute-du-Diable station downscaled with SDSM, DANN and LARS-WG models. The analysis is made on the outputs of the downscaling models using both NCEP and CGCM1 datasets for the time period of 1961-2000. Some aspects of model errors in downscaled data are presented in section 5 by comparing bar charts of observed and simulated data as well as calculating root mean square errors (*RMSE*). The presentation in this section is a further extension in model errors evaluations in terms of hypothesis testing and confidence intervals for the difference of means and ratios of variances of the observed and simulated data at 95% confidence level. Uncertainty in the estimates of means and variances of the observed and downscaled meteorological variables are evaluated by establishing 95% confidence intervals about those estimates. The statistical software, S-PLUS and its relevant functions are used for the analysis.

6.1. Exploratory data analysis

Three exploratory data analysis (EDA) plots for checking normality and outliers in the observed daily precipitation, Tmax and Tmin data of the Chute-du-Diable (CDD) station are shown in Figure 10. Another three plots are presented in Figure 11 showing autocorrelation amongst consecutive data points in the time series. The plots shown in Figure 10(a) for daily precipitation reveal a distinctly

skewed distribution, skewed toward the left (that is, toward smaller values). That suggests the distribution for daily precipitation is not normal. The data also exhibit outliers which are illustrated by box and qq-plots. The time series and the auto correlation function (ACF) plots in Figure 11(a) suggest no significant serial correlation, or serial dependency amongst consecutive daily precipitation time series data. The horizontal lines are 95% confidence for ACF.

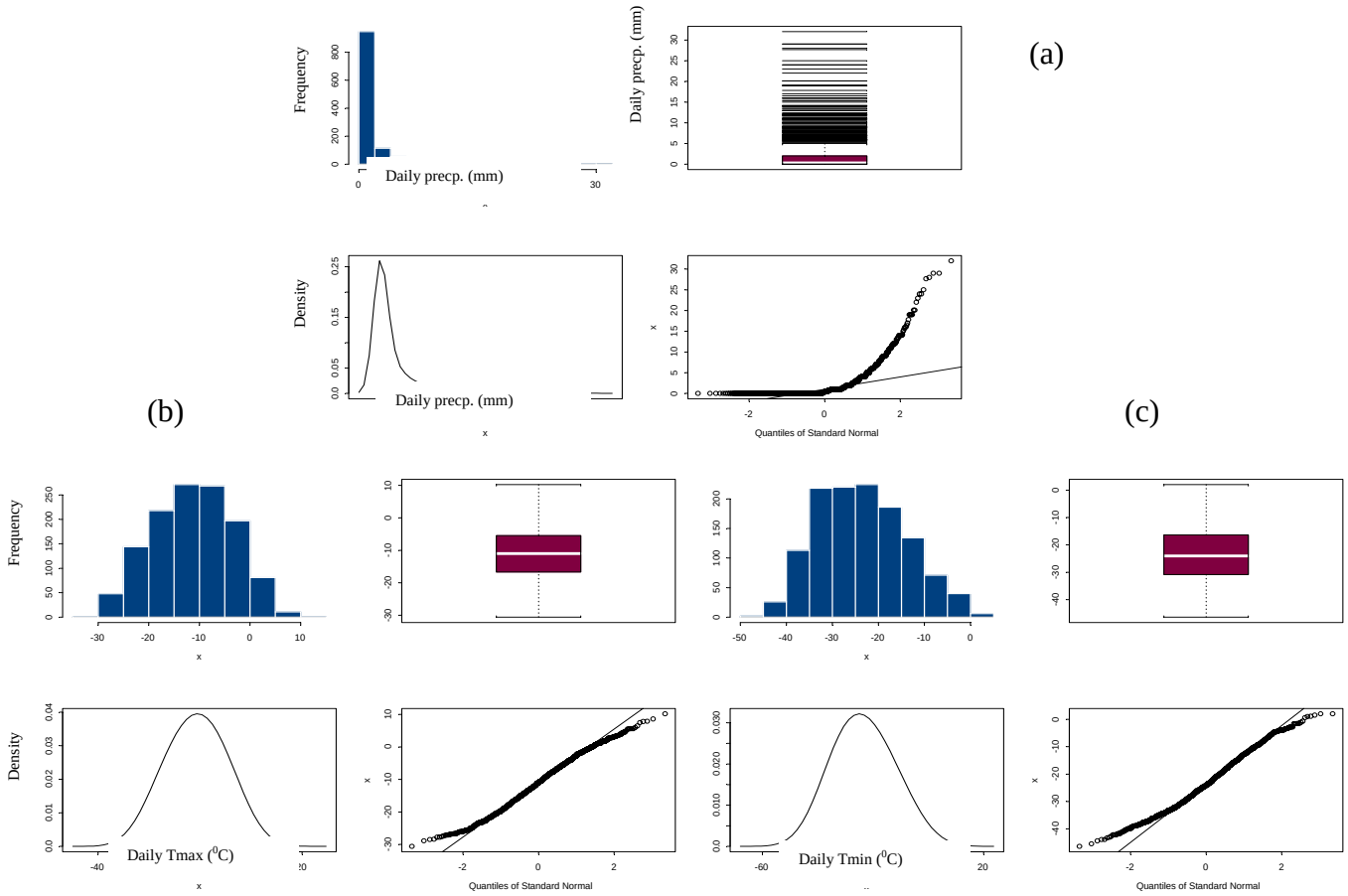

Figure 10 Exploratory data analysis plots (a) precipitation (b) Tmax and, (c) Tmin

The resulting plots for Tmax and Tmin as shown in Figure 10 (b) and (c) indicate that the data come from a nearly normal distribution, and there is no indication of outliers. In Figure 11(b) and (c), the ACF plots show that at *lag 1* the correlation coefficients in both Tmax and Tmin at about 0.6, which is relatively high even though a value of 0.7 is what is usually considered as significantly high value of correlation coefficient. However, the autocorrelation values diminish further after the *lag 1*. The exploratory data analysis (EDA) plots of downscaled daily precipitation, Tmax and Tmin, which are not shown here, also support the same conclusions. Thus the EDA plots suggest that the daily precipitation does not satisfy all the assumptions of parametric data analysis, while the Tmax and Tmin can be considered nearly normal variables and do satisfy those assumptions.

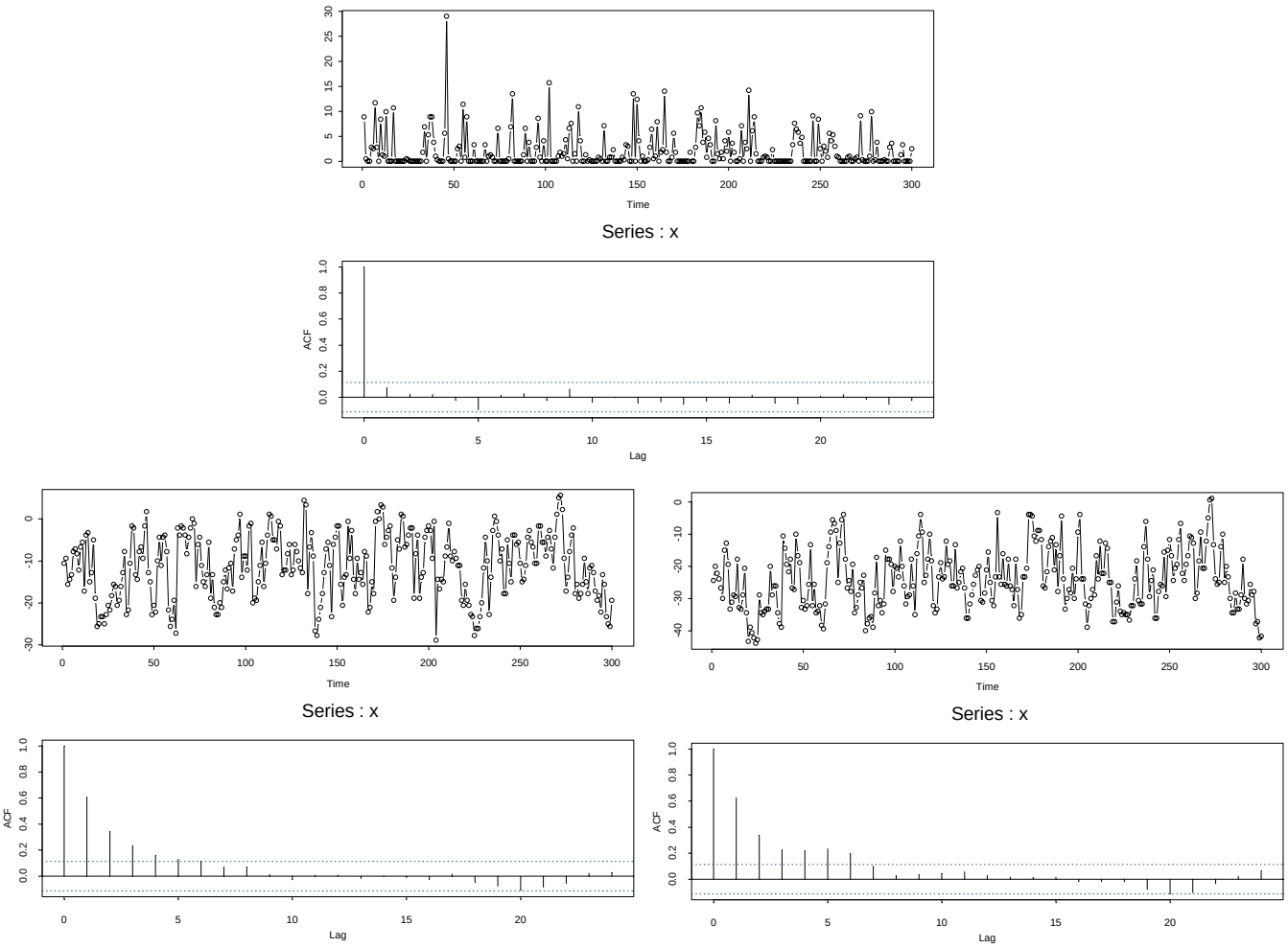

Figure 11 Time series and ACF plots (a) precipitation (b) Tmax, and (c) Tmin

Error Evaluation in Mean Estimates

Model error in the estimates of mean values for each month is calculated as the difference between observed and simulated mean values of daily precipitation, Tmax and Tmin. The simulations are made with each downscaling model using historical data of large scale atmospheric variables for the period of 1961-2000 as input. The plots of those model errors are shown in Figure 12. They are tested at 95% significance level using non-parametric Wilcoxon rank-sum test for precipitation, and using parametric hypothesis test (*t*-test) for Tmax and Tmin. In mean daily precipitation estimation at CDD station, the SDSM and ANN model errors for all months found insignificant at 5% level of significance because all reported *p*-values are found high above 0.05 and confidence interval of $\mu_1 - \mu_2$ does not include '0'. In terms of formal hypothesis testing, *p*-value has the following interpretation: the *p*-value is the level of significance for which observed test statistic lies on the boundary between acceptance and rejection of the null hypothesis. At any significance level greater than the *p*-value, one rejects the null hypothesis, and at any significance level less than the *p*-value one accepts the null hypothesis. For example, if *p*-value is 0.03, one rejects the null hypothesis at a

significance level of 0.05, and accepts the null hypothesis at a significance level of 0.01. LARS model errors are found significant in the month of June, July and September while for the other months the LARS model errors found insignificant at 5% significance level. Among all three downscaling models, the ANN model produced the least error in all months except October and November, however all months *p*-value found high above 0.05 in Wilcox rank sum test. In the month of October and November, the SDSM model errors are the least.

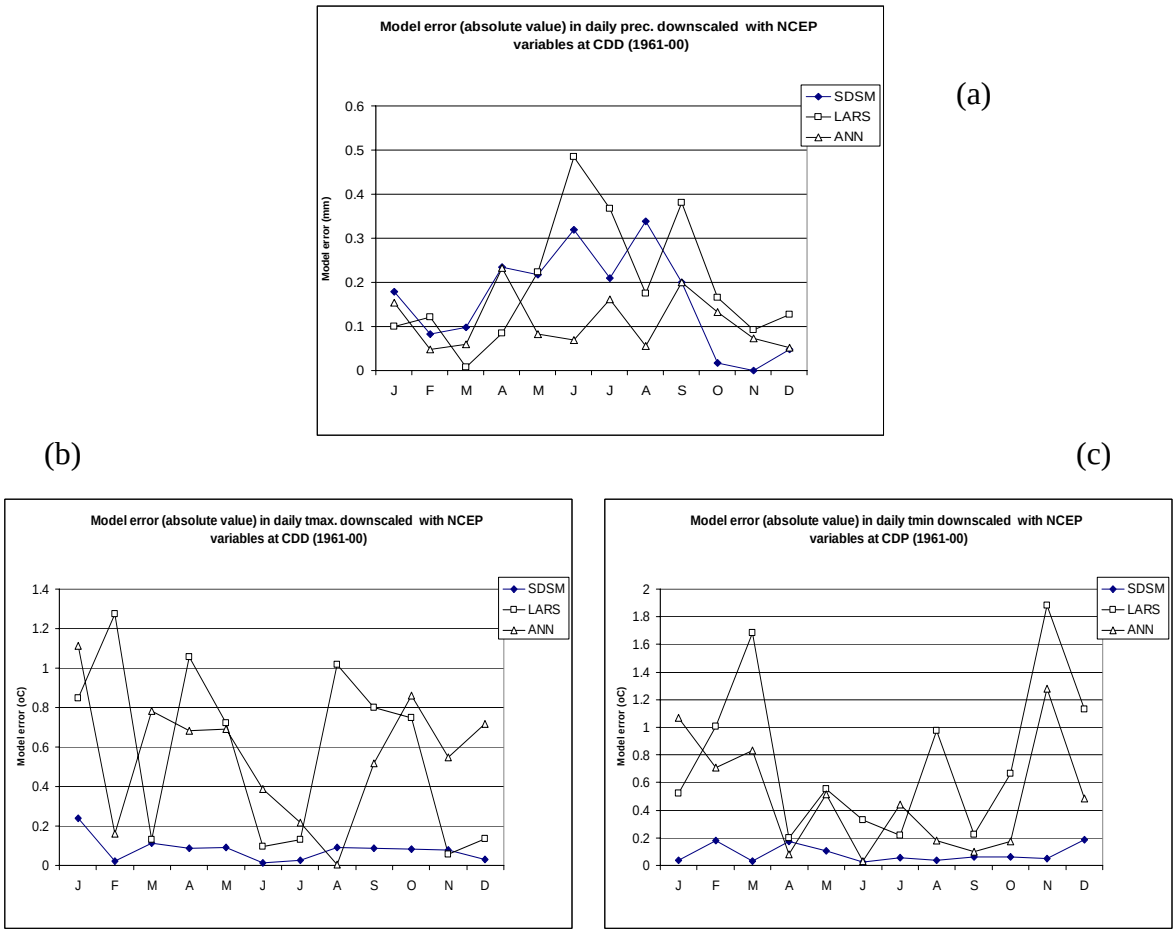

Figure 12 Model error (absolute value) in downscaled daily, a) precipitation, b) Tmax and c) Tmin

Model errors in downscaled daily maximum temperatures shown in Figure 12, indicate that the SDSM model error is the least and insignificant in all months at 5% significant level. The *p*-values are found high and the confidence interval for $\mu_1 - \mu_2$ include the value '0' for all months. During hypothesis and interval testing for $\mu_1 - \mu_2$ for Tmax, it was found that, a model with error above 0.6 (see Figure 3) is significant at $\alpha = 0.05$. Based on that observation, from Figure 12 it can be said that both ANN and LARS models do not produce insignificant errors for all months of the year, in some months their errors are significant and in some months insignificant. Similar type of conclusion can be drawn about the model errors in the estimates of means of Tmin, as shown at the bottom of

Figure 12. The SDSM produces the least error in all months at 95% significance level while the ANN and LARS are mixed of both significant and insignificant errors.

Error Evaluation in Variance Estimates

Comparative plots of variances of observed and downscaled precipitation, Tmax and Tmin are presented in Figure 13. In case of precipitation variability, it seems that the ANN model does not preserve variability closer to the observed data, rather they show less variability, while SDSM and LARS models variability is closer to the observed data. This variability (σ_1^2 / σ_2^2) is tested with 95% statistical significance according to the theorem discussed in section 2.3. Hypothesis test and confidence interval estimates have been evaluated at 5% significance level for each month between observed and simulated data of various downscaling models. In case of ANN, the *p*-values are all found below 0.05 for all months and the confidence interval does not include the value 1. This evidence supports that the observed variance and the ANN simulated variances are not same at 5% significance level. The variability of SDSM simulated precipitation and observed precipitation is not found same at 95% significance level for all months. In the months of June, July and August the SDSM variability is not the same with observed while in rest of the months they are the same at 95% significance level. In case of LARS model, the variances are not equal in July and August.

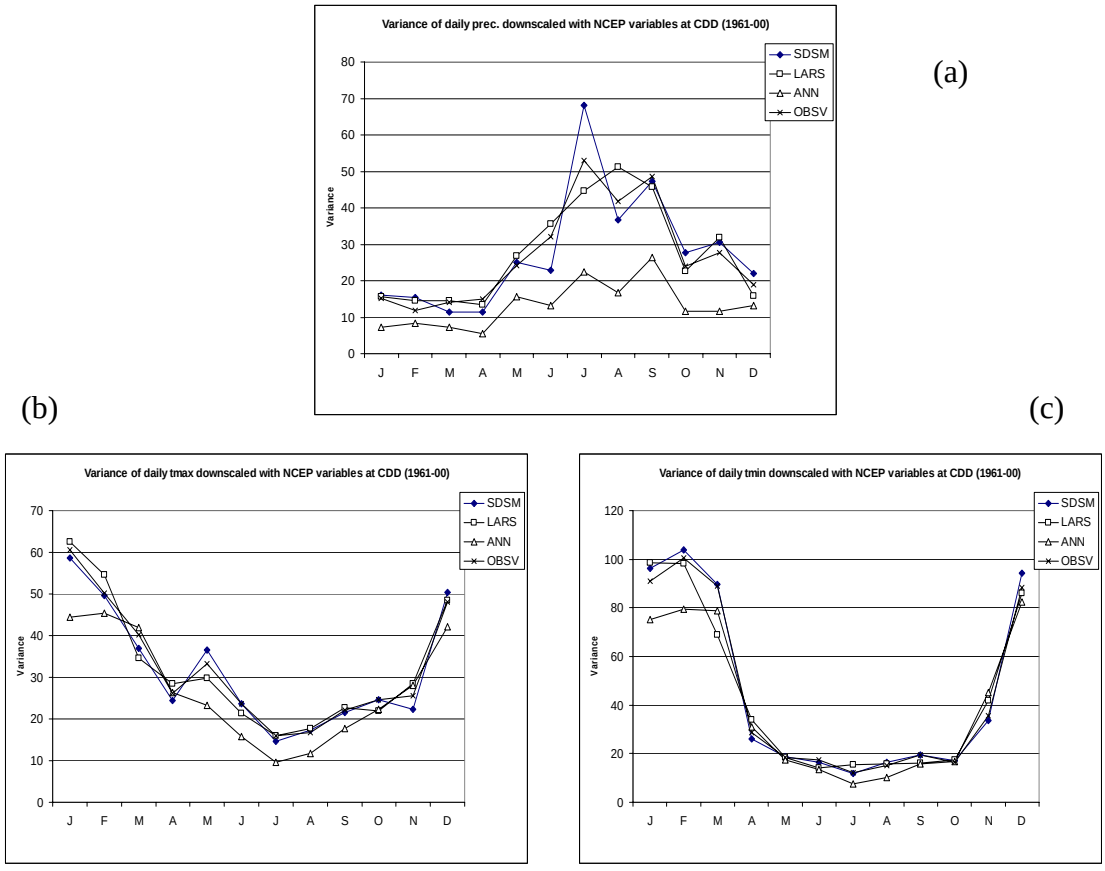

Figure 13 Variances for downscaled daily, a) precipitation, b) Tmax and c) Tmin

In case of Tmax, the variance test at 95% confidence level, indicate that the ANN model variability is equal with observed variability only in months of March, April, October and November while the SDSM model's variability is found to be equal in all months. For LARS model, the variance test indicates same variability in almost all months except in the months of February and March. In case of Tmin, at station CDD, the ANN model variances are not equal with the observed in months of January, February, March and November at 95% significance level while for SDSM, the variability was found to be equal in all months. For LARS model, the variability is found to be equal for all the months with the exception of March.

6.2. Uncertainty Evaluation in Mean Estimates

Uncertainty in the estimates of means has been quantified by the estimates of confidence intervals for means. According to the results of exploratory data analysis as discussed in the previous section, non-parametric approach for precipitation, and both parametric and non-parametric approach for temperatures can be used to find confidence intervals for means. Here, the non-parametric bootstrap approach is used for precipitation as well as Tmax and Tmin for estimating 95% confidence intervals for their means. The bigger confidence interval means large uncertainty and the smaller confidence interval means less uncertainty. The plots are shown in Figures 14 to 16 and the results are discussed below.

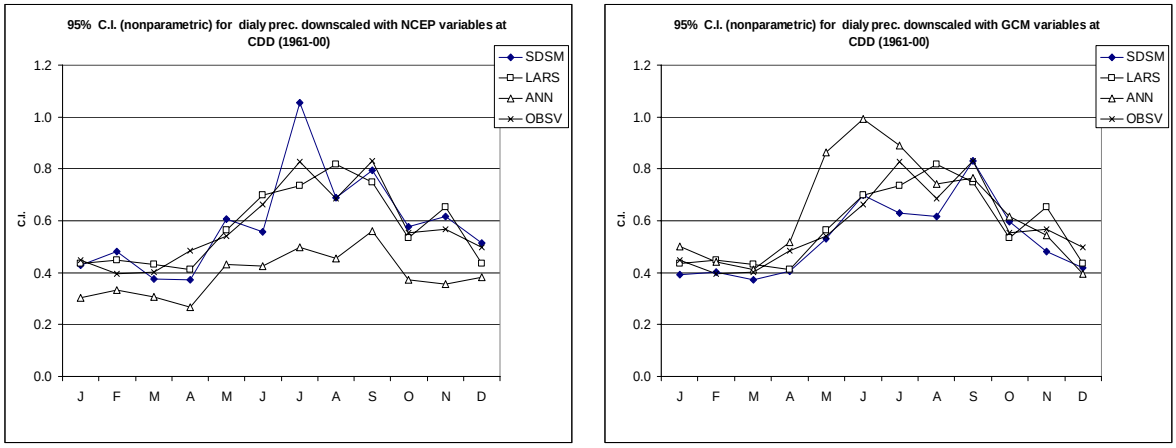

Figure 14 95% non parametric confidence interval for mean daily precipitation

In case of daily precipitation (Figure 14) downscaled with NCEP variables at CDD station, the ANN model exhibited the least uncertainty in terms of confidence interval for mean daily precipitation while the other two models exhibited uncertainty at the same level as exhibited by the observed precipitation. In the case of mean daily precipitation downscaled with GCM variables, the SDSM downscaling model exhibited the least uncertainty for almost all months.

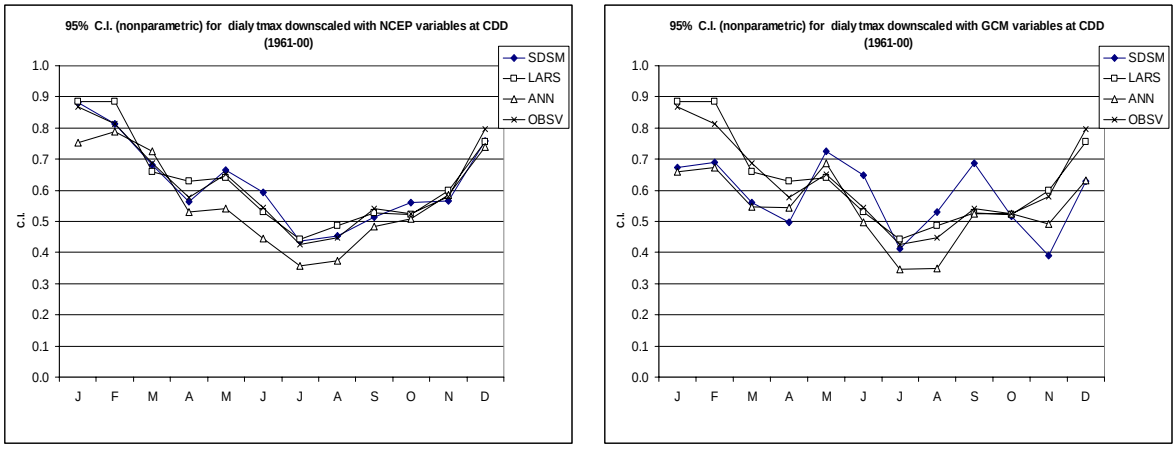

Figure 15 95% non parametric confidence interval for mean daily Tmax

In terms of 95% non parametric confidence interval for daily Tmax (Figure 15) downscaled with NCEP variables at station CDD, it was found that the ANN model exhibited the least uncertainty in all months except for the month of March and November. In March, LARS showed the least uncertainty and in November the SDSM. Tmax downscaled with ANN model and GCM large scale atmospheric variables exhibited the least uncertainty except for the month of April, May and November. In April and November the SDSM and in May the LARS exhibited the least uncertainty.

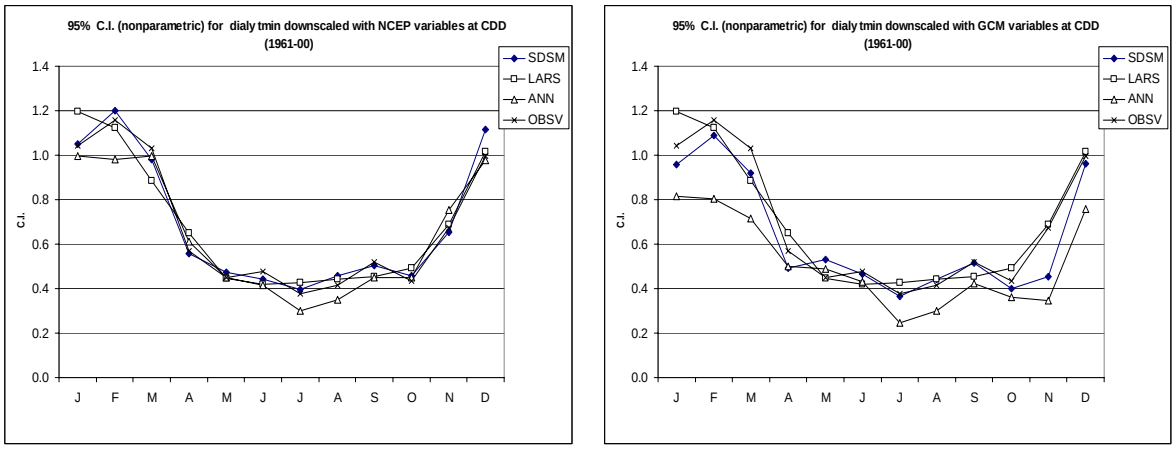

Figure 16 95% non parametric confidence interval for mean daily Tmin

Uncertainty in terms of non-parametric confidence interval for mean daily Tmin are shown in Figure 16. The ANN model exhibited the least uncertainty in NCEP case for nine months except for the month of March, April and November. In March, the LARS model exhibited the least uncertainty and in the months of April and November the SDSM exhibited the least uncertainty. In case of confidence interval for mean daily Tmin downscaled with GCM large scale atmospheric variables, the ANN model exhibited the least uncertainty for nine months except for the months of April, May and June. In April, the SDSM model exhibited the least uncertainty and in May and June the LARS exhibited the least uncertainty.

6.3. Uncertainty Evaluation in Variance Estimates

Uncertainty in the estimates of variance can also be quantified by calculating the confidence intervals for variances. Bootstrapping method has been used in estimating 95% confidence intervals for variances for daily precipitation, Tmax and Tmin which are graphically shown in Figures 17 to 19. For precipitation, in NCEP case the ANN model exhibited the least uncertainty for 11 months except for the month of June, in which the SDSM showed the least uncertainty. In GCM case, the ANN, SDSM and LARS models showed the least uncertainty for four months each.

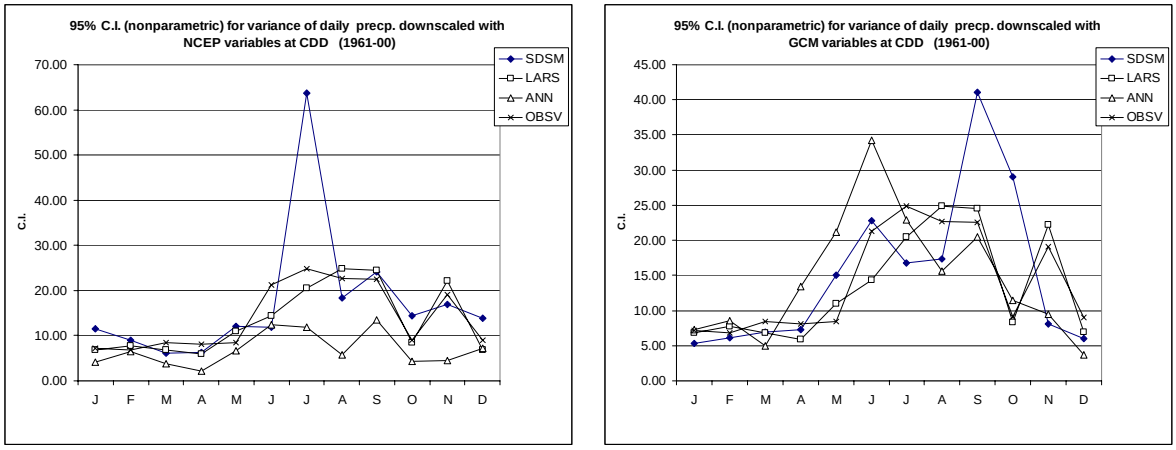

Figure 17 95% non parametric confidence interval for variance of daily precipitation

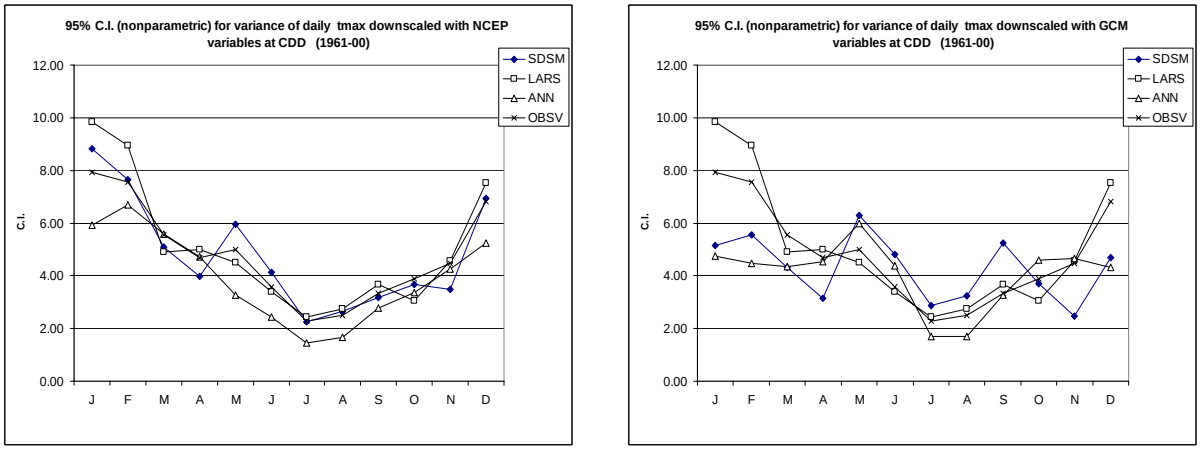

Figure 18 95% non parametric confidence interval for variance of daily Tmax

In terms of 95% confidence interval for variances for downscaled daily Tmax corresponding to NCEP data (Figure 18), the ANN model exhibited the least uncertainty for eight months of the year while the SDSM and LARS gave the least uncertainty for two months each. In the case of GCM, the ANN model exhibited the least uncertainty for six months, the SDSM model for three months and the LARS model for three months. Uncertainty quantification in terms of 95% confidence interval for variances for daily Tmin is shown in Figure 19. In NCEP case, the ANN model exhibited the least

uncertainty for nine months except for April, October and November. In those months, the SDSM model exhibited the least uncertainty. In the case of GCM, the ANN model exhibited the least uncertainty for eleven months except for the month of April, in which the SDSM exhibited the least uncertainty. While considered the GCM case, the ANN model exhibited the least uncertainty for all twelve months.

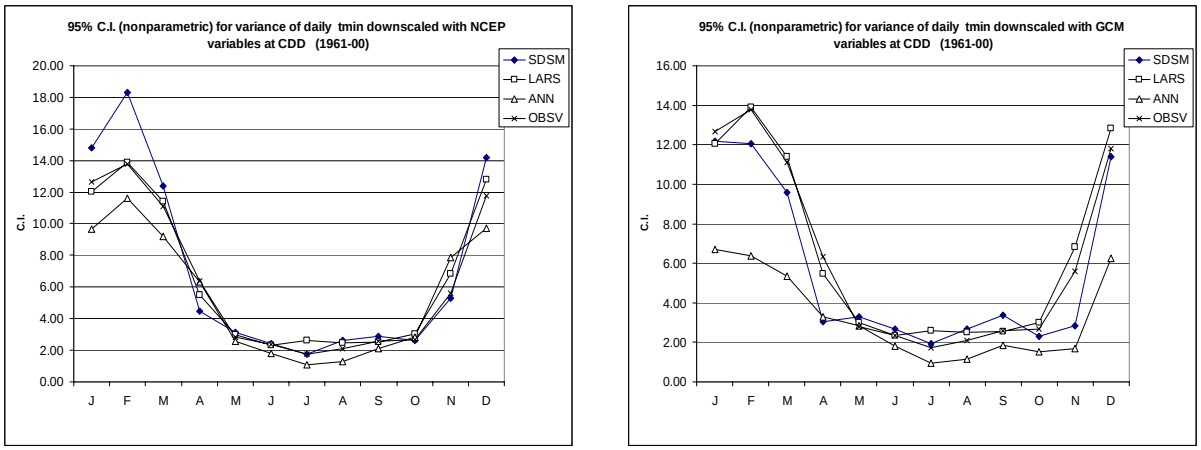

Figure 19 95% non parametric confidence interval for variance of daily Tmin

6.4. Summary of Uncertainty Analysis Results

The objective of the uncertainty analysis is two folds: firstly to investigate which downscaling model produces the least error at 95% significance level in estimating means and variances and, secondly to assess uncertainties in those estimates of means and variances in terms of their 95% confidence intervals. The exploratory data analyses indicate, the distribution of daily precipitation is not normal and even not nearly normal and includes many outliers. It also shows that the precipitation data does not have any serial correlation at 95% significance level. These characteristics indicate that a non-parametric test is a suitable approach for precipitation data analysis. The distribution of daily maximum and minimum temperatures are nearly normal, do not have outlier and they are not serially correlated at 95% significance level. This permits both parametric and non-parametric approaches of data analysis for daily temperature data. The analyses also indicate that DANN is the most accurate model in downscaling daily precipitation with 95% confidence level while SDSM is the least error model in downscaling daily maximum and minimum temperatures with 95% confidence level.

Uncertainty in the estimates of means of downscaled daily precipitation is the least for DANN model evaluated in terms of 95% confidence intervals. LARS and SDSM models exhibit uncertainty in the estimates of means of daily precipitation almost at the same level of the observed data. Uncertainty in the estimates of means of daily Tmax is the least in almost all months for DANN model while NCEP large scale atmospheric variables are used for downscaling. However, while GCM large scale atmospheric variables are used, only in few months the DANN uncertainty is found the least. Uncertainty in the estimates of means of daily Tmax downscaled with SDSM and LARS

models using NCEP data is found to be at the same level as that calculated from the observed data. In cases where GCM data is downscaled, the uncertainty in the estimates of means of daily Tmax is in general at the same level as found for the observed data. Uncertainty in the estimates of means of Tmin with DANN model is found the least in almost all months for both NCEP and GCM cases. Uncertainty in the estimates of means of Tmin, for SDSM and LARS models from both the NCEP and GCM data are found almost at the same level as that of the observed one.

Uncertainty in the estimates of variances of daily precipitation for DANN model is found the least for all months in NCEP case. For SDSM and LARS models those uncertainties are found almost at the same level of the uncertainty of the observed data. Uncertainty in the estimates of variance of daily Tmax for DANN model is the least for almost all months in NCEP case. For SDSM that uncertainty in most of the months is at the same level as the observed uncertainty. For LARS model, in most of the months they are at the same level, while in few months they are higher than the observed. Uncertainty in the estimates of variances of Tmin, both for NCEP and GCM cases, the DANN model exhibited the least uncertainty. For SDSM, the uncertainty is found less than the observed in almost all months except few, in which the SDSM uncertainty is higher than the observed. For LARS model, the uncertainty is at the same level as observed, in few months they are higher than the observed.

Based on the uncertainty analysis results and their description so far provided above, a general conclusion may be drawn as follows. In terms of model errors and their uncertainty evaluation, the DANN model seems to exhibit the least error and the least uncertainty in daily precipitation downscaling at 95% confidence level though the model does not preserve the variability well. Based on the same criterion, the SDSM seems to be the least error model at 95% confidence level for downscaling daily maximum and minimum temperatures; the variability is well preserved but the exhibited uncertainties are sometimes slightly higher than the DANN model. On the same criterion, the LARS model cannot compete to be considered as the least error and the least uncertain model. However, to be more ascertain about this type of general conclusion, one requires further investigation including more stations data and more criterions for model error and uncertainty evaluation.

7. Developing Standalone DANN Downscaling Model

It has been explained in section 3 that a NeuroSolutions development Environment has been used to develop different types of dynamic ANNs. During the development phase, all the training and testing of a DANN is done within the NeuroSolutions development environment. The optimal DANN model structure is identified by interactive training and testing of different structures for the downscaling of daily precipitation or temperature values of the observed climate. Then, this model can be used to predict daily precipitation or temperature values corresponding to a climate change scenario with the corresponding predictors from GCM provided as inputs to the network. This particular step of the process where we use the developed models with new inputs is sometimes referred to as 'production' phase of the model. However, it will be more convenient if it is possible to run the once trained DANN model on any other computer where the NeuroSolution software may not be installed. In fact this is made possible by a NeuroSolutions extension tool called the Custom Solution Wizard that will take an existing neural network created with NeuroSolutions and automatically generate and compile a Dynamic Link Library (DLL). This allows the modeller to easily incorporate the trained neural network models into any custom application. The Wizard will display a series of panels that will guide the modeller step-by-step through the creation of a neural network DLL. Upon completion, the Custom Solution Wizard will create a neural network DLL which (along with the corresponding weights file) provides a simple protocol for assigning the network input and producing the corresponding network output. The weights file holds the weights for each component and the input and output normalization coefficients contained within the NeuroSolutions breadboard at the time of creation. Furthermore, the Custom Solution Wizard supports learning which allows the modeller to re-train the generated neural network and/or retune the network after gathering new data.

While using the wizard to create the DLL, the modeller is also given the option of creating a shell for a number of programming environments such as Visual Basic, Visual C++ and Microsoft Excel. Each shell provides a sample application along with source code to give the modeller a starting point for integrating the generated DLL into his application. During this particular research study, two prototypes of stand alone DANN applications were developed for downscaling precipitation and temperature at each station in the study area. The first one is developed as "*excitable Visual Basic application*" while the second is developed as "*Visual Basic macro*" which runs under Microsoft Excel. While using the stand alone applications, the user has to specify (by browsing through the file folders) the DLL and the weight files corresponding to the trained DANN downscaling at a particular station. The user should also specify file name of the *input* data (containing time serious of the GCM predictor variables) which is going to be downscaled and the name of the *output* file where the downscale precipitation or temperature data is going to be stored. If the DLL is to be used in a training mode, then the name and location of the *desired* file should also be specified. A typical user interfaces for stand alone DANN downscaling applications is shown in Figures 20a. For the application running under the Microsoft Excel environment, the locations of the DLL and weight files are specified in the Visual Basic macro and the *inputs, output* and *desired* data for the station are

organised under excel worksheets and the worksheet names are provided through the user interface shown in Figures 20b which is launched from the introduction worksheet.

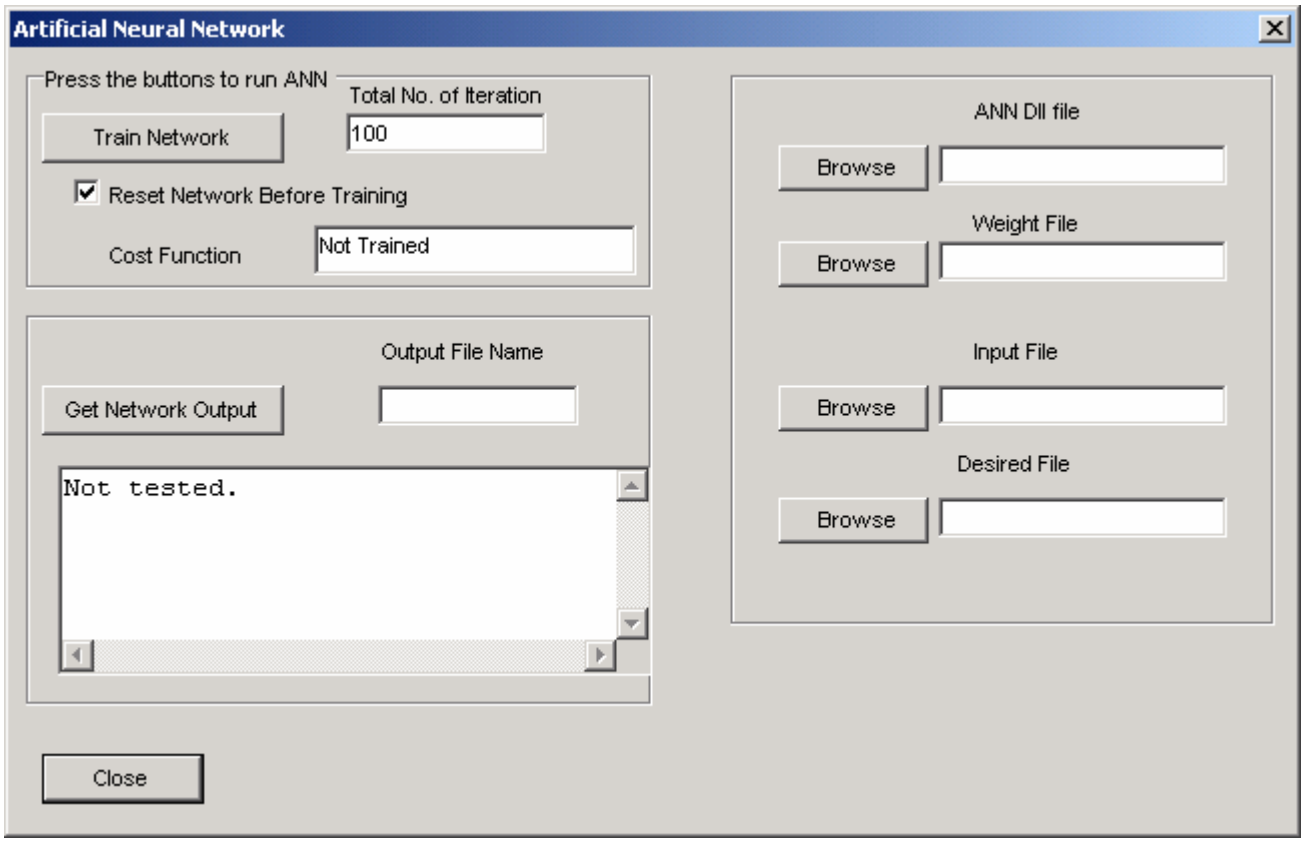

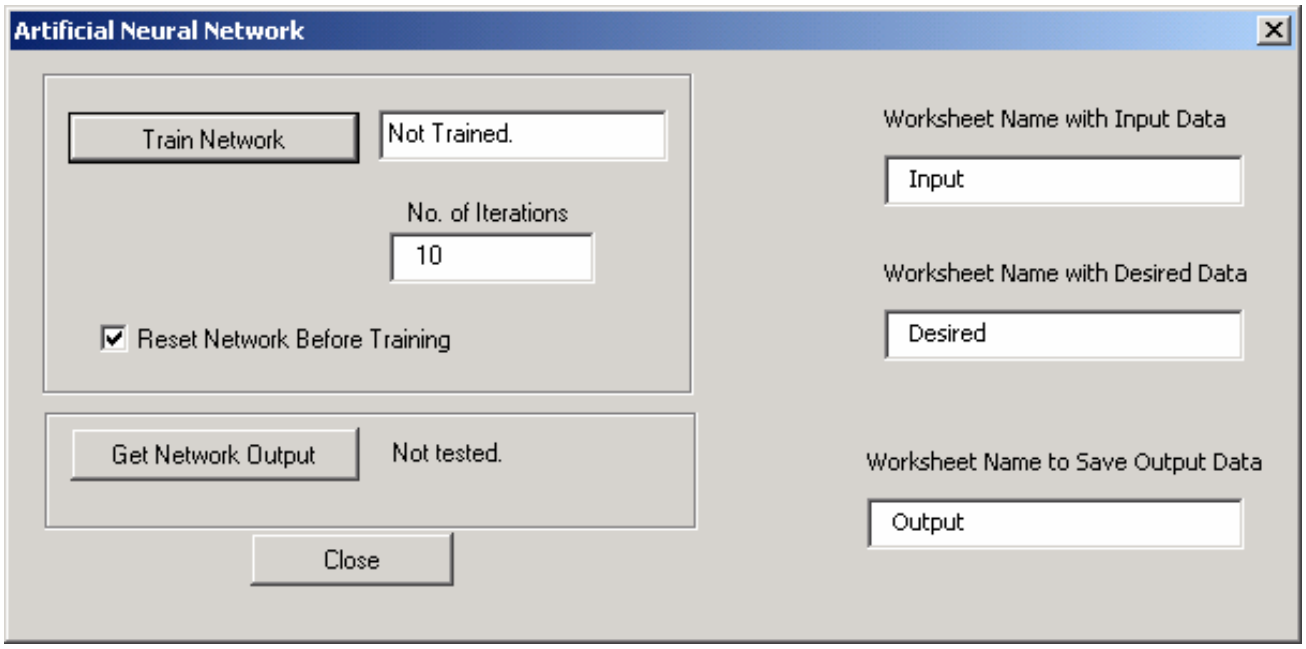

Figure 20a&b. User interfaces of the stand-alone DANN downscaling application prototypes

The question of whether a DANN downscaling model developed with observed data at a particular location can be used at some other location by retraining the same model with observed data of another location is very interesting. However, the answer lies whether the large scale predictor variables identified as input at the first location will be the same as the once appropriate for the second location. If that is the case, then the DLL (containing the optimum DANN architecture) can be retrained with the corresponding input and output data set of the second location. This will result in a new parameter (weight) file that could be used for downscaling GCM scenario data at this location. However, if the geographical and other meteorological factors affecting precipitation and temperature at the two locations are different, then, there is no guaranty that the same set of predictor variables, and hence, the same DLL with identical DANN structure used in the first station will also be the most optimal DANN for the second location. In the latter case, the user will need to first select new predictor variables that are the most relevant to the study area. A brief user manual of the DANN downscaling model is included in Annex 2.

8. Hydrological Impact of Anticipated Climate Change

Changes in global climate are believed to have significant impacts on local hydrological regimes, such as in stream flows which support aquatic ecosystems, navigation, hydropower, irrigation systems, etc. In addition to the possible changes in the total volume of flow, there may also be a significant change in the frequency and severity of floods and droughts. Such hydrologic impacts of climate change on a watershed can be estimated by developing hydrological models of the watershed and simulating river flows resulting from the downscaled precipitation and temperature data corresponding to the climate change scenario considered. Each of the hydrological modeling systems used in this study are described briefly in the following section. But the general steps followed in using hydrologic models in the study of the hydrological impact of climate change in the study area are described below:

- Setting up and calibration (and verification) of a hydrologic model with precipitation, temperature, potential evapo-transpiration, stream flow or reservoir inflow data representing the current climate (1961 – 2000).
- Simulation of stream flow and reservoir inflow corresponding to future climate change scenarios based on the downscaled future precipitation and temperature data.
- Analyses of the simulated stream flow and reservoir inflows corresponding to the different time periods (2020s, 2050s, 2080s) and see if there will be a significant trend in the annual stream flow and reservoir inflow volume as well as frequency of high and low flows.

8.1. Hydrologic models

Hydrological models are mathematical formulations which determine the runoff signal which leaves a watershed basin from the rainfall signal received by this basin. They provide a means of quantitative prediction of catchment runoff that may be required for efficient management of water resources systems. Such hydrological models are also used as means of extrapolating from those available measurements in both space and time, in particular in ungauged catchments and into the future to assess the likely impact of future hydrological changes (Beven, 2001). Three well known hydrological modelling systems are applied in this study for simulation of flows in the rivers located in the Saguenay watershed so that the possible effect of the type of hydrological model employed in climate change impact study could be analysed. The first two are lumped conceptual modelling systems called HBV-96 (Bergström and Forsman, 1973) and CEQUEAU (Morin et al. 1983). The third one is a physically based distributed parameter modelling system called WatFlood (Kouwen et al., 1993). While a single WatFlood model cover the whole Saguenay watershed and flows in each of the rivers in the region are simulated simultaneously, HBV-96 and CEQUEAU have to model each sub-basin and simulates the river flows at the outlet of each of these sub-basins separately. HBV-96 and CEQUEAU are also used to simulate the total daily inflows into the Chute-du-Diable reservoir located on the Peribonka River. Chute-du-Diable is one of the large reservoirs in the region operated

by ALCAN for hydroelectric production. In general, the power generation capacity of the station is proportional to the amount of water available in the reservoir which is in turn proportional to the rate of reservoir inflow from the surrounding catchment. Therefore, having a good estimate of the possible impact of climate change on the reservoir inflow could be very beneficial in planning the operation policy of the power generation facility and other possible measures in order to reduce the adverse effects in case such climate changes become a reality.

HBV-96 Hydrologic Modeling System (IHMS)

IHMS-HBV is an integrated hydrological modelling system developed at the Swedish Meteorological and Hydrological Institute, and has been applied to a wide range of applications including analysis of extreme floods, effects of land-use change and effects of climate change (Arheimer, 1998; Brandt, 1990; Harlin, 1992; Lidén, 2000). It can best be described as a semi-distributed conceptual model. It has a routine for snow-accumulation and snowmelt based on a degree-day relation with an altitude correction of temperature. The soil moisture accounting routine accounts for soil field capacity and change in soil moisture storage due to rainfall/snow melt and evapotranspiration while the runoff generation routine transforms water from the soil moisture zone to runoff (see Figure 21). The model parameters are determined through a calibration process, where the parameters are adjusted until simulated and observed runoff shows a good agreement. The calibrated model can then be used as a simulation tool in numerous applications. A more detailed description of the HBV-96 can be found at http://www.indic-airviro.smhi.se/HBV/

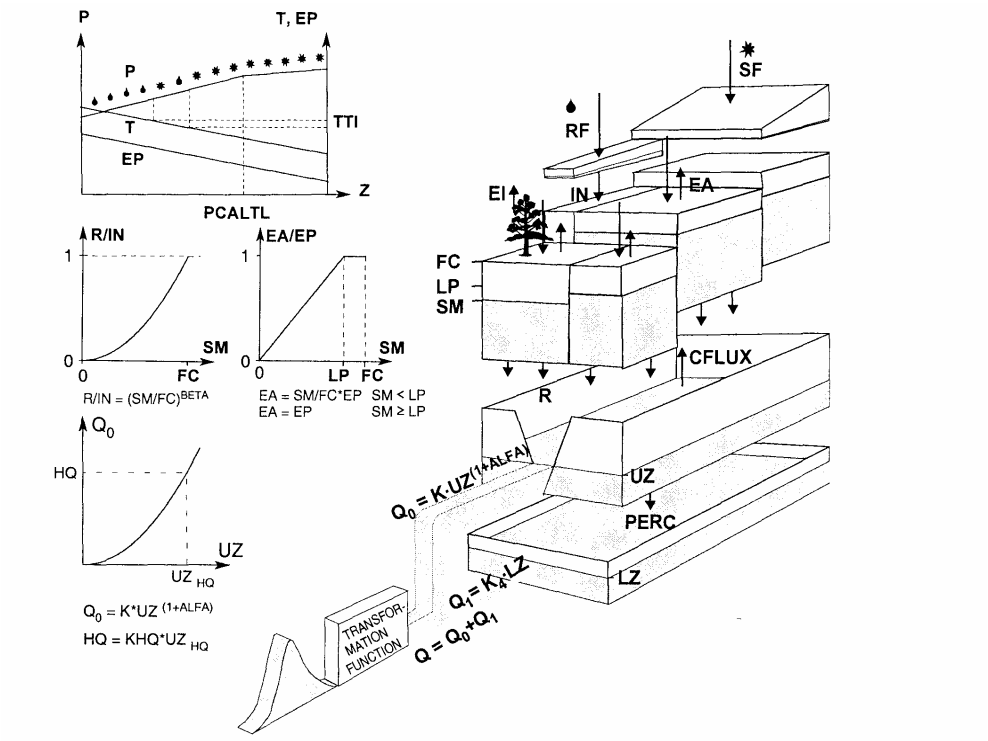

Figure 21. The principal structures of the IHMS -HBV-96 conceptual hydrologic model

CEQUEAU Hydrological Modelling System

CEQUEAU is a distributed hydrological model, which takes into account the physical characteristics of the basin by subdividing it in elementary representative areas (ERA), also called whole squares, which are assumed to have homogenous features (Morin et al. 1983). It is a water-balance-type conceptual model with distributed parameters. ERAs are further divided according to sub-basin divides, which allows following the formation and evolution of streamflow in time and for proper routing of runoff. In addition to physiographic data, the model requires meteorological inputs (daily solid and liquid precipitation, as well as maximum and minimum daily air temperature). Calculations are performed to quantify the vertical movement of water through the so-called production function, while downstream routing (or advection) of water is calculated with a transfer function. The production function is modeled by a series of interconnected reservoirs representing the ground (Fig. 23). Mass transfers are represented by mathematical equations to simulate the different components of the hydrological water balance (snowpack formation and melt, evapotranspiration, water in the unsaturated zone, water in the saturated zone and lakes and marshes).

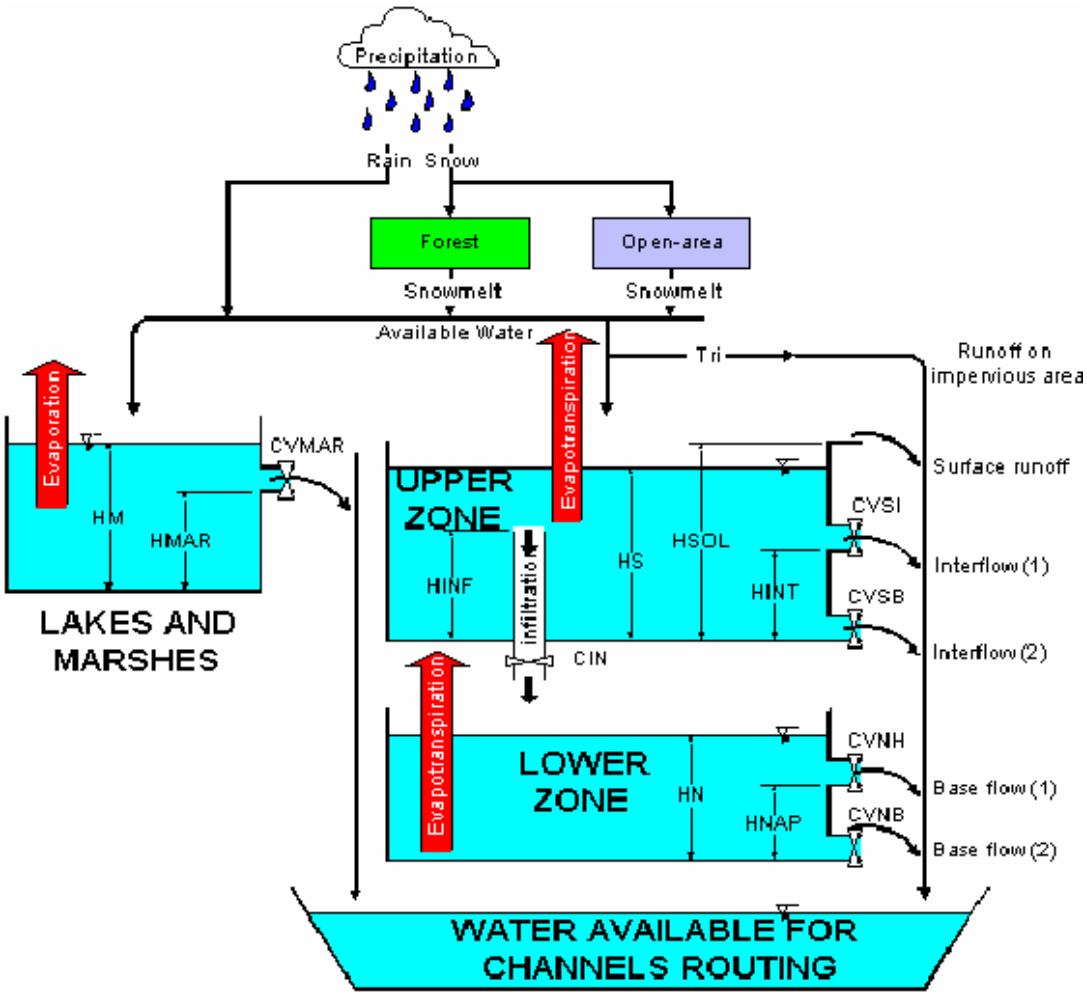

Figure 22 Schematic representation of CEQUEAU hydrological model.

WATFLOOD Distributed Hydrologic Modeling System

WATFLOOD is an integrated modelling system that can simulate river flows for watershed having response times ranging from one hour to several weeks. The system is aimed at flood forecasting and long-term hydrologic simulation using distributed precipitation data. The processes modeled include interception, infiltration, evaporation, snow accumulation and ablation, interflow, recharge, baseflow, and overland and channel routing (Kouwen et al., 1993). The snow melt process in WATFLOOD is modelled by an index method; in this case, a degree-hour based heat input or loss. An accounting of the heat content of the snow pack allows re-freezing. For overland flow, an explicit method is used that is based on continuity and Manning's formula and incorporates the average surface slope for each grid. River flows are similarly based on continuity and Manning's formula but separate roughness parameters are used for channel and floodplain roughness. Base flow is calculated by a two parameter, non-linear storage-discharge function. The total inflow to the river system is found by adding the surface runoff contributions from the various land cover classes to the base flow. These flows are then added to the channel passing through the grid and the outflows from upstream grids are added as inflow to lower grids, where outflows from other contributing grids are added to the local flow and routed to the next downstream grid. Computed flows can be compared to measured flows wherever measured flows are available.

WATFLOOD uses the Grouped Response Unit (GRU) method to model large watersheds (see Figure 23). The GRU is a technique that is designed to greatly improve the computational efficiency for modelling large watersheds. It is well known that the hydrological response from such land covers as, for instance, forests and alpine tundra, differ greatly but it can be expected that for example, two or more similarly forested areas that experience the same meteorological conditions would have the same response. The same logic applies to other land covers. In the GRU method, all similarly vegetated areas (not necessarily contiguous) within a sub-watershed or element are grouped as one response unit and called a GRU. The GRU is the basic computational unit in the model. An element has one GRU for each hydrologically significant land cover type. The hydrologic response of each class is computed as if that class covered the whole grid but its response (flow) is weighted according to its percent coverage in that grid or sub- watershed. The hydrological responses from each GRUs in an element are summed to give its total response. The modelling parameters are tied to the land cover type and as such should apply to other watersheds where the land cover mix may be different, but where similarly vegetated areas can be expected to respond in the same way to meteorological conditions.

For the grid in Figure 23 there are four hourly runoff computations and four overland flow routing segments. The flows are then combined for the grid. It is as if there are four sub-watersheds in this grid in a pie-shaped configuration, with each segment contributing runoff according to its percent coverage. The four runoff amounts are added in each grid and routed downstream from grid to grid.

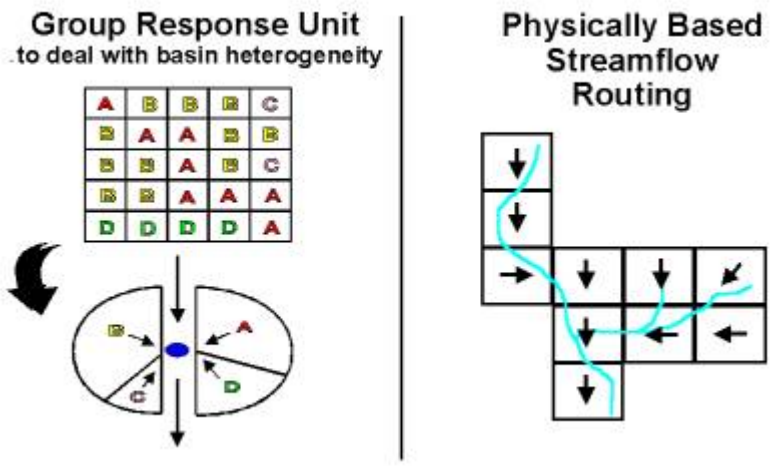

Figure 23 - Group response unit and runoff routing concept (Donald, 1992)

The essential property of this arrangement is that the parameters are associated with the land cover classes A, B, C and D. All grids in this method have the same hydrological parameters, even though the land cover makeup of each grid is not the same. The advantages of this scheme are: 1) the parameters can be used in other physiographically similar watersheds without recalibration, and 2) the parameters do not have to be recalibrated if land use in the watershed changes over time. For the latter, only the land cover map and the fractions in each grid need to be redefined.

In addition to the modelling systems described above, the popular HEC-HMS hydrological modeling system (HMS) developed at the Hydrologic Engineering Center (HEC) of the US Army Corps of Engineers was also used. However, at the moment HEC-HMS model does not have a snowmelt component which can represent the different flow dynamics in such cold and snowy region and as a result it was not able to accurately simulate peak flows which usually occur in the spring as a result of spring snowmelt. Therefore, the HEC-HMS results are not included in this report.

8.2. Hydrologic model calibration and validation results

Hydrologic Modelling is done using all the three models explained in the previous section. The simulation results of HBV-96, CEQUEAU and WATFLOOD on some selected rivers are presented in this report. Observed precipitation and temperature data from the thirteen meteorological stations that were used in the downscaling exercise in section 5, are once again used for calibration and validation of the hydrologic models. As it has been mentioned earlier, while WATFLOOD models the whole Saguenay watershed and simulates stream flows in all the eleven rivers at once, HBV-96 and CEQUEAU models each sub-catchment and simulates the stream flow in each of the rivers separately. While precipitation and temperature data at all the thirteen stations are used to the WATFLOOD model, stations which are closer to each of the sub-catchments were used in modeling each of these sub-catchments with HBV-96 and CEQUEAU. The required outputs from these models are the mean daily discharge in each of the eleven rivers in the watershed. In addition, the total inflow

into the Chute-du-Diable reservoir is also simulated with HBV-96 and CEQUEAU. However, since the modelling exercise and overall trend in most of the stream flows is similar, the simulation results of the reservoir inflow and only four of the rivers from representative set of sub-catchments are presented in this report. Moreover, the CEQUEAU models are developed and applied for simulation of flows in only two rivers, namely, for Serpent River flow and Chute du Diable reservoir inflow.

The historical precipitation and temperature data from each metrological station are divided into two sets, one for calibration and the other for validation of the hydrological models. Because of limited stream flow data available for some of the rivers, eleven years of daily stream flow data between 1986 and 1996 are used for calibration and six years of data between 1997 and 2002 is used for model validation. These data sets associated with the calibration and validation periods reflect the current climate condition in the region. Combinations of manual and automatic optimization are used to calibrate the models in such a way that the observed and simulated flow values be as close as possible. The performances of the best calibrated models are presented in Figures 24. The root mean square error values (RMSE), the coefficient of determinations (R^2) and the correlation coefficients (r) between the model outputs and the observed data are further summarized in Table 10. In general, the model validation results show that the performance of HBV-96 and CEQUEAU models is slightly better than that of WATFLOOD in most of the cases. This is not unexpected because of the fact that WATFLOOD model is set up to simulate the stream flow in all the eleven rivers in the watershed simultaneously while HBV-96 and CEQUEAU are optimised to simulate the flows in each of the rivers separately.

Table 10. The performances of the three hydrologic models in simulating the flows during the validation period

River Basin	Catchment Area in Km^2	RMSE			R^2			r		
		HBV-96	WATFLOOD	CEQUEAU	HBV-96	WATFLOOD	CEQUEAU	HBV-96	WATFLOOD	CEQUEAU
Serpent	1760	17.5	30.9	22.5	0.84	0.50	0.77	0.93	0.81	0.92
Mistassibi	9320	98.5	113.8	-	0.75	0.64	-	0.91	0.86	-
Mistassini	9870	99.0	116.6	-	0.79	0.71	-	0.91	0.88	-
Ashu - Aval	15300	148.2	153.8	-	0.70	0.68	-	0.88	0.88	-
Chute Du Diable	9700	100.9	-	58.6	0.80	-	0.93	0.90	-	0.96

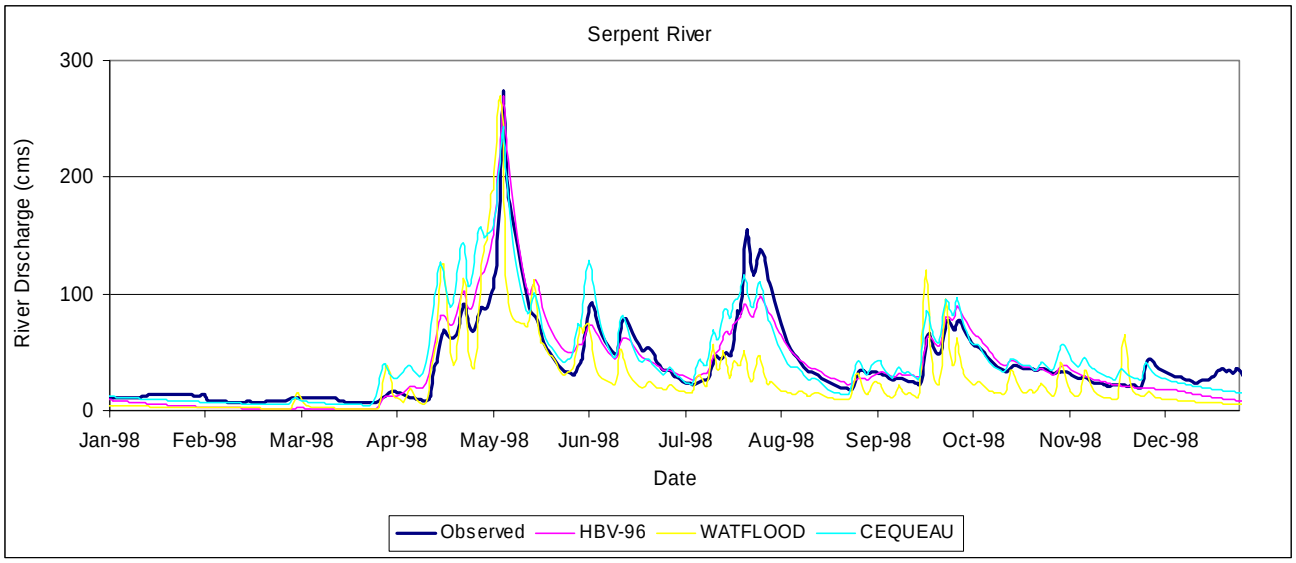
Serpent River
River Drscharge (cms)
300
200
100
0
Jan-98
Feb-98
Mar-98
Apr-98
May-98
Jun-98
Jul-98
Aug-98
Sep-98
Oct-98
Nov-98
Dec-98
Date
Observed
HBV-96
WATFLOOD
CEQUEAU

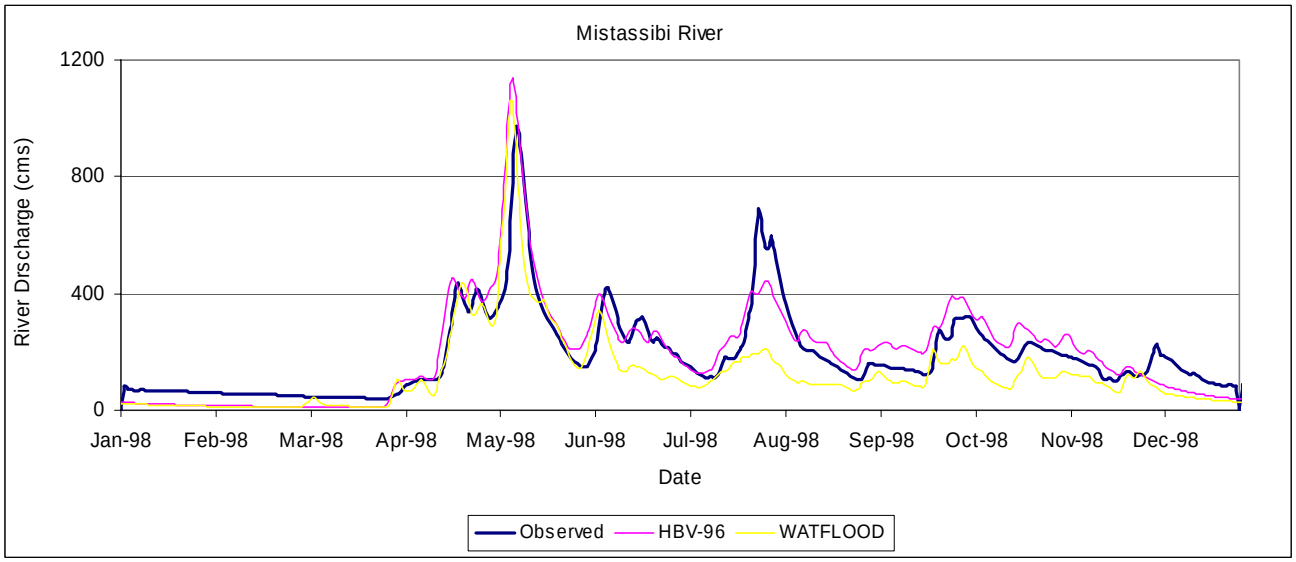
Mistassibi River
River Drscharge (cms)
1200
800
400
0
Jan-98
Feb-98
Mar-98
Apr-98
May-98
Jun-98
Jul-98
Aug-98
Sep-98
Oct-98
Nov-98
Dec-98
Date
Observed
HBV-96
WATFLOOD

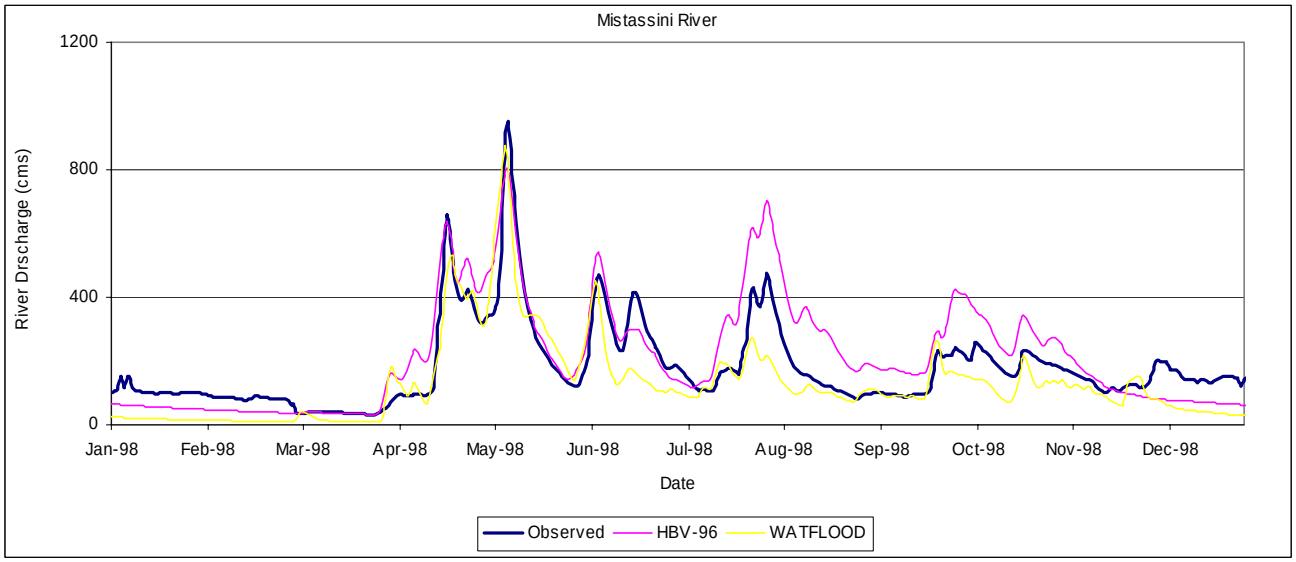
Mistassini River
River Drscharge (cms)
1200
800
400
0
Jan-98
Feb-98
Mar-98
Apr-98
May-98
Jun-98
Jul-98
Aug-98
Sep-98
Oct-98
Nov-98
Dec-98
Date
Observed
HBV-96
WATFLOOD

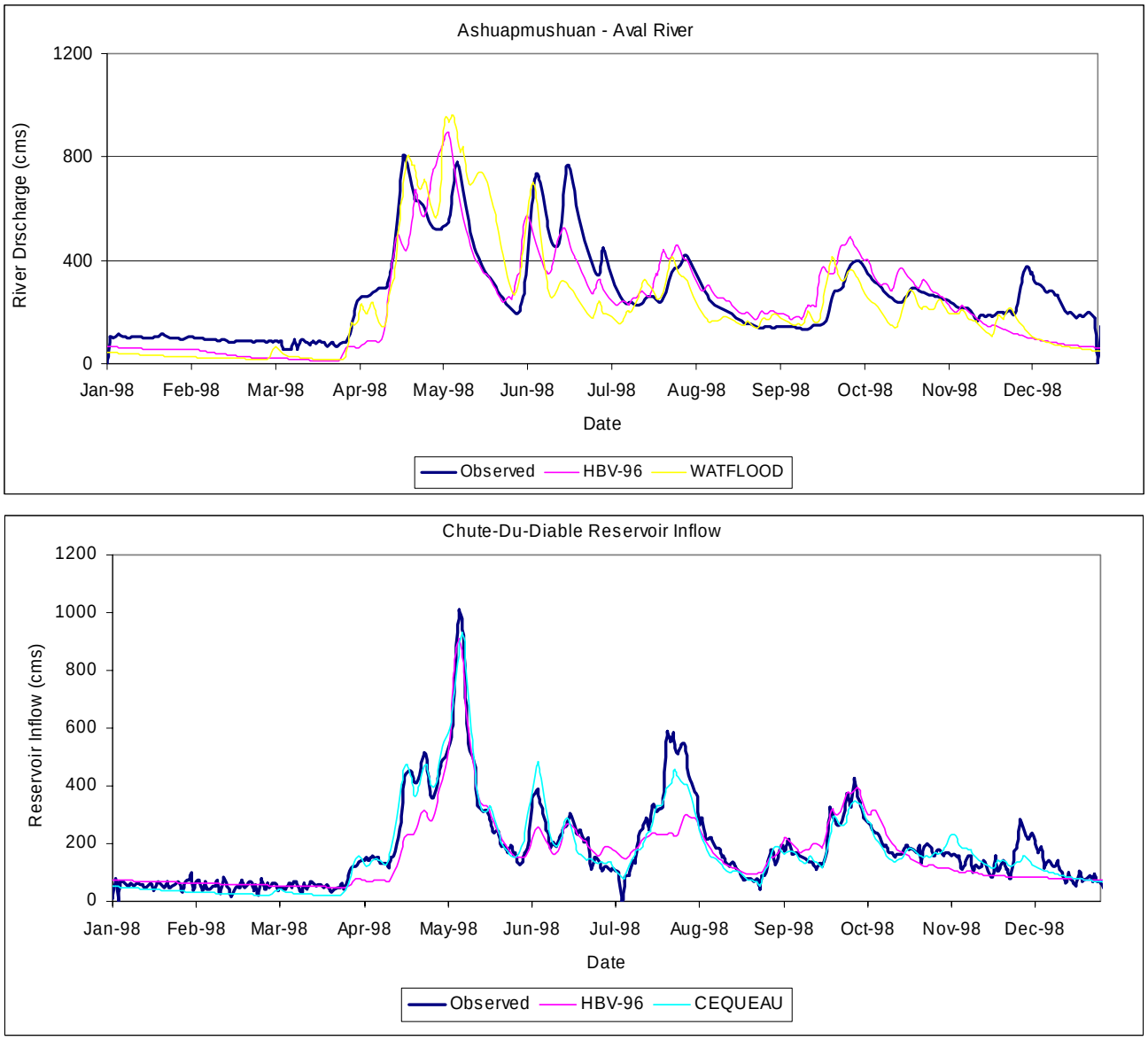

Figure 24. Comparison of validation results of the three hydrologic models for the simulation of flows in the different rivers.

8.3. Hydrologic impact of future climate change scenario

The ultimate objective of the downscaling exercise is to generate a reliable estimate of meteorological variables corresponding to a given scenario of the future climate so that these meteorological variables will be used as basis for different types of impact studies. Therefore, after calibrating the hydrological models with the historical record, the next step in the investigation is to simulate river flows in the watershed corresponding to future climate conditions by using the downscaled precipitation and temperature data described in section 5 as input to the hydrologic

models. Such simulation helps to identify the possible trend in the mean flow as well as low and peak flow values corresponding to the 'business as usual' climate change scenario.

The simulation is done with each hydrological model described in the previous sections. Inputs to the hydrological model consist of future precipitation and temperature data downscaled with SDSM, LARS-WG and DANN. Then simulation results correspond to each of the downscaling scenario time periods (Current, 2020s, 2050s and 2080s) are analyzed for all months of the year. Monthly mean, high and low flows are calculated for each year and then averaged over the number of years in each scenario period. The simulation results corresponding to each combination of downscaling techniques and hydrological models for the Chute-du-Diable reservoir inflow and the flow in four selected rivers in the Saguenay watershed are summarized in Table 11. The scenario simulation outputs corresponding to each hydrologic model are also presented in Figure 25. The figure shows simulated changes in monthly mean flows between the current and the 2080s time period corresponding to precipitation and temperature downscaled with all the three different downscaling methods. Similar results corresponding to scenario simulations of flows in the other rivers can be found in Annex 1C.

Table 11. Simulated changes in mean river flow corresponding to different downscaling and hydrologic models

Hydrologic Model	**River**	Average Increase / Decrease (%)								
		SDSM			**LARS**			**DANN**		
		2020s	2050s	2080s	2020s	2050s	2080s	2020s	2050s	2080s
WATFLOOD	Serpent	9.0	21.7	30.8	-6.8	-3.4	-6.1	15.1	11.6	14.7
	Mistassibi	-0.1	2.8	3.0	-3.0	-2.7	-7.6	15.6	11.3	19.4
	Mistassini	1.2	5.2	8.2	-2.0	-2.9	-7.1	-3.2	-8.4	-8.1
	Asham_Aval	0.2	6.4	13.5	-2.6	-1.9	-6.2	0.0	-4.6	1.4
		Average Increase / Decrease (%)								
		SDSM			**LARS**			**DANN**		
		2020s	2050s	2080s	2020s	2050s	2080s	2020s	2050s	2080s
HBV-96	Serpent	12.4	28.2	39.1	-4.9	-4.1	-6.4	13.6	12.6	20.5
	Mistassibi	-5.1	-11.2	11.4	0.8	-4.4	-7.5	14.5	21.3	31.0
	Mistassini	6.0	13.8	24.1	1.4	-5.9	-6.2	-9.0	-13.4	-16.0
	Asham_Aval	-1.2	4.6	16.2	-1.9	-0.8	-8.0	10.3	7.5	31.3
	Chute Du Diable	11.4	22.9	39.2	0.2	-2.6	-8.4	6.3	2.2	15.7
		Average Increase / Decrease (%)								
		SDSM			**LARS**			**DANN**		
		2020s	2050s	2080s	2020s	2050s	2080s	2020s	2050s	2080s
CEQUEAU	Serpent	5.3	12.4	16.1	-4.7	-9.4	-15.3	25.0	24.6	44.6
	Chute Du Diable	0.8	4.7	7.4	-3.7	-8.6	-17.3	44.2	43.5	70.9

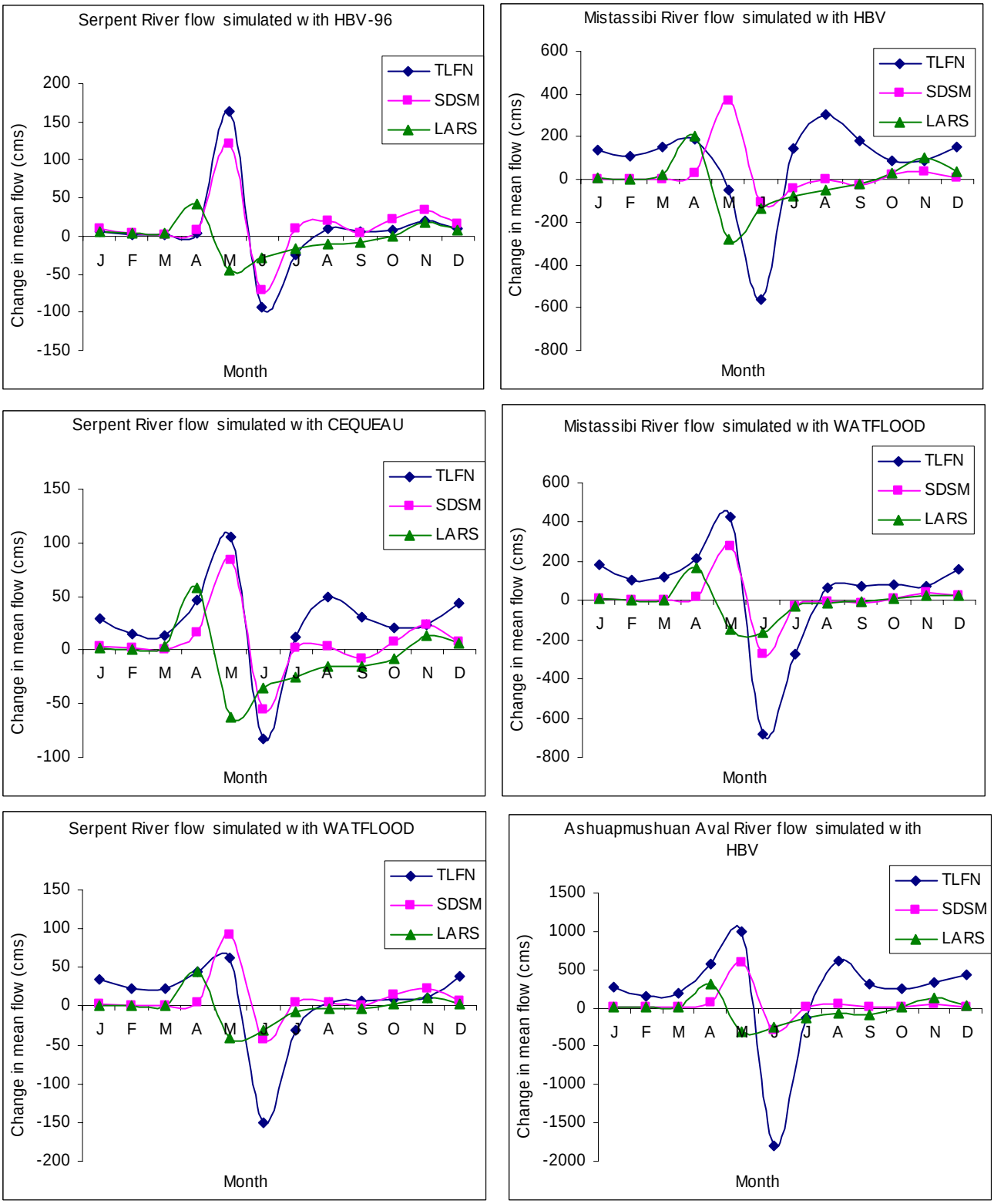

Figure 25. Comparison of simulated changes (between the current and the 2080s time period) in monthly mean flows of selected rivers corresponding to the 'business as usual' scenario.

The results in Table 11 show that, for the period between the current and the 2080s, the GCM data downscaled with SDSM and DANN and simulated with each of the hydrologic models resulted in an increasing trend of average stream flow in most of the rivers. In general, the once downscaled with SDSM resulted in a change in the mean annual flow of between +3% and +39% while the once downscaled with DANN resulted in a change in mean annual flow of between -16% to +31%. However the once downscaled with LARS-WG and simulated with the same hydrological models resulted in a decreasing of mean annual flow in the rivers in the range of -6% to -17%. Once again, this result is consistent with the downscaling results discussed in section 5 whereby precipitation downscaled with DANN and SDSM show an increase in annual precipitation while the one downscaled with LARS-WG does not show any significant increase during the same time period. The results in Table 11 also shows that the overall changes in mean annual flows simulated by the two lumped conceptual hydrologic models are very comparable. However, Figure 25 shows that the GCM scenario data downscaled with DANN and SDSM and simulated with HBV-96 resulted in the highest increase in the river flow in May, and the highest decrease in June. The same scenario data simulated with WATFLOOD resulted in increasing river flows between December and May and a decrease in flow in June and July. Conversely, the GCM data downscaled with LARS-WG resulted in the largest increase in the river flow in April, with a flow decrease for the rest of the spring and summer months. This is all consistent with the predicted increase in the temperature, particularly the winter temperature (about 5 to 6 °C), and the associated earlier beginning of snow melting which would increase the runoff effect. Moreover, all the three downscaling methods resulted in an increase in low flow during the winter months once again consistent with the overall increase in winter temperature and its effect in reducing freezing. However, the hydrologic simulation corresponding with the DANN downscaled data resulted in the highest increase in the spring mean and peak flow in May and the highest decrease in mean flow in the following months also consistent with the highest increase in temperature predicted by the same downscaling technique.

8.4. Flood frequency analysis of river flow simulation outputs

Flood frequency analysis is the determination of the magnitude of flood flows at different frequencies or recurrence intervals. Due to its large economical and environmental impact, such analysis remains a subject of great importance in watershed infrastructures design and management. Flood frequency analyses are usually based on annual flood series. The standard procedure to determine probabilities of flood flows consists of fitting the observed stream flow record to specific probability distributions. Assuming independence and stationarity, a statistical distribution is fitted to the data using a given estimation method, and a flood with pre-specified exceedance probability can then be inferred from this distribution. There are a number of two- and three-parameter distributions described in the literature (Cunnane, 1987), such as: Gumbel, Generalized Extreme Value, Generalized Logistic, log-Normal, Gamma, and log-Pearson III. However, the log-Pearson III method is generally recommended for frequency analysis of annual flood serious (Klemes, 1993).

The possible consequence of climate change in the mean monthly or annual flow of rivers in the Saguenay watershed has been shown in section 6.3 above. However, that analysis doesn't explain the effect of climate change on the frequency of extreme or heavy flood events. In this section, the possible impact of climate change on the flood frequency of the rivers in the Saguenay watershed is investigated. The result will show the possible trend in the frequency of flooding in each of the rivers corresponding to the 'business as usual' climate change scenario. The US Army Corps of Engineers' flood frequency analysis software known as HEC-FFA is used in this study. HEC-FFA is used to compute flood frequencies in accordance with "Guidelines for Determining Flood Flow Frequencies" Bulletin 17B of the U.S Water Resources Council (WRC), March 1982. This guideline is designed for computing flood flow frequency curves where systematic stream gauging records of sufficient length (at least 10 years) to warrant statistical analysis are available as the basis for determination. When developing a flood flow frequency curve, the analyst should consider all available information; which could be either observed flood discharge data or flood discharges estimated from climatic data (rainfall and/or snowmelt). Such estimates require adequate climatic data and a calibrated watershed model for converting precipitation to discharge. Once the discharge data is made available, flood events can be analyzed using either annual or partial-duration series. The annual flood series is based on the maximum flood peak for each year. A partial-duration series is obtained by taking all flood peaks equal to or greater than a predefined base flood. The analysis in this section is based on the annual flood series. The Pearson Type III distribution with log transformation of the flood data (log-Pearson Type III) is recommended as the basic distribution for defining annual flood series and is implemented in HEC-FFA. The method of moments is used to determine the statistical parameters of the distribution from station data.

Once again, the river flow simulations made for the current and future time periods by the three hydrological models describe earlier (HBV-96, CEQUEAU, and WATFLOOD) are the basis for the flood frequency analysis. The hydrologic simulations are also based on the precipitation and temperature data downscaled with the three downscaling models (SDSM, LARS-WG and DANN) described in section 3. Therefore, the flood frequency analysis of each river may give different outcomes based on the particular combination of downscaling technique and hydrological model employed for the simulation of flow in that river. Figures 26 to 28 show the result of such flood frequency analysis of the simulated flows in Serpent River corresponding to all the possible combinations of downscaling techniques and hydrological models described in previous section. Flood frequency analysis graphs of the Chute du Diable reservoir inflow and three more rivers in the Saguenay watershed are presented in Annex 1D. All the results are also summarized in Table 12 which presents the percentage increase in peak flow (from the current period) in each river corresponding to different return periods (20, 50 and 100) by the 2080s. These results indicate that, on average, the GCM output downscaled with DANN gave relatively larger increases in the frequency of peak flows than those downscaled with SDSM and LARS. SDSM seems to result in a relatively smaller increase in the frequency of flood events than the other two. Moreover, the analysis indicates that the overall increasing trend in the frequency of flood event is not a linear one. This can

be witnessed from the graphs where frequency curves corresponding to the 2020s are above the one for 2080s. Interestingly, the results of the frequency analysis of peak flows simulated with all the three hydrological models are found to be relatively consistent. However, simulations made by the HBV-96 seems to give the highest increase in the frequency of peak flow followed by WATFLOOD and CEQUEAU. For instance, the increase in the magnitude of 100 year flood in the Serpent River is found to vary in the range of around 8% to 36% depending on the particular choice of downscaling technique and hydrologic model used in each study. Similar variations are also shown in the case of the other simulated rivers. But in general, the 100 year flood of the current climate seems to reduce to a flood event of 20 to 50 years return period by the 2080s. This will, of course, have profound implications in the design of hydraulic structure in the Saguenay watershed.

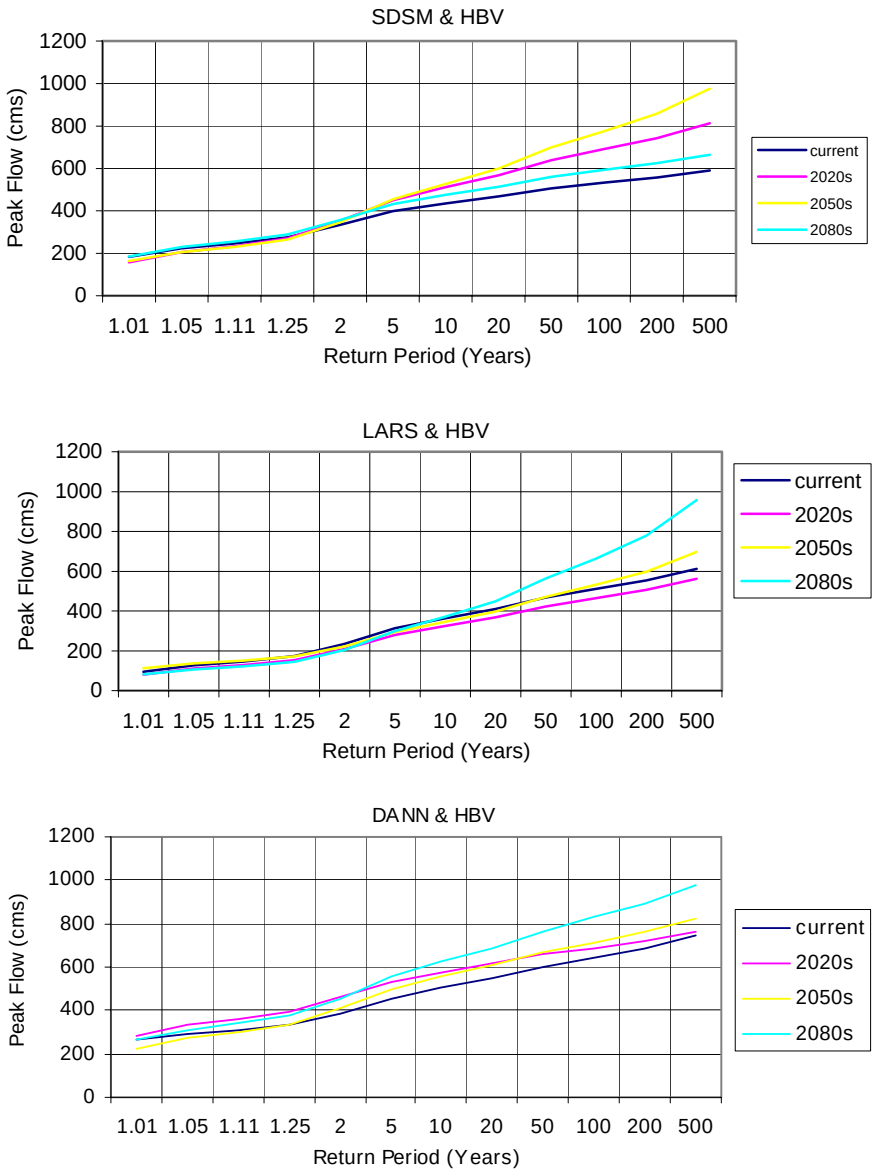

Figure 26 Flood frequency curves for Serpent River based on scenario simulations with HBV hydrologic model and input data downscaled with SDSM, LARS-WG and DANN respectively

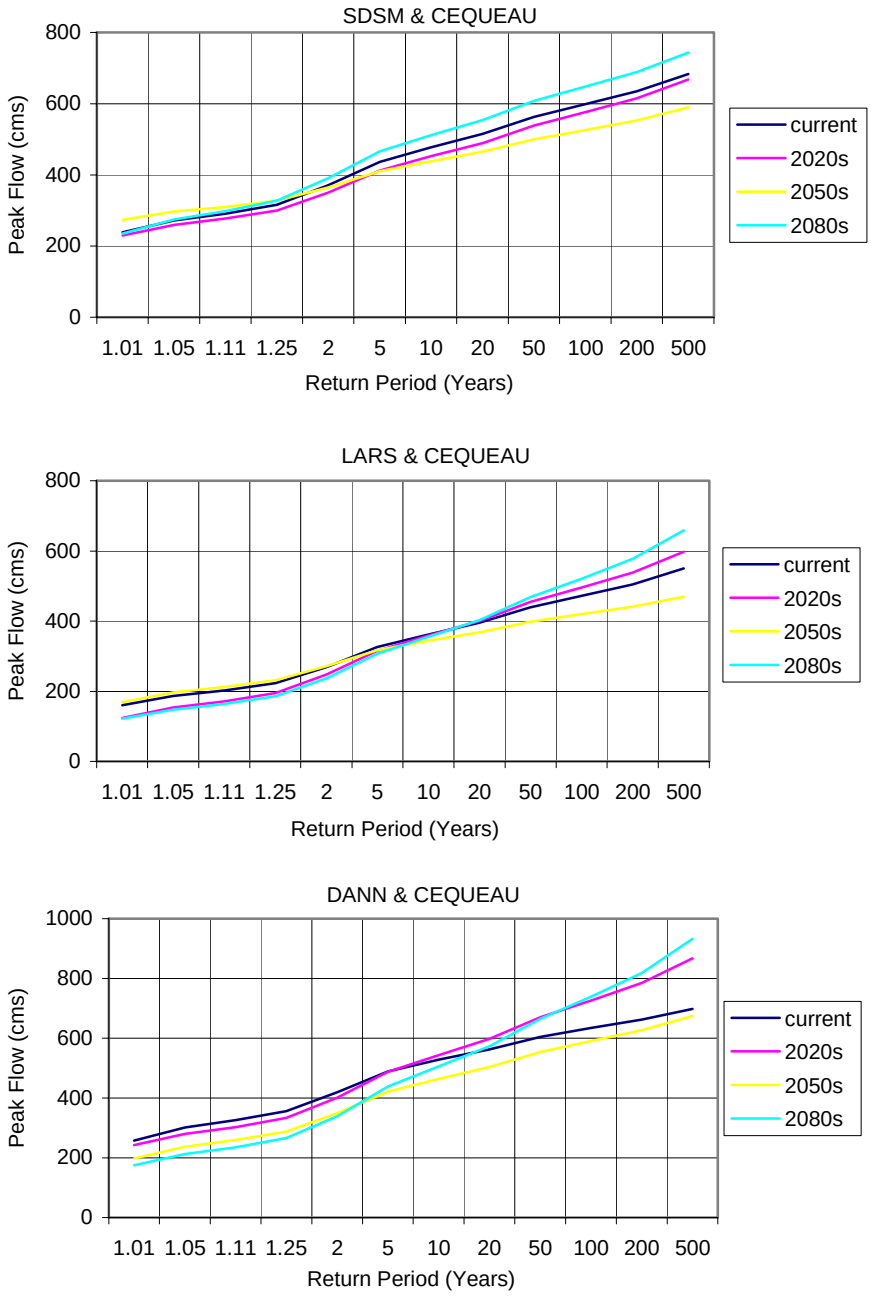

Figure 27 Flood frequency curves for Serpent River based on future scenario simulation with CEQUEAU hydrologic model and input data downscaled with SDSM, LARS-WG and DANN models respectively

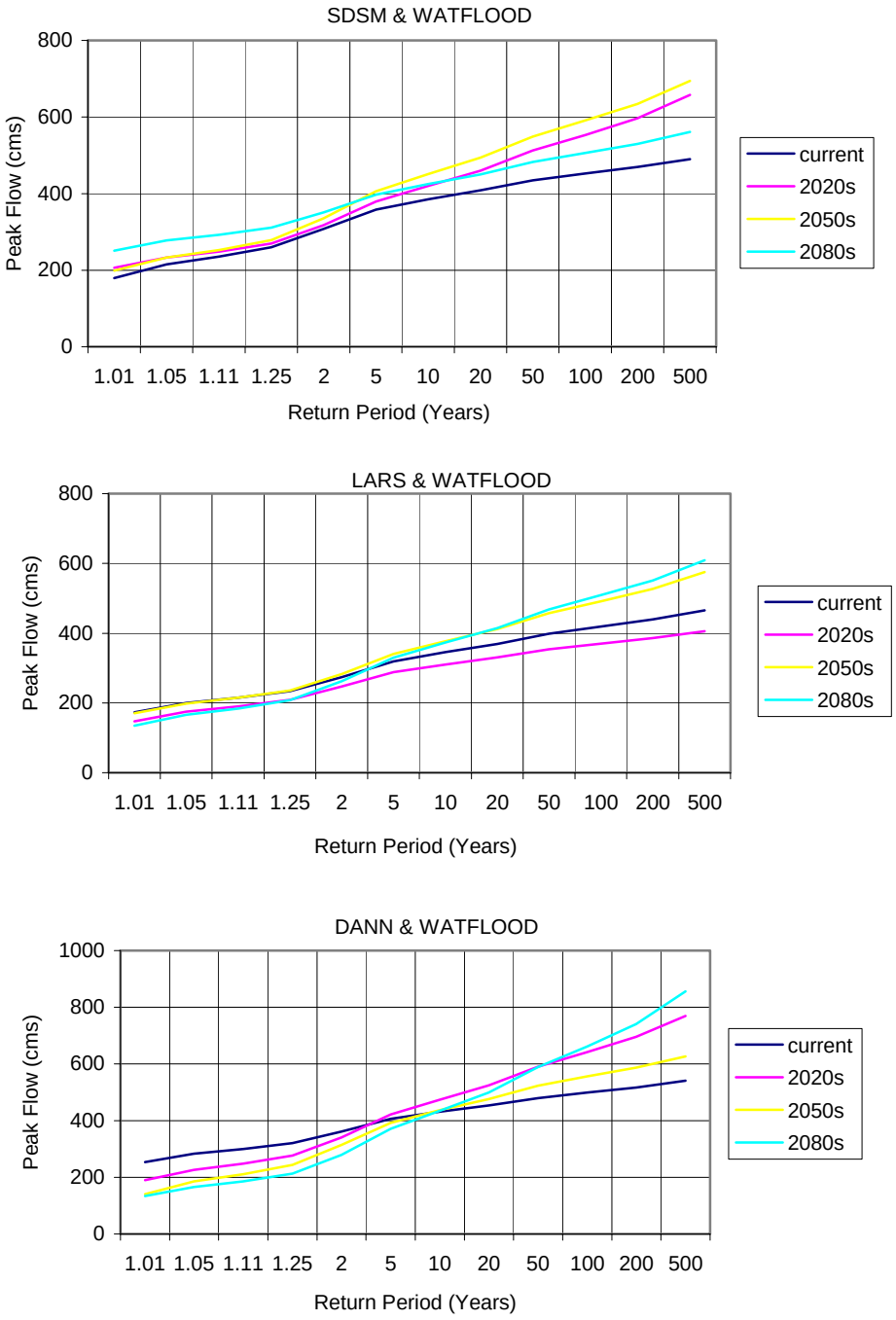

Figure 28 Flood frequency curves for Serpent River based on future scenario simulation with WATFLOOD hydrologic model and input data downscaled with SDSM, LARS-WG and DANN models respectively

Table 12. Changes in flood magnitudes between the current and the 2080s time period corresponding to different modelling systems and return periods (%)

Downscaling Techniques	**Rivers**	**Hydrologic Models**								
		HBV-96			**WATFLOOD**			**CEQUEAU**		
	Return Per ->	**20**	**50**	**100**	**20**	**50**	**100**	**20**	**50**	**100**
	Serpent	9.9	10.7	11.4	10.3	10.9	11.8	7.6	8.0	8.3
	Mistassibi	23.9	21.3	19.6	0.9	1.2	1.6	-	-	-
SDSM	Mistassini	19.3	20.9	22.1	12.0	12.8	13.6	-	-	-
	Asham_Aval	16.0	18.9	21.3	23.3	26.6	29.5	-	-	-
	Chute Du Diable	19.3	19.0	18.6	-	-	-	3.5	4.2	4.9
		Hydrologic Models								
		HBV-96			**WATFLOOD**			**CEQUEAU**		
	Return Per ->	**20**	**50**	**100**	**20**	**50**	**100**	**20**	**50**	**100**
	Serpent	9.5	20.6	30.0	12.2	17.5	21.5	1.9	6.8	10.5
	Mistassibi	-0.6	1.4	2.4	7.8	13.0	16.7	-	-	-
LARS	Mistassini	-6.8	0.7	7.0	-2.3	0.6	2.8	-	-	-
	Asham_Aval	74.8	68.3	63.1	-1.7	0.8	2.7	-	-	-
	Chute Du Diable	-12.7	-14.3	-15.5	-	-	-	-9.3	-7.4	-5.8
		Hydrologic Models								
		HBV-96			**WATFLOOD**			**CEQUEAU**		
	Return Per ->	**20**	**50**	**100**	**20**	**50**	**100**	**20**	**50**	**100**
	Serpent	25.6	27.4	28.5	10.1	22.7	32.7	1.8	10.0	16.6
	Mistassibi	-2.1	13.0	25.3	8.8	19.6	27.6	-	-	-
DANN	Mistassini	-6.9	2.1	9.1	-8.1	-3.8	-0.9	-	-	-
	Asham_Aval	-11.6	-5.4	-0.8	-4.8	4.1	11.2	-	-	-
	Chute Du Diable	-11.7	-4.3	1.6	-	-	-	12.7	21.7	28.6

9. Summary and Conclusion

This report presents the results of a study on downscaling of large scale atmospheric variables simulated with Global Climate Models (GCMs) to meteorological variables at regional and local scale in order to investigate the hydrological impact of a possible future climate change scenario. Downscaling is necessary since the hydrological models normally used for impact studies require local meteorological time series which are compatible with the size of the watershed for which the possible impacts of climate change are to be analysed. There are various downscaling techniques available to convert GCM outputs into daily meteorological variables appropriate for hydrologic impact studies. However, the interest in nonlinear regression methods, namely, artificial neural networks is nowadays increasing because of their high potential for complex, nonlinear and time-varying input-output mapping. This study investigated the applicability of dynamic artificial neural networks (DANN) as downscaling methods for daily rainfall and temperature prediction at a number of stations in the Saguenay-Lac-Saint Jean watershed and compares the results with that of the most widely used *multiple linear regression* (SDSM) and *stochastic weather generator* (LARS-WG) techniques. The downscaled temperature and precipitation data are also used to investigate the possible impact of climate change on the hydrology of the region by simulating possible future flows in a number of rivers which are located in the watershed. The impact analysis was done using three types of hydrological models in order to see the effect of the type of models used on the outcome of the hydrologic impact analysis.

The study found the *time lagged feedforward network* (TLFN) to be the best DANN for downscaling daily precipitation and temperature data while the results of the other DANN methods, namely the Elman and Jordan networks, were not satisfactory. While these networks were able to estimate the monthly mean precipitation and temperature data, they were unable to properly capture the variability of these data as well as the average dry and wet-spell lengths. Seasonal analysis of the downscaled results also shows that, the DANN has consistently resulted in lower root mean square error (RMSE) in simulating precipitation for each of the four seasons than the SDSM and LARS-WG downscaling techniques. Te uncertainness analysis in terms of model errors also shows the DANN model to be the least error and the least uncertain model in daily precipitation downscaling at 95% confidence level though the model does not preserve the variability well. Based on the same criterion, the SDSM seems to be the least error model at 95% confidence level for downscaling daily maximum and minimum temperatures; the variability is well preserved but the exhibited uncertainties are sometimes slightly higher than the DANN model. With respect to future trends, the DANN model has predicted an increase in average annual precipitation of the Saguenay watershed by the 2080s to be in the range of 16 to 36 percent while SDSM predicted an increase in annual precipitation in the range of 22 to 44 percent in the same time period. On the other hand, LARS-WG downscaling results have not shown any significant change in precipitation for the same time period. Moreover, downscaling result for daily temperature corresponding to all the three models show a comparable and consistently increasing trend in the mean annual temperature ranging between 4 to 5 ^{o}C for the next 100 years.

At the same time, the hydrological simulation which was based on the downscaled precipitation and temperature data showed an overall increasing trend in the mean annual flow in most of the rivers in the

Saguenay watershed. However, the magnitude of this change for the next hundred years varies between -8 and +40 percent depending on the type of hydrological model and the particular catchment for which the river flow or reservoir inflow is being simulated. In general the hydrologic simulation result shows that, while the data downscaled with DANN and SDSM resulted in an increase in mean annual flow in the range of 10 to 40 percent in the next 100 years, the one downscaled with LARS-WG resulted in a decrease in mean annual flow of up to 10 percent for the same time period. When we consider climate change impact on monthly basis, the data downscaled with DANN and SDSM resulted in the highest increase in river flows (and reservoir inflow) in May, and the highest decrease in June which seems to be the result of earlier spring snow melt effect. However, the same data downscaled with LARS-WG resulted in the increased river flow in April followed by decreased flow for the rest of the spring and summer months. Nevertheless, all the three downscaling methods resulted in an increase in low flow during the winter months in most of the simulated rivers which is consistent with the overall increase in winter temperature and its effect in reducing freezing.

The flood frequency analysis done on the simulated peak flows indicated an overall increasing trend in the frequencies of flood events in most of the major rivers in the Saguenay watershed. The study also indicated that, on average, the GCM output downscaled with DANN gave relatively larger increases in the magnitude of less frequent events (events with high return periods) than those downscaled with SDSM and LARS. SDSM seems to result in a relatively smaller increase in the frequency of flood events for the next 100 years than the other two. Interestingly, the results of the frequency analysis of peak flows simulated with all the three hydrological models are found to be relatively consistent. However, simulations made with HBV-96 seem to give the highest increase in the frequency of peak flow followed by WATFLOOD and CEQUEAU. This is a clear indication of how the outcome of a hydrologic impact study (or any other impact study based on downscaled data) can be affected by the choice of any one particular downscaling technique and hydrological model combination over the other.

Acknowledgement

This work was made possible through a grant from the Canadian Climate Change Action Fund, Environment Canada, and a grant from the Natural Sciences and Engineering Research Council of Canada to the first author. The authors gratefully acknowledge the contribution of a number of students who were involved at various stage of the project.

References

Arheimer, B., 1998: Riverine Nitrogen – analysis and modelling under Nordic conditions. Kanaltryckeriet, Motala. pp. 200.

ASCE Task Committee on Application of Artificial Neural Networks in Hydrology (2000a) Artificial Neural Networks in Hydrology. I: Preliminary Concepts, *ASCE Journal of Hydrologic Engineering*, Vol. 5, No. 2, pp. 115-123.

Bergström, S. and Forsman, A.,1973: Development of a conceptual deterministic rainfall-runoff model. *Nordic Hydrology*, 4, 147-170.

Beven, K.J. 2001. *Rainfall-Runoff Modeling: The Primer*, John Wiley & Sons Ltd., England.

Brandt M. 1990. Simulation of runoff and nitrate transport from mixed basins in Sweden. *Nordic Hydrology* **21**: 13–34.

Buletin 17B, 1982, *Guidelines for Determining Flood Flow Frequency*, Revised Bulletin 17B of the Hydrology Committee, U.S. Water Resources Council.

Cannon, A.J., Whitfield, P.H. 2002. Downscaling recent streamflow conditions in British Columbia, Canada using ensemble neural network models. *Journal of Hydrology*, 259: 136-151.

Carter**,** T.R., M.L. Parry, H. Harasawa, and S. Nishioka, 1994: IPCC Technical Guidelines for Assessing Climate Change Impacts and Adaptations. University College, London, United Kingdom, and Centre for Global Environmental Research, Tsukuba, Japan, 59 pp.

Conway, D., Wilby, R.L. and Jones, P.D. 1996. Precipitation and air flow indices over the British Isles. *Climate Research*, **7**, 169–183.

Coulibaly P., Anctil F., Aravena, R. & Bobée, B. 2001a. ANN modeling of water table depth fluctuations. Water Resources Research, 37(4): 885-896.

Coulibaly, P., Anctil F. & Bobée. B. 2001b. Multivariate reservoir inflow forecasting using temporal neural networks. Journal of Hydrologic Engineering, ASCE, 6(5): 367-376.

Cunnane, C., 1987. Review of statistical methods for flood frequency estimation, in *Hydrologic Frequency Modeling*, edited by V.P. Singh, pp. 49-95, D. Reidel, Dordrecht.

Dibike, Y.B. and Coulibaly P. 2003. Downscaling of global climate model outputs for flood frequency analysis in the Saguenay River system, Progress report to Climate Change Action Fund, Environment Canada.

Dibike, Y.B., Solomatine, D., and Abbott, M.B. (1999). On the encapsulation of numerical-hydraulic models in artificial neural network, Journal of Hydraulic research, Vol. 37, No. 2, pp. 147-161.

Elman, J. (1990) Finding structure in time, Cognitive Science, No. 14, pp. 179-211.

Gautam, D.K., and Holz, K.-P. 2000. Neural network based system identification approach for the modelling of water resources and environmental systems, In Schleider and Zijderveld (eds.) Artificial Intelligence Methods in Civil Engineering Applications, pp. 87-100.

Harlin, J., Kung, C.-S., 1992. Parameter uncertainty and simulation of design floods in Sweden. *Journal of Hydrology* 137, 209-230.

Hughes, J.P., P. Guttorpi and S.P. Charles, 1999: A non-homogeneous hidden Markov model for precipitation occurrence. Appl. Statist., 48, 15–30.

Haykin, S. 1999. *Neural Networks: A Comprehensive Foundation*, Prentice-Hall Inc., New Jersey.

Jordan, M.L. (1986) Attractor dynamics and parallelism in a connectionist sequential machine. *Proc. of the 8th conference of the Cognitive Science Society*, pp. 532-546.

Kistler, R., Kalnay, E., Collins, W., Saha, S., White, G., Woollen, J., Chelliah, M., Ebisuzaki, W., Kanamitsu, M., Kousky, V., Dool, H.v.d, Jenne, R., and Fiorino, M., 2001. The NCEP/NCAR 50-Year Reanalysis, *Bulletin of the American Meteorological Society*, Vol. 82, No. 2, pp. 247-267.

Klemes, V., Probability of extreme hydrometeorological events---a different approach, in *Extreme Hydrological Events: Precipitation, Floods and Droughts*, pp. 167-176, IAHS, Publ. No. 213, 1993.

Kouwen, N., E.D. Soulis, A. Pietroniro, J. Donald, and R.A. Harrington, Grouped response units for distributed hydrologic modeling. *Journal of Water Resources Planning and Management, Vol. 119*, No. 3, pp. 289-305, 1993.

Liden, R., J. Harlin,2000. Analysis of conceptual rainfall-runoff Modelling performance in different climates. *Journal of Hydrology* 238, 231-247

Lidén, R., 2000: Conceptual runoff models for material transport estimations. Doctoral thesis, Dept. Water Resources Engineering, Lund Insitute of Technology, Lund University, Report No 1028, Lund, Sweden. 88 pp.+ appendices.

Lorrai, M., and Sechi, G.M. (1995) Neural Nets for Modelling Rainfall-Runoff Transformations, In: *Water resources management*, Vol. 9, pp. 299-313.

Morin, G., Cluis, D., Couillard, D., Jones, G., and Gauthier, J.M. 1983. *Modélisation de la température de l'eau à l'aide du modèle quantité-qualité CEQUEAU*. Scientific Report 153,INRS-Eau, Sainte-Foy, Que

Principe, J.C., Euliano, N.R., and Lefebvre, W.C. (2000*) Neural and Adaptive Systems: Fundamentals through Simulations*, John Wiley, New York.

Schoof, J.T., Pryor, S.C. 2001. Downscaling temperature and precipitation: a comparison of regression-based methods and artificial neural networks. *International Journal of Climatology*, 21: 773-790.

Schubert, S. and A. Henderson-Sellers, 1997. A statistical model to downscale local daily temperature extremes from synoptic-scale atmospheric circulation patterns in the Australian region. *Climate Dynamics*, 13, 223-234.

Semenov, M.A., Barrow, E.M. 1997. Use of stochastic weather generator in the development of climate change scenarios. *Climatic Change*, 35: 397-414.

Semenov, M.A., Barrow, E.M. 2002. LARS-WG: *a stochastic weather generator for use in climate impact studies*, Version 3.0, user manual

Societe d'electrolyse et de chimie Alcan Ltee (ALCAN),. 1982. Rapport Technique Final Du Projet: Nouvelle Technologie Pour Accroitre La Puissance Generee Par Un Systeme Hydroelectrique Complexe Deja Existant. Energie electrique Quebec. Jonquiere Quebec.

Trigo R.M., Palutikof J.P. 1999. Simulation of daily temperatures for climate change scenarios over Portugal: a Neural Network Model approach. *Climate Research* (13, 45-59).

US Army Corps of Engineers (US-ACE). 2000. Hydrologic Modeling System HEC-HMS Technical Reference Manual. Hydrologic Engineering Center. Davis, California.

von Storch, H., Hewitson, B. and Mearns, L. 2000. Review of Empirical Downscaling Techniques, in *Regional climate development under global warming*. General Technical Report No.4. Conf. Proceedings, Torbjornrud, Norway.

Weichert, A., Burger, G. 1998. Linear versus nonlinear techniques in downscaling. *Climate Research*, 10: 83-93.

Wigley, T. M. L., P. D. Jones, K. R. Briffa, and G. Smith, 1990: Obtaining subgrid scale information from coarse-resolution general circulation model output. J. Geophys. Res. 95, 1943-1953.

Wilby, R.

L., Dawson, C.W., Barrow, E.M. 2002. SDSM – a decision support tool for the assessment of regional climate change impacts. *Environmental Modelling & Software,* 17: 147-159.

Wilks, D.S. 1999. Multisite downscaling of daily precipitation with a stochastic weather generator. *Climate Research*, 11: 125-136.

Wilks, D. S. and R. L. Wilby, 1999: The weather generator game: A review of stochastic weather models. Prog. Phys. Geography, 23, 329-358.

Williams, R. J. and Zipser, D. (1995) Gradient-based learning algorithms for recurrent networks and their computational complexity. In: Y. Chauvin and D. E. Rumelhart (eds.) *Back-propagation: Theory, Architectures and Applications*, Hillsdale, NJ: Erlbau

Xu, C.Y. 1999. From GCM to River flow: A review of downscaling methods and hydrologic modeling approaches, *progress in physical Geography*, 23(2), pp. 229-249.

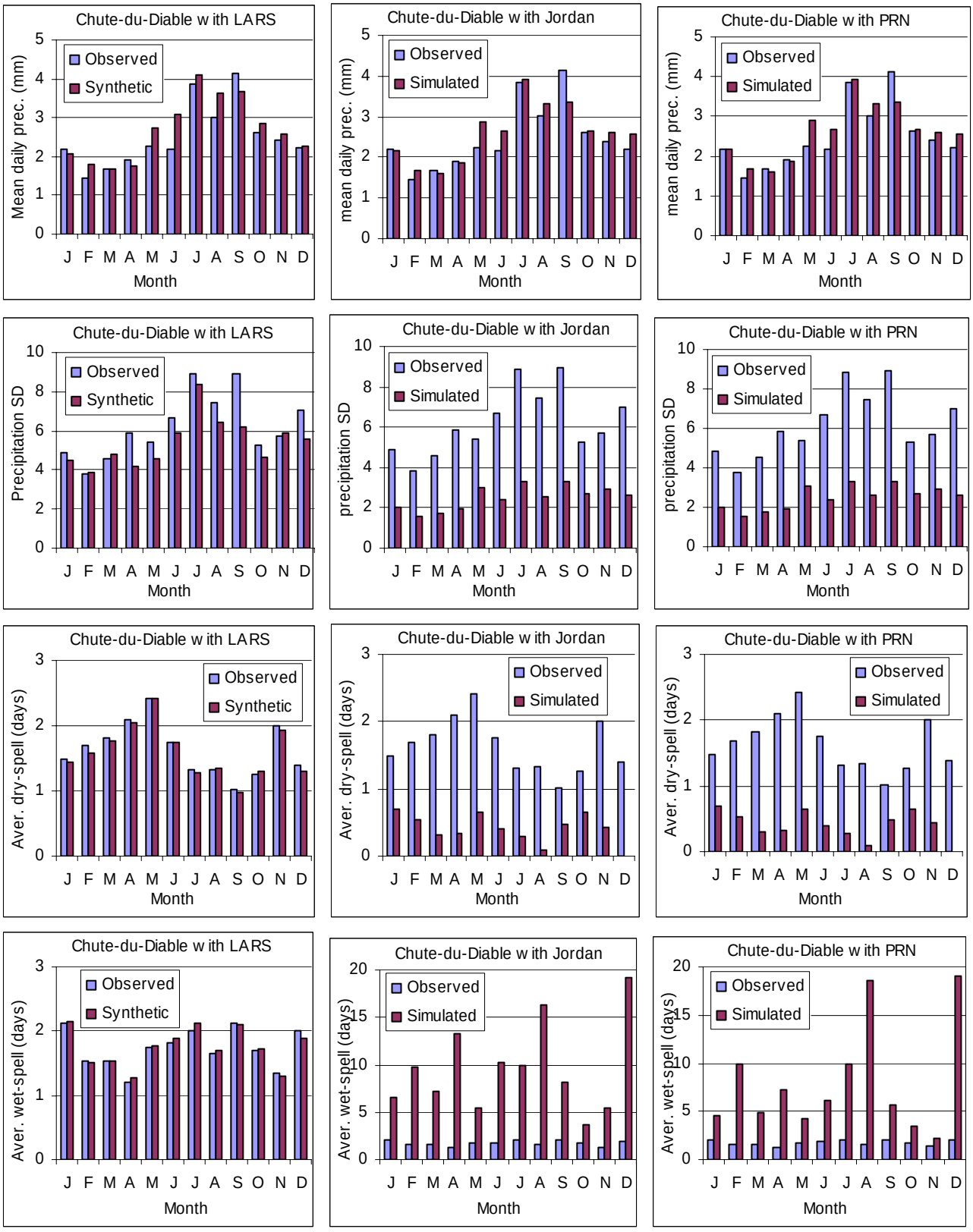

Annex A1 Validation performances of the three downscaling methods (LARS, Jordan & PRN networks) in downscaling daily precipitation data at the Chute-du-Diable

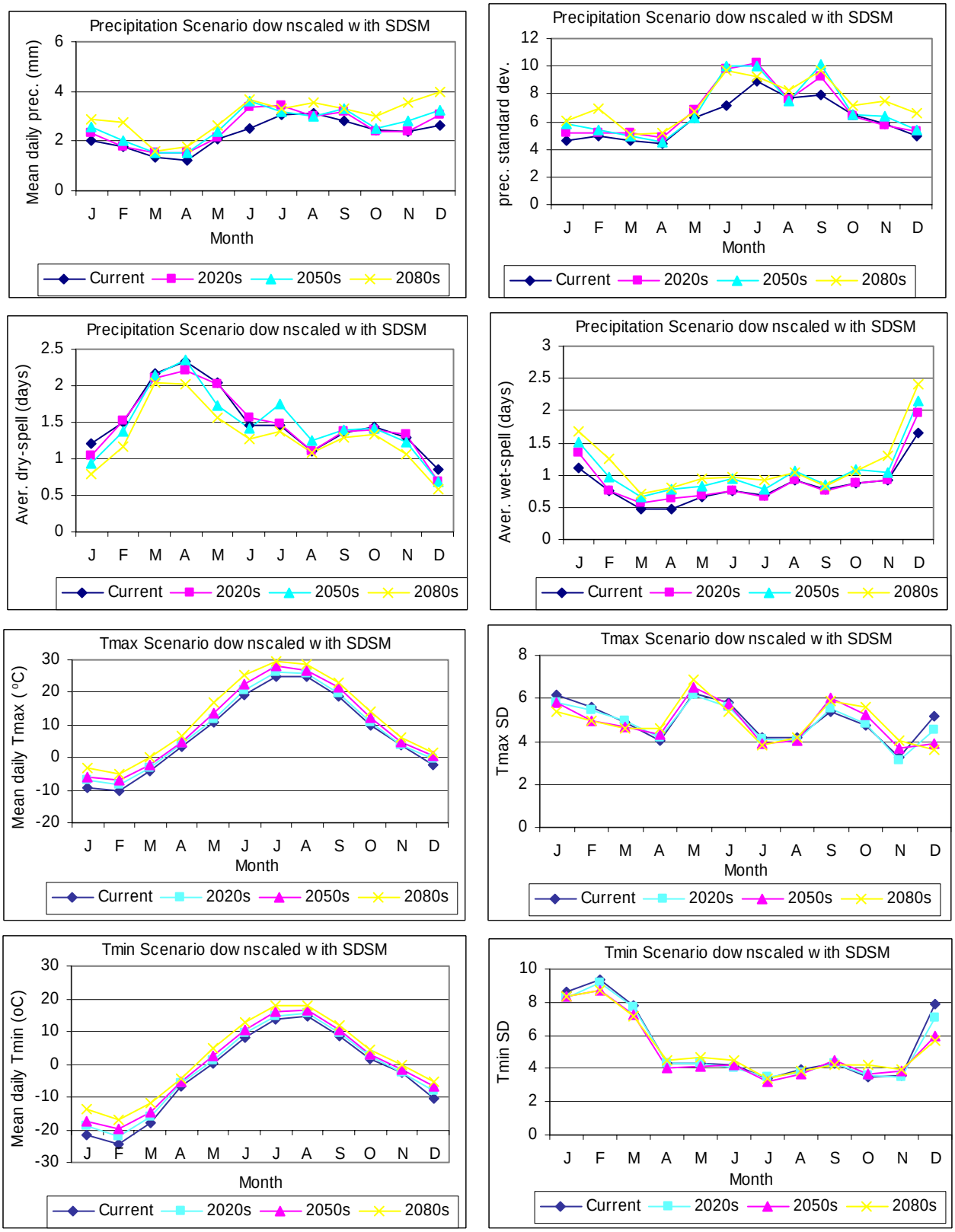

Annex A2. General trend in precipitation and temperature at Chute-du-Diable corresponding to a climate change scenario downscaled with SDSM

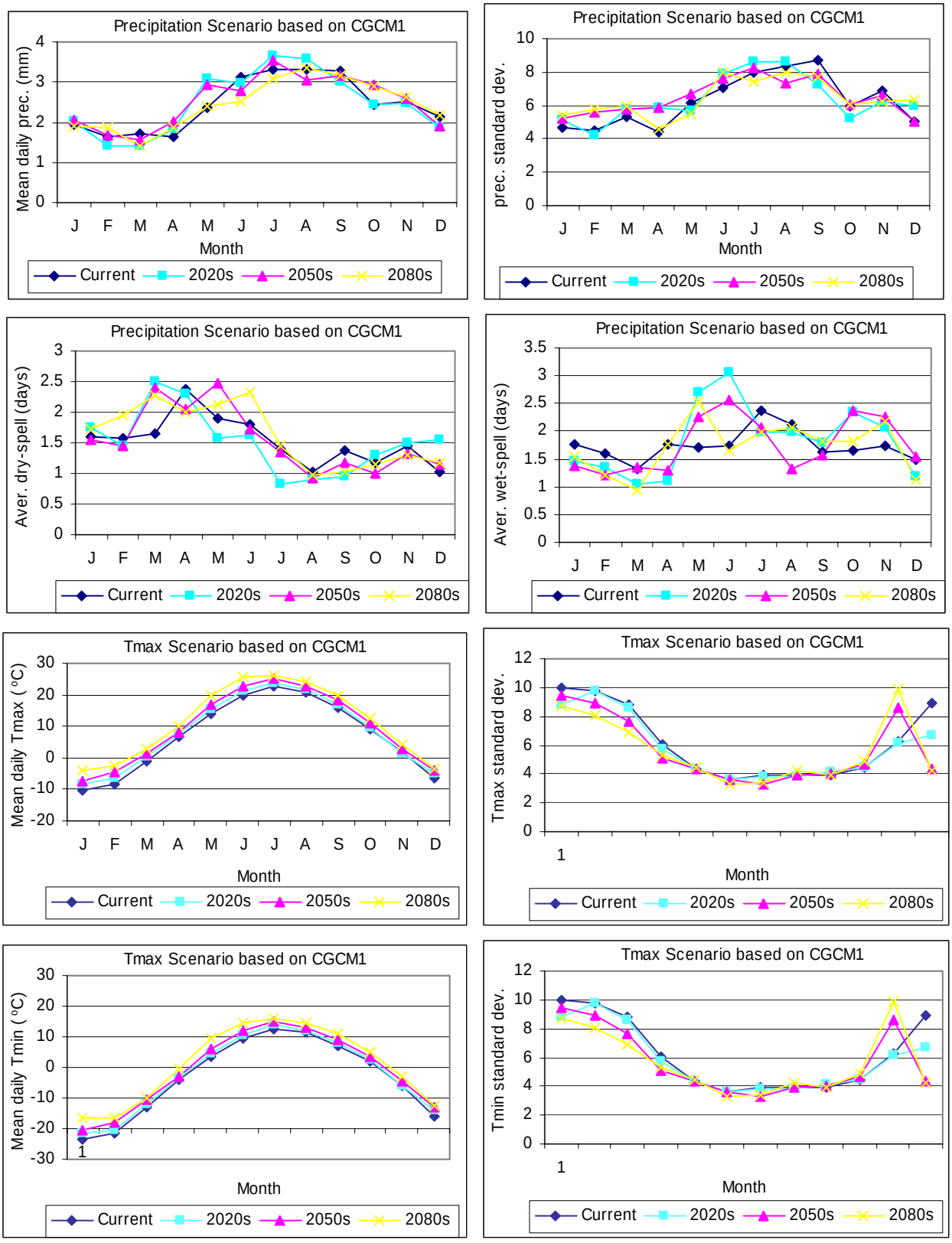

Annex A3. General trend in precipitation and temperature at Chute-du-Diable corresponding to a climate change scenario downscaled with LARS-WG

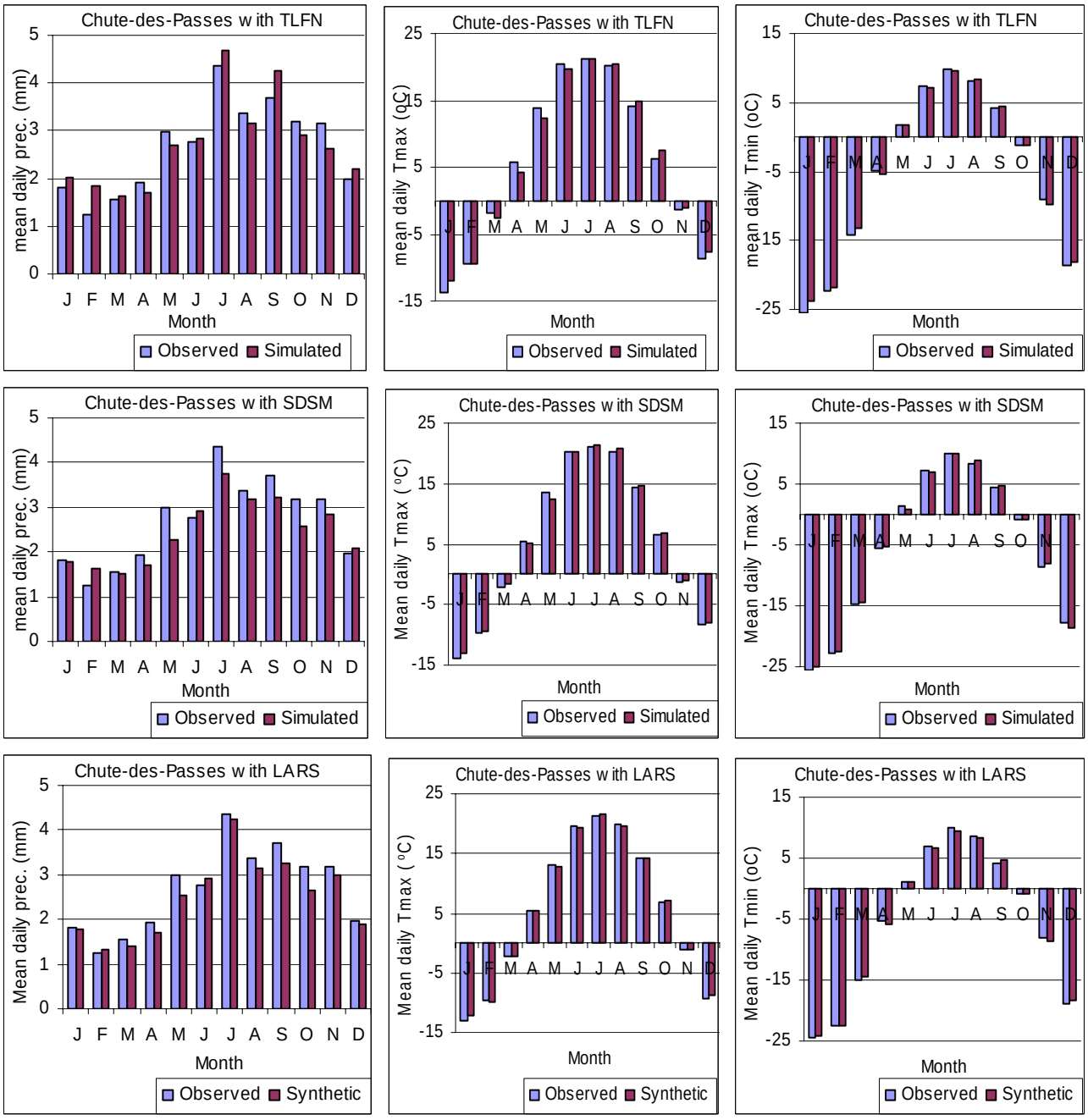

Annex B1. Validation performances of the three downscaling methods (DANN, SDSM, LARS) in downscaling daily precipitation and temperature data at the Chute des Passes station

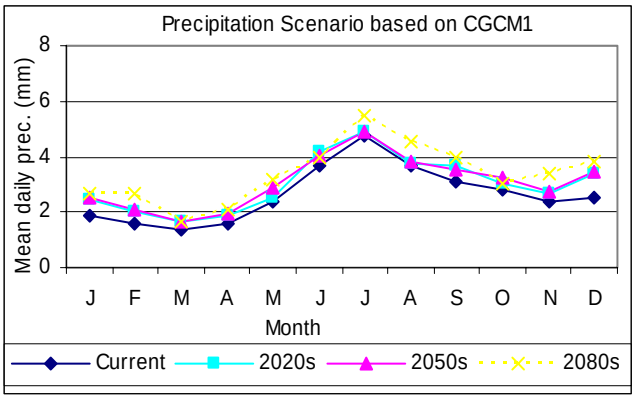

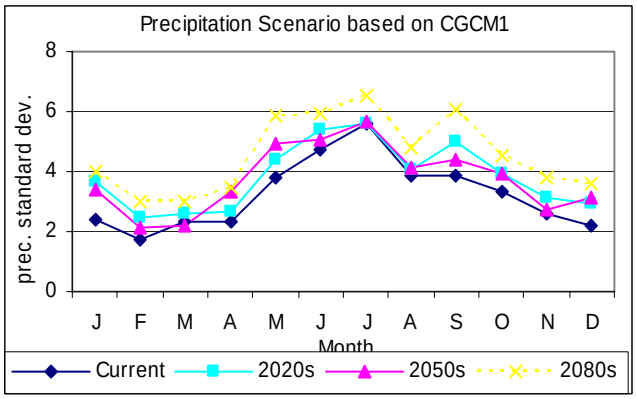

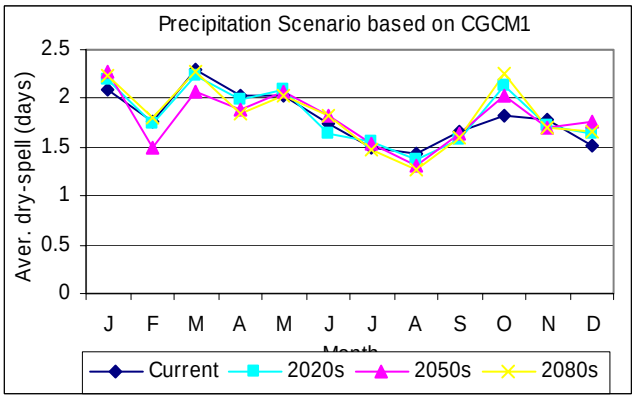

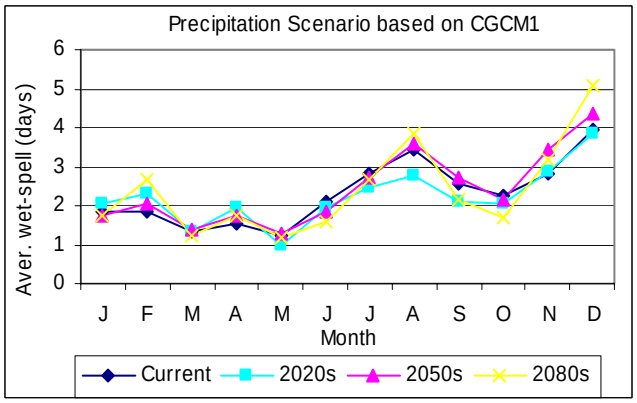

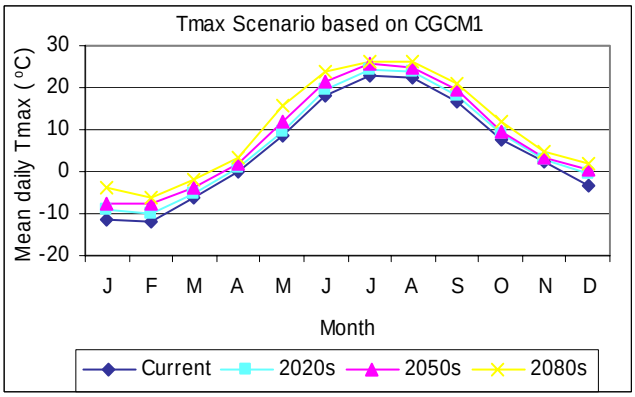

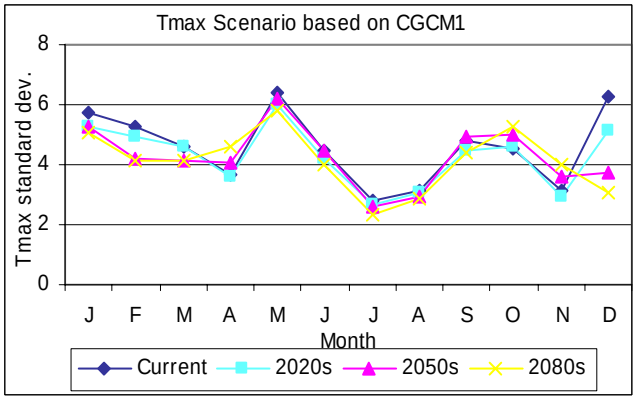

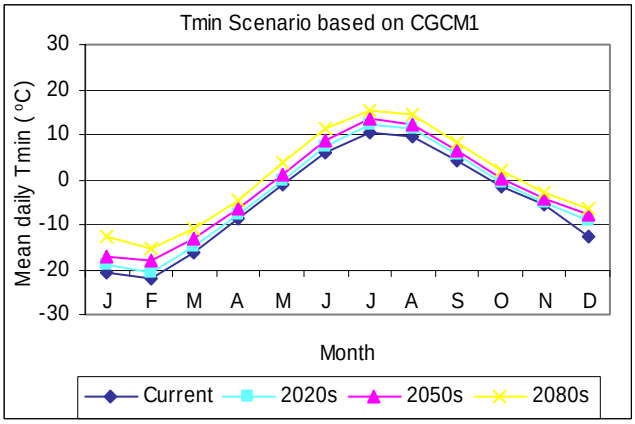

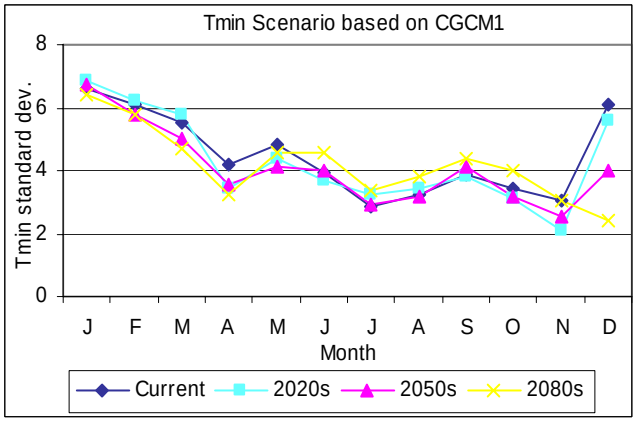

Annex B2. General trend in precipitation and temperature at Chute-des-passes corresponding to a climate change scenario downscaled with DANN

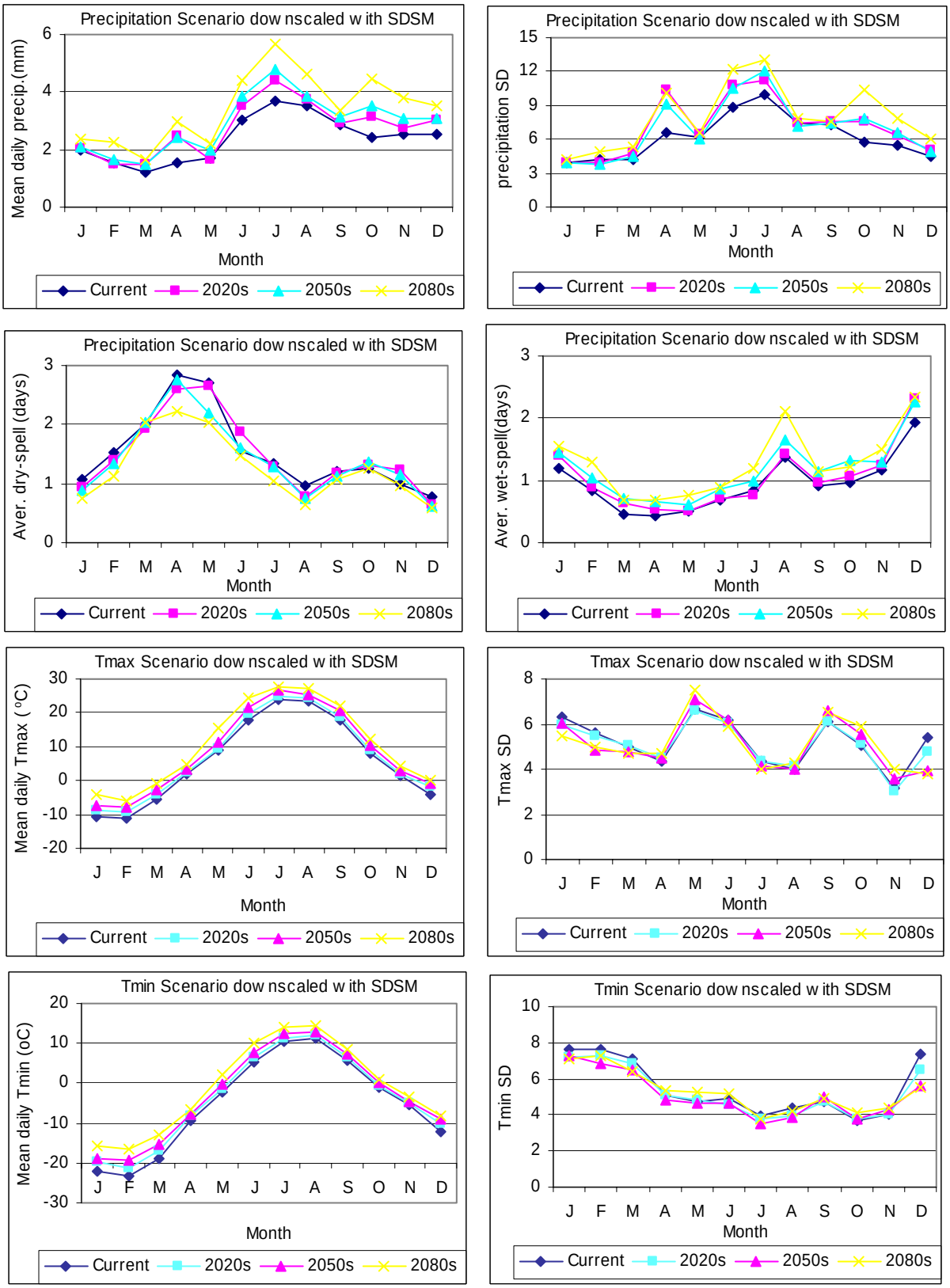

Annex B3. General trend in precipitation and temperature at Chute-des-passes corresponding to a climate change scenario downscaled with SDSM

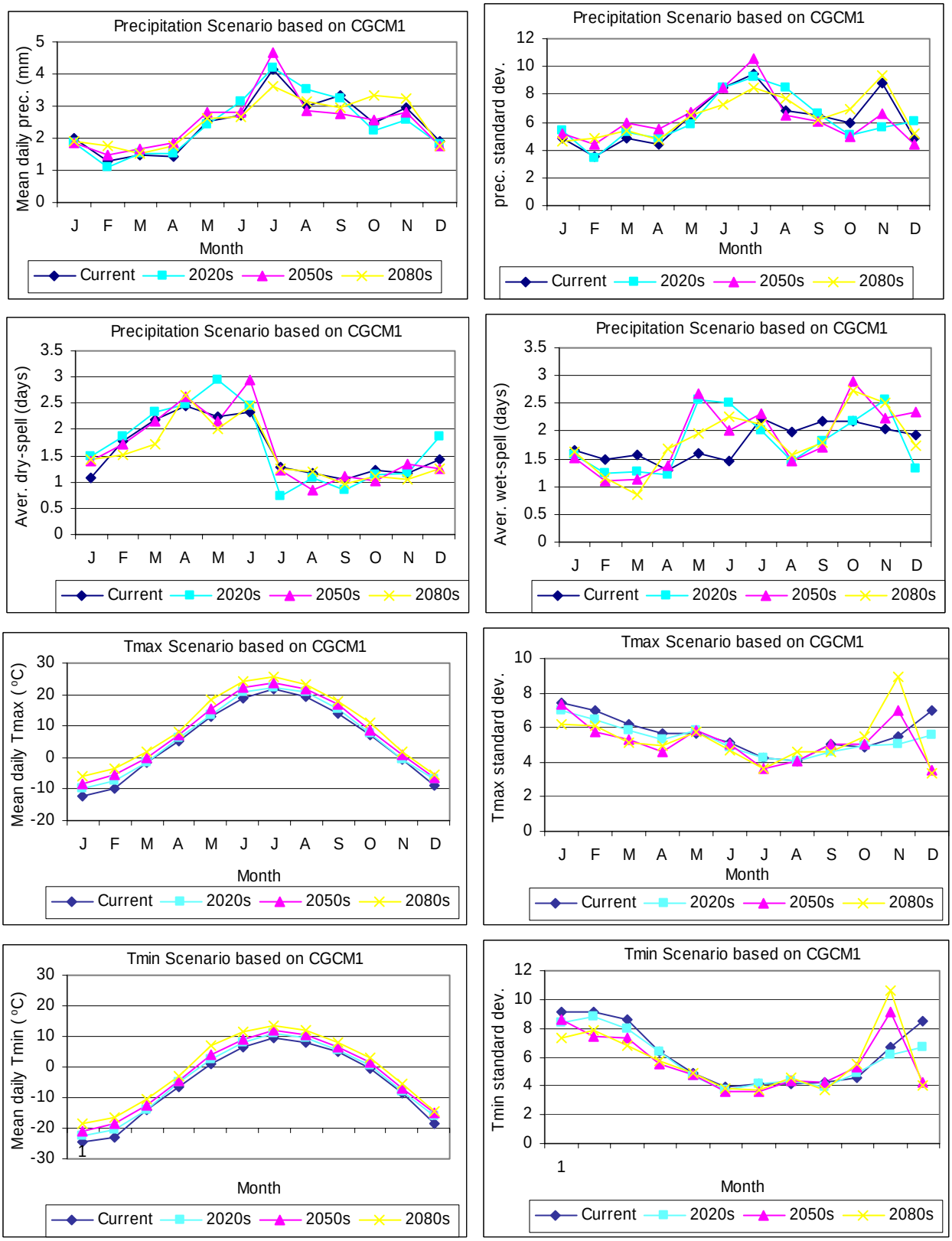

Annex B4. General trend in precipitation and temperature at Chute-des-passes corresponding to a climate change scenario downscaled with LARS-WG

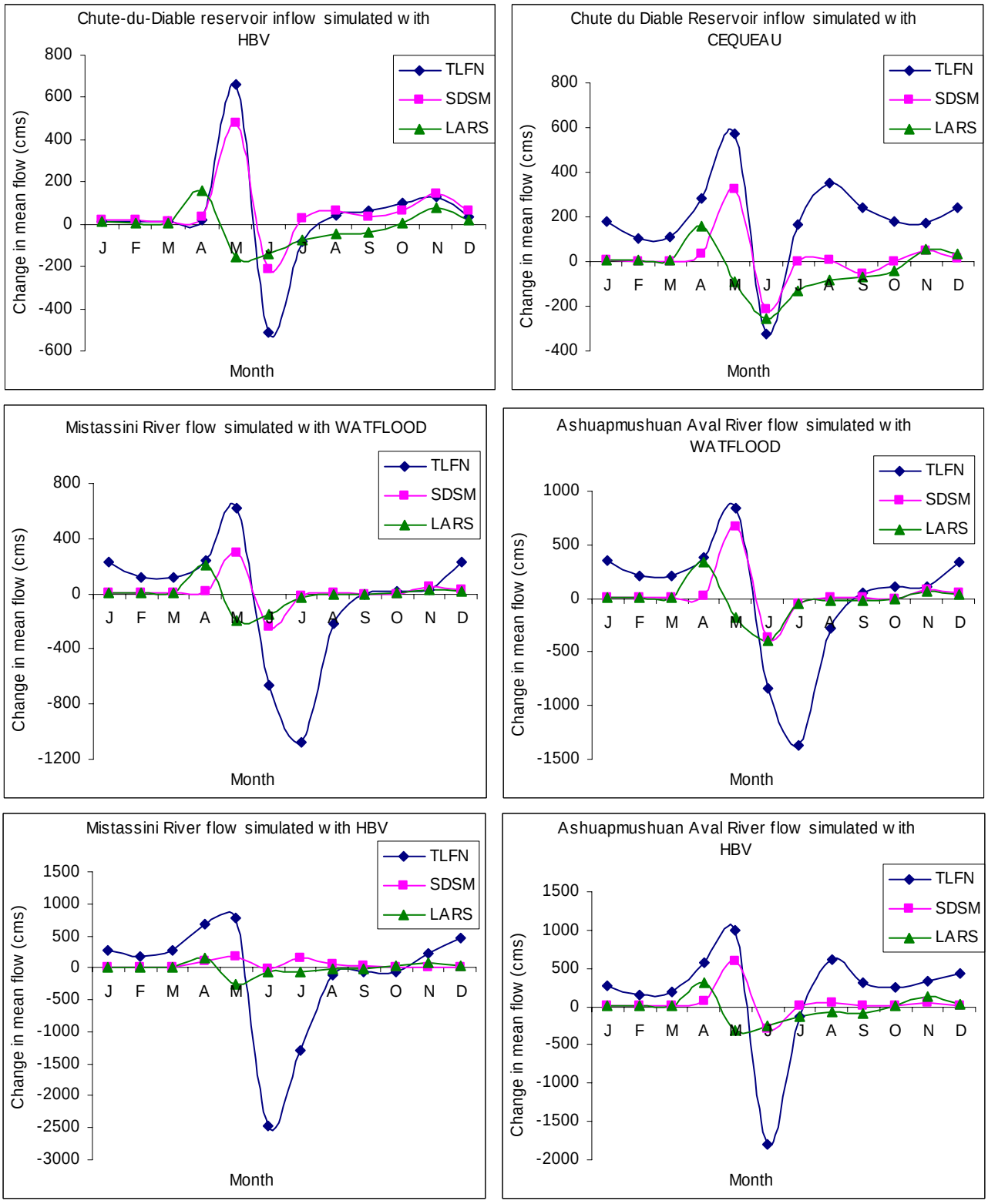

Annex C1. Comparison of changes in monthly mean, high and low flows (between the current and the 2080s time period) at Chute-du-Diable reservoir

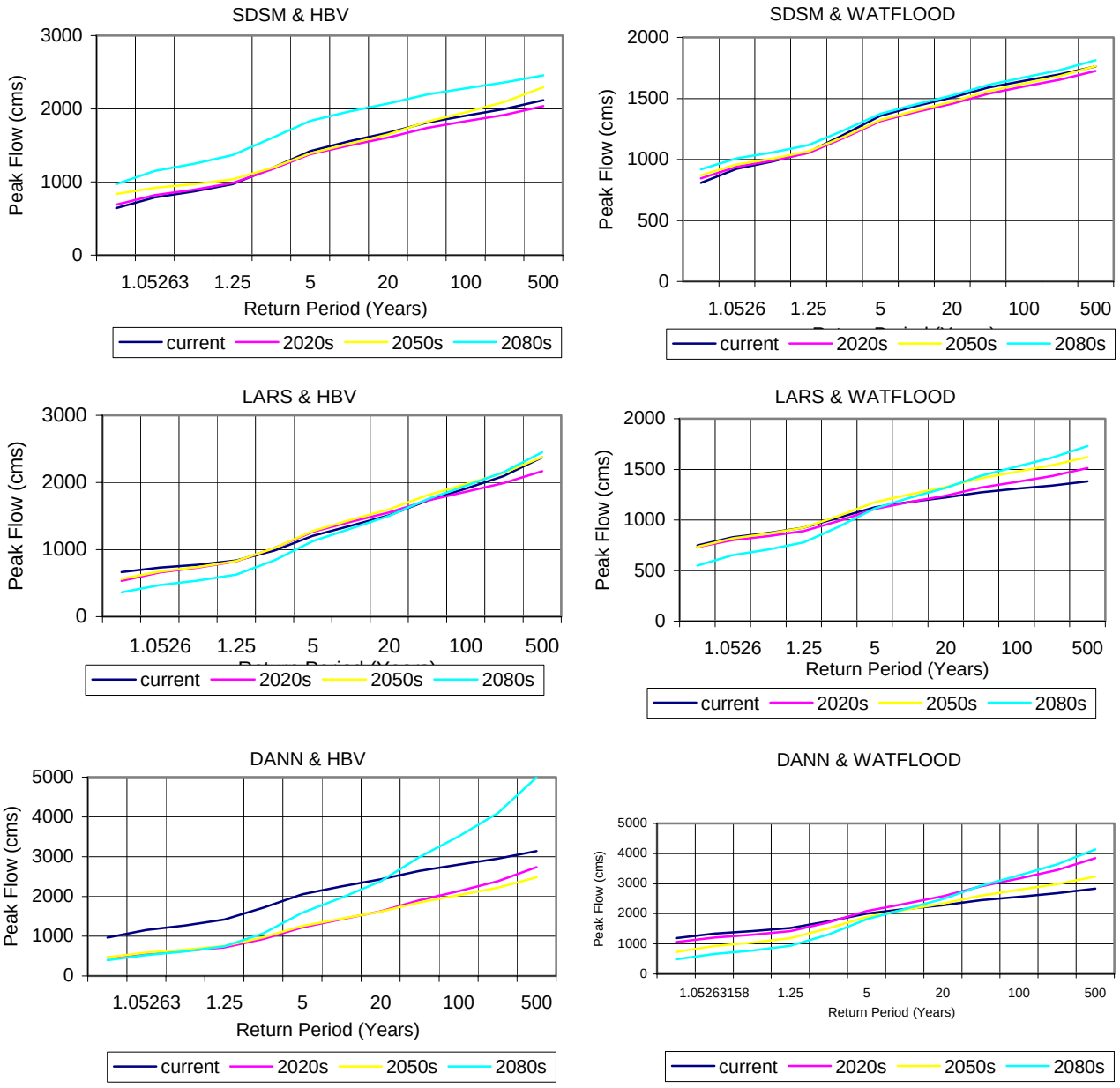

Annex D1. Flood frequency curves for Mistassibi River flow based on future scenario simulation with different downscaling techniques and hydrologic models

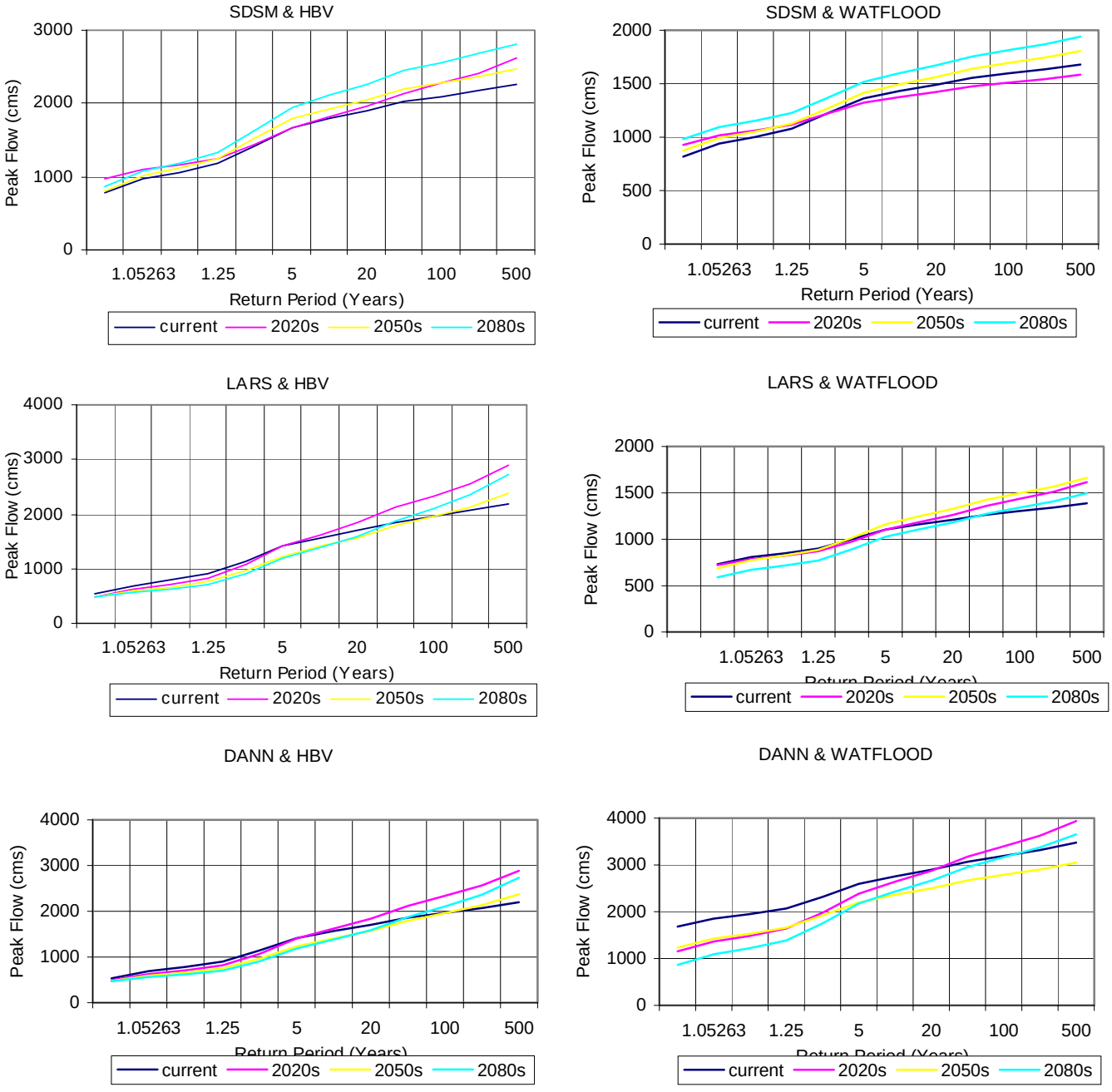

Annex D2. Flood frequency curves for Mistassini River flow based on future scenario simulation with different downscaling techniques and hydrologic models

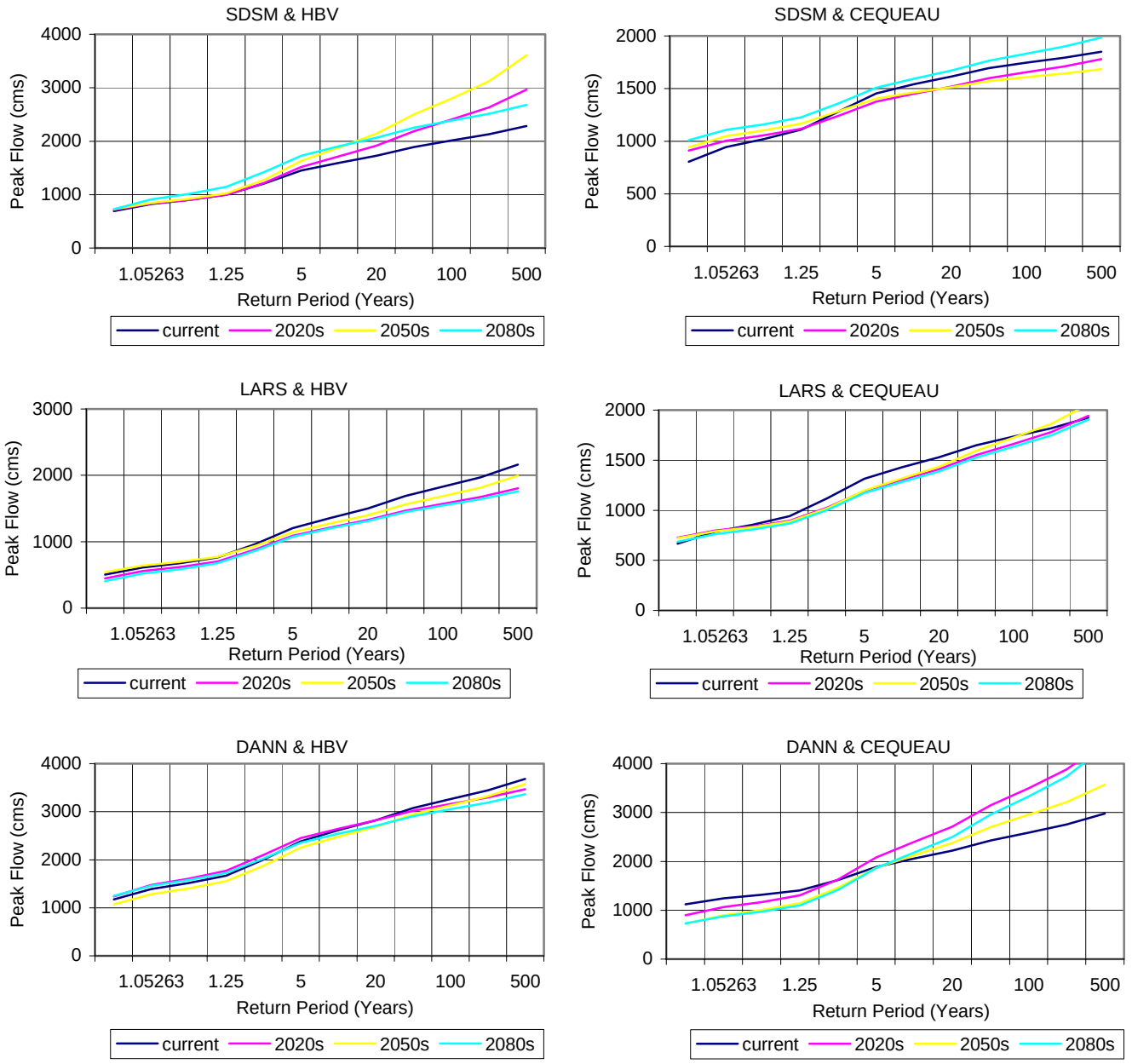

Annex D3. Flood frequency curves for Chute du Diable Reservoir inflow based on future scenario simulation with different downscaling techniques and hydrologic models

ANNEX 2: Summary on how to Downscale GCM Outputs Using Dynamic Artificial Neural Network (DANN) Model

This summary presents the steps required downscale Global Climate Model (GCM) using the neural network development tools called NeuroSolutions and NeuroSolutions for Excel. This Annex described the procedure followed in developing the Time Delay Neural Networks described in the main report. Two sets of models are described here: the TDN1 model which uses all atmospheric variables to predict the output, and the TDN2 model which uses the 8 best variables based on a sensitivity analysis to predict the output.

TDN 1 Model

- A spreadsheet must be made in Microsoft Excel consisting of the 22 atmospheric variables and one additional output column (either Precipitation, Max Temperature, or Min Temperature). Each row on the spreadsheet represents a daily predictor and predictand values. The spreadsheet must be saved and a good practice is to keep names consistent. For example, a spreadsheet may be saved as Norm_Prec_TDN1.xls where it gives, respectively: the weather station, Prec/Tmax/Tmin, and the type of model.
- After setting up the spreadsheet, the model must now be created. Make sure there is a pull-down menu for NeuroSolutions. If there is not, go to Tools/Add-ins and check off *NeuroSolutions for Excel*. It is now necessary to Tag the data for the model. The atmospheric variables columns are tagged as *Input*, and the output column is tagged as *Desired*. Similarly, the rows must be tagged as well. First, check the bottom of the spreadsheet to count the number of rows or being analyzed. Tag the first 75% of the rows as *Training* and the remaining 25% as *Testing*. The model is now ready to be created.
- Again using the NeuroSolutions pull-down menu, choose *Create/Open Network*. NeuroSolutions will now open and a command box will open. Follow these steps, where the bold names are the titles of consecutive command boxes:
  (i) **Neural Model:** Choose *Time-Lag Recurrent Network*. >>
  (ii) **Time-Lag Recurrent:** Change Memory to *TDNNAxon* (or *GammaAxon* for Gama model). Also change *Depth in Samples* to 3 for Tmax/Tmin and 6 for Precipitation. >>
  (iii) **Hidden Layer #1:** Change *Processing Elements* to 30 for TDN1 (22 variables). Also change *Learning Rule* to DeltaBarDelta. >>
  (iv) **Output Layer:** Leave the Output Layer box as it is. >>
  (v) **Supervised Learning Control:** Change the epochs as appropriate. 2000 epochs is good for Tmin and Tmax Models, and 3000 to 5000 epochs is best for Precipitation Models (but this makes the model creation very time consuming – approximately 1 hour).
  (vi) **Probe Configuration:** There are five boxes on this page. Leave Input, change *Output, Desired,* and *Error* to Data Graph and check off Training Set. Next under *Performance Measures*, check off General and Training Set.
  (vii) Click Build and the model will be constructed. The model must be saved before it can be used. Use a filename consistent with the rest of the project.

- The model must now be trained before it can be tested. Returning to the Excel spreadsheet, under the NeuroSolutions menu, choose *Train Network/Train*. Use a consistent name such as Norm_Tmax_TDN1_Train. You are also given the option to change the number of epochs. If you are training the model for the first time, check off *Randomize Initial Weights***,** but if you are

resuming a model that had been training and was paused, make sure this is NOT checked off or else the model will begin training from scratch. The training process can take anywhere from 5 minutes to 2 hours, depending on the amount of data as well as the number of epochs.

- Two tests must now be performed to check the validity of the model. Under the NeuroSolutions menu, choose *Test Network/Test*. Test 1 tests the Training dataset, and Test 2 tests the Testing dataset. Name each test and indicate within the command box which dataset is being tested. Once the tests are complete, Excel will compare the Experimental vs. Theoretical results in the form of a graph. The better the model, the more similar the graphs will look, and the closer to 1 your r-value will be.
- The final step needed for the TDN1 model is the Sensitivity Analysis. From the NeuroSolutions menu, choose *Test Network/Sensitivity about the Mean*. This will give a bar graph showing all the atmospheric variables and how much they affect the model over time. Write down the 8 best variables which will be used in constructing the TDN2 model.
- Save the Excel file for a final time. The file now contains all the work you have just done: the model, the training report, the test reports, the sensitivity analysis, and the data spreadsheet.

TDN2 Model

- Another spreadsheet must be created. Find the top 8 variables in the TDN1 Sensitivity Analysis (the highest bars on the bar graph). Copy and paste these columns to a new spreadsheet as well as the output column, giving a total of 9 columns.
- The steps for setting up the model are very similar to the TDN1 Model. Recapping:
    - Tag Data.
    - Create new model. The only difference in creating this model is the number of Processing Elements. Use 12 PE's for the 8 variables. (A good rule-of-thumb is to use #PE = 3/2*#variables)
    - Train Model.
    - Test 1 using Training Dataset.
    - Test 2 using Testing Dataset.
- A Sensitivity Analysis does not need to be performed since the 8 best variables are already being used.
- The next task is to perform a Cross Validation Test to predict future conditions. The time periods used are Current (1961-2000), the 2020s (2010-2039), the 2050s (2040-2069) and the 2080s (2070-2099). No data is given for (2000-2010). Given a GCM data sheet with predicted atmospheric variables, copy the 8 variable columns corresponding to the particular TDN2 Model. Paste these columns at the bottom of the TDN2 spreadsheet and tag these added rows as *Cross Validation*. For the output column, place all zeros for the Cross Validation data.
- Before testing the Cross Validation data, make sure the correct NeuroSolutions model (or breadboard) is open. For example, if you are working on Metab_Tmax_TDN2.xls, make sure the active model is Metab_Tmax_TDN2.nsb. NeuroSolutions menu: *Open Active Network*.
- Test the Cross Validation data. NeuroSolutions menu: *Test Network/Test*. Name the test 'Production' and use the Cross Validation dataset.

Data analysis using statistical downscaling model (SDSM)

The SDSM model is used to analyze observed data or data attained from a previous model (in our case, the TDN2 model). The SDSM program organizes the data and provides statistical information for a period of time. This analysis is only concerned with the output columns from the previous models.

For a given station and output, say Bonard_Tmin, there are eight outputs that are of interest for analysis. These are: **Current**, **2020s**, **2050s**, **2080s**, which are all taken from the Production output, **Observed Training** and **Observed Testing**, which are the actual conditions measured, and the **TDN Training** and **TDN Testing**, which are the outputs from the TDN model.

*Current: 1960 – 2000
*2020s: 2010 – 2039
*2050s: 2040 – 2069
*2080s: 2070 – 2099

- Click Start to begin.
- From the Menus at the top of the page, choose *Analyse: Analyse Other Data*.
- The first step required is to set the beginning and finishing dates for the desired period of analysis. If this is unknown, open the data in excel to find out how many days the data spans. The exact starting and finish date do not have to be exact, as long as the correct number of days are used and the years are correct. Go to *Settings* to adjust the date.
- Next, the Input file must be specified (*Select File* on the left). The Input file must be a *.dat file to be read correctly. The input file will consist of a long column of numbers, ie. Bonard_Current_Tmin. This line of data is copied from the TDN2 model into Notepad and saved as a new data file.
- Next, the Output file must be specified (*Select File* on the right). The Output file will be created by the SDSM program in the form of a *.txt file. A good practice is to name the output file the same as the input file to keep things organized.
- Next step is to identify the *Statistics* to be analyzed. For Tmax and Tmin, check off **Mean**, **Maximum**, **Minimum**, **Sum**, **Variance**, **Autocorrelation**, and **Skewness**. For Prec, check off **Mean**, **Maximum**, **Variance**, **Percentage Wet**, **Mean dry spell length**, **Mean wet spell length**, **Maximum dry spell length**, **Maximum wet spell length**.
- Once you have selected an input file, selected an output file, set the date, and chosen the statistics, you are ready to proceed. Click *Analyse*, and the output will be produced. The same output you see on the screen is what is put into the text file.

*NOTE: When creating any of these models, you may find it useful to have a pencil and paper handy to keep notes as you proceed. It will help make it easier to keep track of what has been done and what still needs to be done.